Benthic foraminifera as geochemical and micropaleontological proxies for redox conditions in the Peruvian oxygen minimum zone

Dissertation

zur Erlangung des Doktorgrades

Dr. rer. nat.

der Mathematisch-Naturwissenschaftlichen Fakultät

der Christian-Albrechts-Universität zu Kiel

vorgelegt von

Nicolaas Glock

Dipl.-Chem., Philipps-Universität Marburg

Kiel 2011

1. Gutachter und Betreuer:	Prof. Dr. Anton Eisenhauer
2. Gutachter:	Prof. Dr. Martin Frank
Eingereicht am:	27.07.2011
Datum der Disputation:	22.08.2011
Zum Druck genehmigt:	22.08.2011

Gez. (Titel, Vor- und Zunahme), Dekan

Erklärung

Hiermit versichere ich an Eides statt, dass ich diese Dissertation selbständig und nur mit Hilfe der angegebenen Quellen und Hilfsmittel erstellt habe. Ferner versichere ich, dass der Inhalt dieses Dokumentes weder in dieser, noch in veränderter Form, einer weiteren Prüfungsbehörde vorliegt. Die Arbeit ist unter Einhaltung der Regeln guter wissenschaftlicher Praxis der Deutschen Forschungsgemeinschaft entstanden.

Kiel, den

(Nicolaas Glock, Dipl.-Chem.)

Contents

Abstract

Tropical oxygen minimum zones (OMZ) are the most important regions of low oxygen in the recent ocean and the nutrient cycling in these regions indeed affects the rest of the ocean. They are areas of high bioproductivity and fishing in these areas has indeed influence on the economy in the whole world and even more on the local economy. One of the most distinctive OMZs is located off Peru. Main objective of this work was the calibration and application of a set of geochemical and micropaleontological proxies for the reconstruction of redox conditions in the Peruvian oxygen minimum zone. The main tools in this work were benthic foraminifera collected off the Peruvian continental margin. The shallow infaunal benthic foraminiferal species *Bolivina spissa* was most widespread among habitats with different redox-conditions at the Peruvian oxygen minimum zone and thus bears great potential to be used as a proxy carrier.

In chapter 2 the results of the measurement of redox sensitive elements in foraminiferal calcite are presented. The test calcite of dead foraminifera often is contaminated by diagenetic coatings which previously have been identified as Mn carbonates and Mn and Fe rich (oxyhydr)oxides. These coatings complicate the exact determination of several element/Ca ratios in foraminiferal calcite. Element distribution maps on test cross-sections of *B. spissa* of core top samples from the Peruvian OMZ generated with an electron-microprobe revealed that diagenetic coatings were absent in these tests. A Fe rich organic phase at the inner test walls could be removed successfully with an oxidative cleaning procedure. Due to the limited amount of *B. spissa* specimens at some sampling sites and to avoid remainings of contaminations Fe/Ca and Mn/Ca ratios were determined at the inner part of the test walls in test cross-sections with secondary-ion-mass-spectrometry (SIMS). Bulk analyses with ICP-MS of samples where enough specimens were available were compared to the SIMS data and agree in a good way. Mn/Ca ratios are relatively low but in the same magnitude as in the pore waters. Indeed the permanently anoxic OMZ off Peru causes MnO_2 reduction in the water column and only minor amounts of particulate bound Mn arrive the seafloor. Thus Mn/Ca ratios in benthic foraminifera from the Peruvian OMZ could be used to trace the amount of oxygen depletion in the OMZ. Higher Mn/Ca ratios would indicate a better oxygenation because more particulate bound Mn would reach the seafloor and be remobilised in the pore waters. The Fe/Ca ratios in *B. spissa* were the lowest at a location at the lower boundary of the OMZ which was strongly depleted in oxygen and showed a strong, sharp Fe peak in the top interval of the pore water. Since no living but plenty of dead specimens of *B. spissa* have

been found at this location during sampling time this might indicate that the specimens died recently because the pore water was turning anoxic. Thus the Fe flux out of the sediment started after the death of *B. spissa* at this site. The sharp peak also indicates that the Fe flux started recently and might hint that ironoxides that precipitated in a period of higher oxygen supply from water masses below the OMZ just recently started to get remobilised when the sediment turned anoxic. The trend of the higher pore water concentrations with increasing water depth at the deeper stations reflects the transition from sulphate reduction to iron reduction. This trend is reflected by the Fe/Ca ratios in *B. spissa*, too, while the more short time fluctuations of pore water Fe/Ca at the lower OMZ boundary seem not to be reflected by the foraminiferal Fe/Ca. The fact that the Fe/Ca ratios in *B. spissa* reflect not always the pore water conditions might complicate approaches in paleoreconstruction in contrast to the Mn/Ca ratios which seem to be a very promising tool. Nevertheless, future downcore studies will show the value of these proxies in paleoreconstruction. An iron and organic rich phase has also been found at the inner sides of the test walls and also in the pores of several specimens of *Uvigerina peregrina.* This phase most propably represents the inner organic lining. The lining is also enriched in Al, Si, P and S. Similar compositions have been found in test walls of allogromiids and the cements and inner organic lining in the agglutinated tests of textulariids. This hints to an evolutionary connection between these test components.

The development of a new proxy, the pore density in *B. spissa*, is presented in chapter 3. Test pores, developed in rotaliid calcareous species, are important features in the test morphology. In earlier publications it has been suggested that pores promote the uptake of oxygen and the release of metabolic CO_2. The pore densities (PD) of 232 *B. spissa* specimens from eight locations at the Peruvian OMZ were determined and a negative exponential correlation between the PD and the bottom water oxygen concentration ($[O_2]_{BW}$) was found. The relationship between the PD and the bottom water nitrate concentration ($[NO_3^-]_{BW}$) is much better constrained than that for PD-$[O_2]_{BW}$. We propose that the pores in tests of *B. spissa* are largely adapted to the intracellular nitrate uptake for nitrate respiration and to a smaller part extend the oxygen respiration. Hence the PD in *B. spissa* could prove as an invaluable proxy for present and past nitrate concentrations. Investigations of thin sections from living fixed *B. spissa* cells with the transmission-electron-microscope (TEM) showed that mitochondria, cell organelles involved in respiration, are clustered behind the pores. Foraminiferal denitrification has not been traced to a specific organelle, yet. These results hint that mitochondria at least are involved in the process of foraminiferal denitrification.

First applications of the knowledge about the PD in *B. spissa* are given in chapter 4. Comparison of recent specimens with specimens from a strong El-nino (1997-1998) from the same area at the Peruvian continental margin showed that there are significant differences ($P = 0.031$) in the PDs of specimens from 830 m water depth between El-nino and non-El-nino conditions. Nitrate profiles through the water column off Peru show that in this water depth nitrate was depleted during that El-nino compared with the non-El-nino conditions. Promoted were these results, because no significant difference was found between the pore densities at a 562 m site during El-nino and a 579 m site during non El-nino conditions ($P = 0.471$). In these water depth nitrate concentrations during El-nino and non-El-nino conditions were similar. Furthermore first steps for the application for paleoreconstruction have been done. The PD was determined downcore at a short core (12 cm) from 579 m water depth (M77-1 487/MUC-39) and a long pistoncore (~13 m) from 630 m water depth (M77-2 47-2). The short core covers a time span of about the last 300 years. Although the PDs did not differ significantly in the several depth intervals of that core ($P = 0.88$) there is a slight minimum in the PD at the end of the Little Ice Age in the beginning of the 19th century when there were mayor shifts in the biogeochemical conditions at the OMZ off Peru. The PDs in the several depth intervals of the long core on the other hand show significant differences ($P < 0.01$). There seems to be a strong shift to higher PDs during the last glacial maximum (LGM). The higher PDs indicate nitrate depletion during the LGM which either might origin from shifts in the biogeochemical conditions, the lower sea level during this time or an interaction of both. Although the PD from specimens collected during El-Nino conditions seem to reflect even short time changes in the nitrate availability it might be hard to trace El-Nino events in the past due to the high sampling resolution which is needed for such studies. The low variability in the PD of that short core on a centennial time scale might be either due to really low nitrate variability at this sampling site or due to a flattening of the signal because of the limited vertical sampling resolution. In this case more studies on cores from different locations are needed. The changes in the PD during the LGM indicate that the PD is sensitive at least on these millennial time scale changes. Together with information from Mn/Ca and Fe/Ca ratios changes in oxygen and nitrate availability might be traced during the last glacial. This might give a much more complete picture about changes in the biogeochemical conditions in the Peruvian OMZ during this time.

Zusammenfassung

Tropische Sauerstoffminimumzonen (SMZ) sind die wichtigsten sauerstoffarmen Gebiete im heutigen Ozean. Der Nährstoffkreislauf in diesen Regionen hat Einfluss auf den gesamten restlichen Ozean. Durch die hohe Bioproduktivität hat der Fischfang in tropischen SMZs nicht nur starken Einfluss auf die regionale Wirtschaft, sondern auf die Wirtschaft der ganzen Welt. Eine der ausgeprägtesten Sauerstoffminimumzonen befindet sich vor Peru. Ziel dieser Arbeit war die Kalibration und erste Anwendungen eines Sets von geochemischen und micropaleonthologischen Proxies zur Rekonstruktion der Redoxbedingungen in der SMZ vor Peru in der Vergangenheit. Benutzt dazu wurden benthische Foraminiferen, gesammelt am Kontinentalhang vor Peru. Am weitesten verbreitet in Habitaten mit stark unterschiedlichen Sauerstoffkonzentrationen war die flach infaunale benthische Art *Bolivina spissa*. *B. spissa* zeigt demnach das größte Potential als Proxieträger.

In Kapitel 2 werden die Ergebnisse von Messungen redoxsensitiver Elemente in foraminiferen Calcit präsentiert. Die Gehäuse von toten Foraminiferen sind oft mit diagenetischen Coatings überzogen. In früheren Arbeiten wurden diese als Mangancarbonate und Mn und Fe reiche (oxyhydr)oxide identifiziert und erschweren die genaue Bestimmung von mehreren Element/Ca Verhältnissen in foraminiferen Calcit. Elementverteilungen, erstellt mit einer Elektronenmikrosonde an Gehäusequerschnitten von *B. spissa* Individuen aus Oberflächenproben, zeigen keine Hinweise auf die Anwesenheit von diagenetischen Coatings. Eine Fe reiche organische Phase an den Gehäuseinnenwänden konnte erfolgreich mit einem oxidativen Reinigungsschritt entfernt werden. Da von einigen Locationen nur eine begrenzte Anzahl von *B. spissa* Individuen verfügbar war und um Rückstände von Kontaminationen zu vermeiden, wurden Fe/Ca und Mn/Ca inmitten der Gehäusewände an Querschnitten mittels Sekundärionenmassenspektrometrie (SIMS) bestimmt. Diese Daten stimmen gut überein mit ICP-MS Messungen an größeren Probenmengen (~40 Exemplare) von Locationen an denen genug Exemplare verfügber waren. Die Mn/Ca Verhältnisse sind relativ niedrig aber dennoch in derselben Größenordnung des Porenwassers. Tatsächlich wird MnO_2 in der permanent anoxischen SMZ vor Peru bereits in der Wassersäule reduziert und nur sehr geringe Mengen von partikelgebundenem Mn erreicht den Meeresgrund. Mn/Ca Verhältnisse in benthischen Foraminiferen aus der SMZ vor Peru können daher benutzt werden um Sauerstoffkonzentrationen relativ zu rekonstruieren. Höhere Mn/Ca Verhältnisse würden erhöhte Sauerstoffkonzentration indizieren, da mehr partikelgebundenes Mn den Meeresgrund erreichen und im Porenwasser remobilisiert würde. Die niedrigsten Fe/Ca Verhältnisse

wurden an einer Lokation an der unteren Grenze der anoxischen SMZ gefunden. Diese Lokation war sehr sauerstoffarm und zeigte einen ausgeprägten, scharfen Fe Peak im oberen Porenwasserintervall. Die Tatsache, dass während der Probennahme keine lebenden aber sehr viele tote Exemplare von *B. spissa* an dieser Lokation gefunden wurden, indiziert, dass das Porenwasser erst kürzlich anoxisch geworden ist. Der scharfe Fe Peak im Porenwasser deutet ebenfalls daraufhin, dass der Fe-Fluss aus dem Sediment erst kürzlich begonnen hat, was vermutlich daran liegt, dass Eisenoxide, die in einer Periode mit erhöhter Sauerstoffzufuhr aus tiefer liegenden Wassermassen unterhalb der SMZ ausgefällt wurden, erst kürzlich remobilisiert worden sind, als das Sediment anoxisch wurde. Die Tendenz höherer Fe Konzentrationen im Porenwasser mit steigender Wassertiefe an den darunterliegenden Lokationen reflektiert den Übergang von SO_4^{2-} zu Fe-Reduktion. Dieser Trend wird auch von den Fe/Ca Verhältnissen in *B. spissa* reflektiert. Der Fakt, dass die Fe/Ca Verhältnisse in *B. spissa* nicht immer direkt die Porenwasserbedingungen wiederspiegeln, könnte Ansätze zur Paleorekonstruktion jedoch komplizieren. Die Mn/Ca Verhältnisse hingegen sehen in diesem Fall wesentlich vielversprechender aus. Nichtsdestotrotz werden zukünftige Studien kernabwärts zeigen, wie gut sich diese proxies zur Paleorekonstruktion eignen. Eine Fe reiche organische Phase an der Innenseite der Gehäusewände und in den Poren wurde auch bei mehreren Exemplaren von *Uvigerina peregrina* identifiziert. Diese Phase ist vermutlich das sogenannte „Inner Organic Lining“ (IOL). Diese Phase ist außerdem angereichert an Al, Si, P und S. Frühere Studien zeigen ähnliche Zusammensetzungen in Gehäusewänden von Allogromiiden und den Zementen und IOLs von agglutinierten Gehäusen der Textulariiden. Diese Ergebnisse indizieren eine evolutionäre Verbindung dieser Gehäusekomponenten.

Die Entwicklung eines neuen Proxies, die Porendichte (PD) in *B. spissa*, wird in Kapitel 3 beschrieben. Poren in den Gehäusen von Rotaliiden sind wichtige Merkmale in der Gehäusemorphologie dieser calcitischen Spezien. In früheren Publikationen wurde nahegelegt, dass die Poren hauptsächlich die Funktion der Sauerstoffaufnahme und der Abgabe von metabolischen CO_2 haben. Die PDs von 232 *B. spissa* Exemplaren von acht Lokationen aus der SMZ vor Peru wurden bestimmt und eine negativ exponentielle Korrelation zwischen PD und der Sauerstoffkonzentration im Bodenwasser ($[O_2]_{BW}$) gefunden. Allerdings ist die Abhängigkeit der PD von der Nitrat Konzentration im Bodenwasser ($[NO_3^-]_{BW}$) wesentlich ausgeprägter als die Abhängigkeit von $[O_2]_{BW}$. Demnach sind die Poren in Gehäusen von *B. spissa* wahrscheinlich zu einem großen Teil angepasst an die intrazelluläre Aufnahme von Nitrat zur Nitratatmung und nur zu einem geringeren Teil an die Sauerstoffatmung. Demnach könnte sich die Porendichte in *B. spissa* als unschätzbarer

Proxy für gegenwärtige und vergangene Nitratkonzentrationen erweisen. Untersuchungen an Dünnschnitten von lebend fixierten *B. spissa* Zellen mit einem Transmissionselektronenmikroskop (TEM) zeigen, dass Mitochondrien (für die Atmung mitverantwortliche Zellorganellen) hinter den Poren gruppiert sind. Denitrifikation in Foraminiferen wurde bisher noch keinem Zellorganell zugeordnet. Diese neuen Resultate indizieren, dass Mitochondrien zumindest in diesen Prozess involviert sind.

Erste Anwendungen dieses neuen Wissens über die PD in *B. spissa* werden in Kapitel 4 dargestellt. Ein Vergleich rezenter Exemplare mit Exemplaren von einem starken El-Nino (1997-1998) aus demselben Gebiet am Kontinentalhang vor Peru zeigen, dass in einer Wassertiefe von 830 m signifikante ($P = 0.031$) Unterschiede zwischen den PDs zwischen El-Nino und nicht-El-Nino Bedingungen bestehen. Nitrat Profile durch die Wassersäule vor Peru zeigen, dass während des El-Nino die Nitratkonzentrationen geringer waren als während der nicht-El-Nino Bedingungen. Untersützt werden diese Resultate durch die Tatsache, dass kein signifikanter Unterschied zwischen den PDs einer Lokation von 562 m Wassertiefe während El-Nino und einer Lokation von 579 m Wassertiefe während nicht-El-Nino Bedingungen gefunden wurden. In diesen Wassertiefen unterscheidet sich Nitratkonzentration kaum zwischen diesem El-Nino und nicht-El-Nino-Bedingungen. Schließlich wurden noch erste Schritte der Anwendung dieses Proxies zur Paleorekonstruktion unternommen. Die PDs wurden in verschiedenen Tiefenintervallen entlang eines kurzen Kerns (12 cm) von 579 m Wassertiefe (M77-1 487/MUC-39) und eines langen Kerns (~13 m) von 630 m Wassertiefe (M77-2 47-2) bestimmt. Der kurze Kern umfasst eine Zeitspanne von ca. 300 Jahren. Obwohl sich die PD zwischen den verschiedenen Tiefenintervallen des Kerns nicht signifikant unterscheidet ($P = 0.88$) befindet sich ein schwaches Minimum der PD am Ende der kleinen Eiszeit zum Beginn des 19. Jahrhunderts. Zu dieser Zeit fanden starke und rapide Veränderungen in den biogeochemischen Bedingungen in der SMZ vor Peru statt. Auf der anderen Seite zeigt die PD in verschiedenen Tiefenintervallen entlang des langen Kerns signifikante Unterschiede ($P = 0.018$). Die PD scheint sich während des letzten glazialen Maximums (LGM) sichtlich zu erhöhen. Die höheren PDs indizieren niedrigere Nitratkonzentrationen während des LGM. Diese entstehen vermutlich entweder durch Veränderungen in den biogeochemischen Bedingungen, dem niedrigeren Wasserspiegel zu dieser Zeit oder einer Wechselwirkung von beidem. Obwohl die PD von *B. spissa* Exemplaren, die während eines El-Nino gesammelt wurden, Veränderungen in der Nitratkonzentration während eines El-Nino Ereignisses reflektiert, dürfte es schwierig sein El-Nino Ereignisse in die Vergangenheit zurückzuverfolgen aufgrund der hohen

Beprobungsauflösung, die dazu von Nöten wäre. Es ist unklar ob die niedrige Variabilität in der Porendichte entlang des kurzen Kerns von einer Dämpfung des Signals aufgrund der Beprobungsauflösung herrührt oder daher, dass an dieser Lokation tatsächlich nur niedrige Schwankungen in den Nitrakonzentrationen während der letzten 300 Jahre waren. Um das zu klären werden mehr Daten von weiteren Probenlokationen benötigt. Die Veränderung in der PD während des LGM zeigt, dass zumindest in dieser Zeitskala die zeitliche Auflösung des Proxies nicht limitiert ist. Zusammen mit Informationen aus den Mn/Ca und Fe/Ca Verhältnissen könnten Veränderungen sowohl in der Verfügbarkeit von Sauerstoff, als auch Nitrat in das letzte Glazial zurückverfolgt werden. Dies könnte ein wesentlich vollständigeres Bild über Veränderungen in den biogeochemischen Bedingungen während des letzten Glazials geben.

1 Introduction

The main objective of this thesis is the calibration and application of a set of geochemical and micropalentological proxies for the quantitative reconstruction of past oxygen levels in the Peruvian upwelling cell.

1.1 Relevance of upwelling cells in the global ocean

Upwelling cells are areas of high bioproductivity because a high amount of nutrients is transported towards the water surface. This results in a high flux of organic material through the water column. Oxygen is strongly depleted through the water column due to remineralisation of this material. An oxygen minimum zone (OMZ) develops. Strong gradients are formed both in bottom-water oxygenation and the input of organic matter when OMZs intercept the continental margin or seamounts (Levin et al., 1991; Levin et al., 2000; Levin et al., 2002). The extension of the OMZs in the Eastern Tropical North Pacific (ETNP) and Eastern Tropical South Pacific (ETSP) are shown in fig. 1.1.

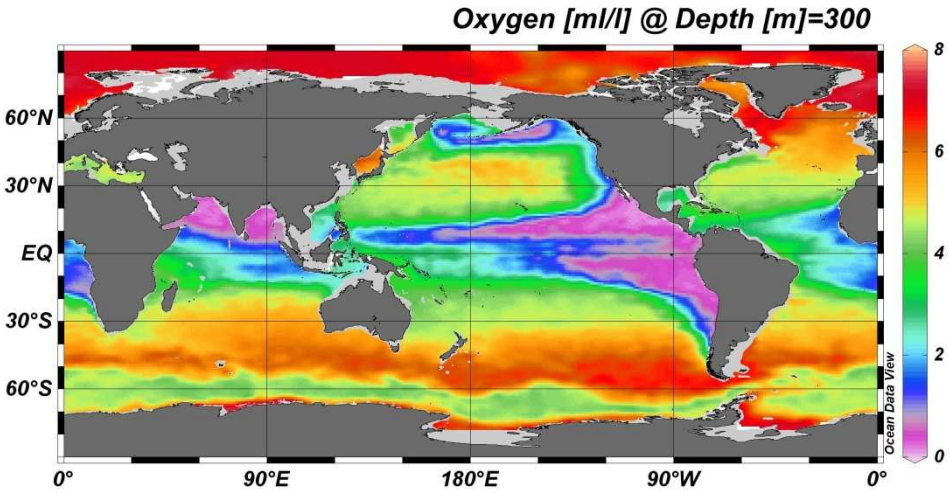

Figure 1.1. Extension of OMZs in the global ocean. Raw data from Boyer et al. (2009).

Tropical OMZs are the most important regions of low oxygen in the recent ocean and the nutrient cycling in these regions indeed affects the rest of the ocean. It has been predicted by model calculations that the ocean will progressively loose oxygen over the next 200 years (Bopp et al., 2002; Matear and Hirst, 2003; Joos et al., 2003). On the one hand this is related to oceanic warming but the main reason is the decreased ocean ventilation due to circulation changes related because of the anthropogenic induced climate change. Indeed a 50-year time series of dissolved oxygen concentrations reveals vertical expansion of the intermediate depth OMZs in the eastern equatorial Atlantic and the equatorial Pacific during this timeframe

(Stramma et al., 2008). One of the most distinctive OMZ is located at the Peruvian upwelling cell. Although coastal upwelling cells cover only about 0.14% of the global ocean (Baturin, 1983; Wolf, 2002) in 2007 15.5 million tons of fish has been caught by commercial fisheries in eastern boundary upwelling ecosystems (Fréon et al., 2009). This corresponds to 17% of the global catches (91.2 million tons; source: FAO FishStat). About 8% of the global catches were located only in the Peruvian upwelling cell (7.2 million tons; source: FAO FishStat). Therefore if the oxygen depletion in this area would vertically extend towards the water surface habitats which are rich in pelagic fish would be endangered. This on the other hand would have significant influences on the global and especially local fishery. Furthermore OMZs are important for the global carbon cycle. Photosynthetic organisms bind atmospheric CO_2 near the water surface which is transported into the deep via the flux of organic material (Berger et al. 1989). On the other hand dissolved CO_2 from deeper water masses is released to the atmosphere via upwelling. The cold, upwelled deeper water masses warm up when they are transported to the water surface, which reduces the solubility of CO_2. Bioproductivity in these regions therefore has a substantial influence on the CO_2 concentrations in the atmosphere. That OMZs are an important source of the greenhouse gas N_2O due to denitrification should only shortly be mentioned. All these topics point out that there is a high importance to understand the processes which control the extension of OMZs. The reconstruction of the Peruvian OMZ in the past will help to understand these processes and give information if the recent oxygen fluctuations are indeed of anthropogenic or if they are more related to natural variability.

1.2 The mechanism of upwelling

Upwelling is the vertical transport of cool deeper water masses which are usually rich in nutrients to the water surface where they replace the warmer, nutrient depleted water masses. This phenomenon results from an interaction of wind stress, coastal currents and the Coriolis force (Gunther, 1936; Hart and Curie, 1960; Wooster and Reid, 1963; Smith, 1983). In an ideal situation the interaction of wind stress and the Coriolis force induce surface currents which flow at a 45° direction of the wind (Ekman, 1905). If the water column is divided vertically into thin layers each layer would put a force towards its flowing direction onto the underlying layer (similar to the wind stress at the surface). This results in a shift of direction in each subsequent layer and in a decrease of velocity until it dissipates. The so called Ekman spiral (fig. 1.2) visualises this effect (Knauss, 1997). The whole layer in the water column from the surface until the spiral ends is called the Ekman layer. Integration of the transport over all thin layers inside the Ekman layer results in a net transport orthogonal to the induced

direction (Ekman, 1905). Due to the different Coriolis effect the direction of the transport depends on the hemisphere. While in the northern hemisphere the net transport is directed 90° to the right of the wind direction it is directed 90° to the left in the southern hemisphere (Colling, 2001). Along the coast of Peru for example the winds blow northwards. Due to its location in the southern hemisphere the Ekman transport would result in a current of the surface waters directed west, offshore. A three dimensional model of the upwelling process (fig. 1.3) has been given by Sverdrup et al. (1942; Wolf, 2002). Winds parallel to the coast cause an alongshore transport of the surface waters in wind direction as well as an offshore (Ekman-) transport. To balance the Ekman transport an onshore current along the seafloor on the shelf emerges, the so called bottom Ekman layer. This causes the replacement of the departed surface water by the upwelling of deeper water masses. Since the wind driven alongshore transport is stronger than the Ekman transport, deep water masses also move greater distances parallel to the coast during upwelling (Smith, 1983).

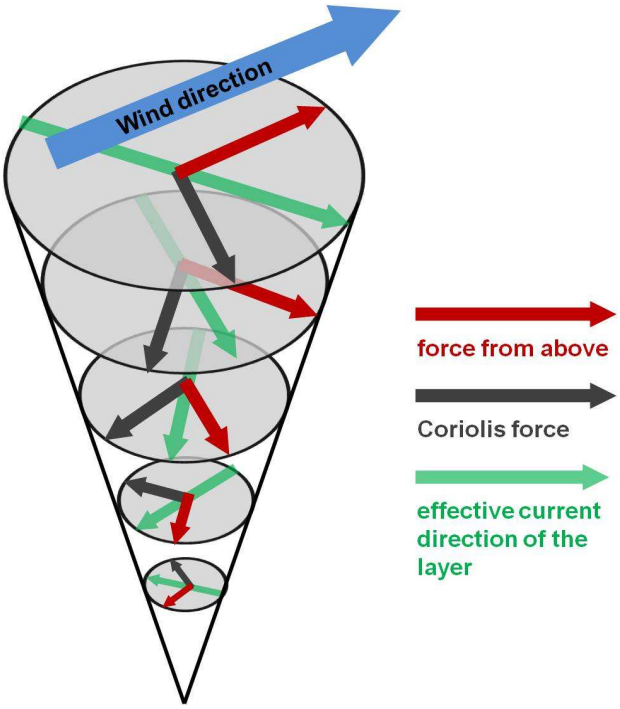

Figure1.2. The Ekman spiral.

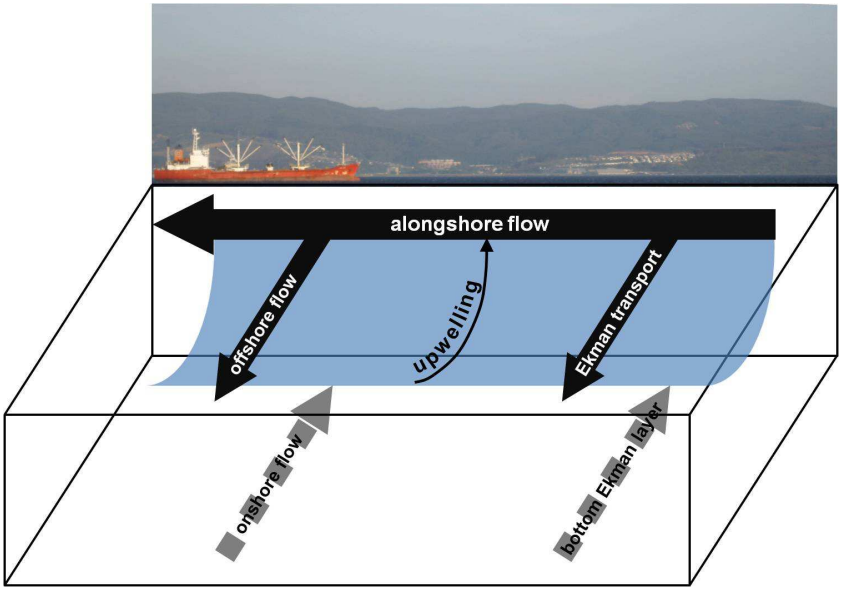

Figure 1.3. Three-dimensional upwelling model (free after Wolf, 2002).

In the tropical Pacific intensity of upwelling and associated enhanced biological productivity has been viewed as a result of variations in the strength of the trade winds (Loubere 2002). The Peruvian upwelling cell located in the ETSP is influenced by the Peru-Chile Current system. This current system, also known as the Humboldt Current System (HCS), is one of the most productive eastern boundary systems of the world. The source of upwelling water in this area is related to the Equatorial Subsurface Water (ESSW; Morales et al., 1999). The ESSW has been associated with Peru-Chile Undercurrent (PUC). The PUC is influenced by the Equatorial Undercurrent, directed polewards and flows over the shelf and upper slope (Wooster et al., 1965). Additionally it has a low temperature, high salinities, low dissolved oxygen and high amount of nutrients (Wyrtki, 1965; Brink et al., 1983). Regions are termed suboxic when oxygen drops down below 10 μmol/kg (Tyson and Pearson, 1991). In suboxic regions nitrate gets involved into respiration and is used as electron acceptor instead of oxygen (Bange et al., 2005; Stramma et al., 2008). In 2008 water masses in the Peruvian OMZ at 11°S were at least suboxic from 50-580 m water depth in 2008 (Glock et al., 2011).

1.3 El-Nino Southern Oscillation

During an El-Nino (EN) the trade winds are weakened on a large scale while the sea surface layers in the eastern and central equatorial Pacific are warming (McPhaden et al., 1998). El-nino events are accompanied with swings in the so called Southern Oscilation (SO), which was identified in the 1920s (Walker, 1923; 1924; 1928; Thurman, 1988). The SO is often described as a seesaw between the South-East-Pacific High Pressure Zone and the North Australian-Indonesian Low Pressure Zone (Philander, 1983, McPhaden et al., 1998). Very high atmospheric sea level pressures occur in the tropical Pacific and Indian regions while on the other hand very low sea level pressures occur in the ETSP during EN. Periods of unusually low sea surface temperatures in the equatorial Pacific linked to very low pressures west and high pressures east of the date line are also known as La-Nina (Phillander, 1990, McPhaden et al., 1998). The full range of the SO including both EN and La-Nina events is called El-Nino Southern Oscillation (ENSO; McPhaden et al., 1998).

The south-east trade winds are affected by the so called Walker Circulation. Under normal conditions they approach the Australian-Indonesian Low Pressure Zone, rise and result in high precipitation rates in the Low Pressure Zone. Off the west coast in South America within the South-East-Pacific High Pressure Zone dry air descends. Thus high rates of evaporation occur at this coast. As a precursor to an EN event the Indo-Australian low-pressure cell starts to move eastwards (Thurman, 1988). This can cause drought conditions in northern Australia,

Indonesia and the Phillipines (McPhaden at al. 1998). Concurrent to this the Intertropical Convergence Zone, where southeast and northeast trade winds meet and rise, moves southward. Usually located between 3°N and 10°N the ITCZ may cross the equator during EN events (Thurman, 1988). This results in excessive rainfalls in the island states of the central tropical Pacific and along the west coast of South America (McPhaden et al., 1998) and is also associated with a weakening of trade winds, coastal upwelling and abnormally high sea surface temperatures in the eastern Pacific (Thurman, 1988). Additionally an intensification of the eastward flow of the Equatorial Undercurrent results in a rise in sea level along the western coast of North and South America polewards in both hemispheres. The severe coastal rains during El-Nino drive away the anchovy of Peru which on the one hand are the basis of fishing there and on the other hand serve as food supply for a large bird population. Thus the effects on the economy of Peru are disastrous due to the strong dependence on fishery and guano industry (Thurman, 1988). But also on other regions along the tropical Pacific and the west coast of North and South America EN events affect the mortality and distribution of commercial valuable fish stocks and other marine organisms in a way that the consequences of this event could be felt worldwide (Barber and Chavez, 1983; Dessier and Donguy, 1987; Pearcy and Schoener, 1987; Lehodey et al., 1997; McPhaden et al., 1998).

1.4 N-cycling in the water column and sediments

Since a major part of this work was the development of a proxy which indicates nitrate availability, there should be a small outline on the oceanic nitrogen cycle. In the oceans nitrate is often a limiting nutrient in bioproductivity (Arrigo, 2005; Lam et al., 2009). In the oceanic nitrogen cycle N_2 becomes bioavailable via N_2-fixation. The fixed nitrogen stays in the ocean bound in different organic and inorganic forms. The loss of nitrogen to the atmosphere in the form of N_2 is dominated by two pathways. On the one hand there is nitrate respiration in facultative anaerobic microorganisms which produces N_2 from NO_3^- (heterotrophic denitrification). On the other hand there is the anaerobic oxidation of ammonium (Anammox) by NO_2^- which yields in N_2, too (van de Graaf et al., 1995). About 20-40% of the global nitrogen loss in the oceans is estimated to occur in OMZs, although OMZ waters occupy only about 0.1% of the global ocean volume (Gruber and Sarmiento, 1997; Codispoti et al., 2001; Gruber, 2004; Lam et al., 2009). Nitrate usually is depleted near the water surface due to utilisation in bioproductivity. Remineralisation of degraded organic matter produces NH_4^+ which is stepwise oxidized to NO_3^- under aerobic conditions (nitrification). Thus the NO_3^-

concentration rises with water depth. The denitrification process proceeds stepwise, too, and a number of intermediates are involved (NO_3^-→NO_2^-→NO→N_2O→N_2). Nevertheless only the complete process with the final product N_2 meets the strict definition of denitrification (Zumft, 1997; Lam et al., 2009). Heterotrophic bacteria release NH_4^+ from organic matter by anaerobic denitrification of NO_3^-. Thus heterotrophic denitrification has been supposed to be the major remineralisation pathway in OMZs, although the expected NH_4^+ accumulation has not been found in OMZs (Richards, 1965; Lam et al., 2009). Another possible source for NH_4^+ is the dissimilatory nitrate reduction to ammonium (DNRA). Recent studies showed that several benthic foraminiferal species are able to switch to nitrate respiration in times when oxygen is too depleted (Risgaard-Petersen et al., 2006). Foraminiferal denitrification has important influences on the benthic N-cycle (Glud et al., 2009; Pina-Ochoa et al. 2010). A scheme for the oceanic N-cycle is shown in fig. 1.4.

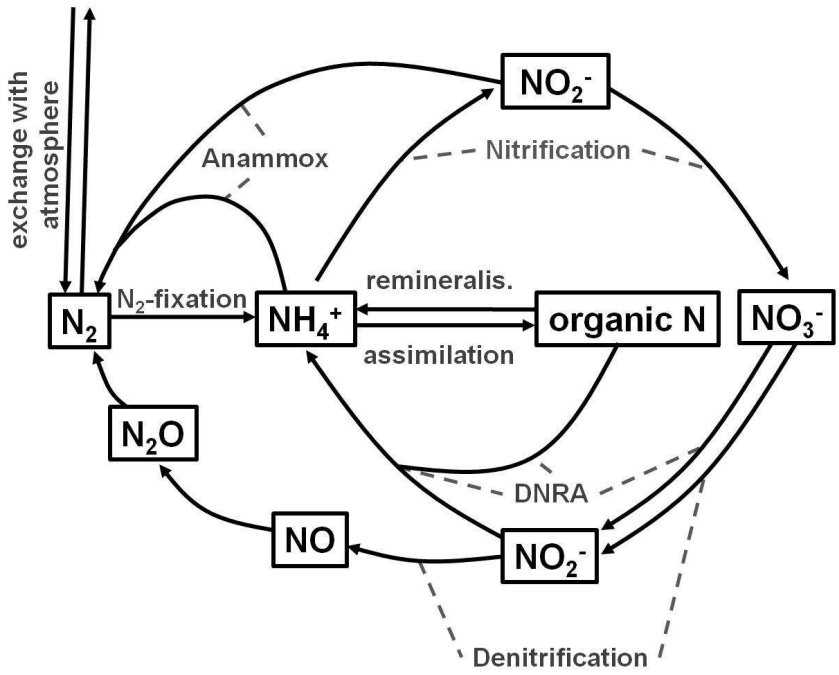

Fig. 1.4. The oceanic N-cycle.

1.5 Foraminifera

Foraminifera are amoeboid protists with reticulating pseudopods. Pseudopodia are fine strands of cytoplasm that branch and merge to form a dynamic net (Hemleben et al., 1989). Foraminifera are typically covered by a test. These tests consist either of calcite (rotaliids and milioliids), agglutinated sediment particles (textulariids) or organic material (allogromiids). The orders mentioned above are only examples for the different test types. On the basis of morphology 15 extant foraminiferal orders are recognized of which 7 are calcitic (Sen Gupta,

2003). To date 2185 foraminiferal species are recorded (Murray, 2007). Only 45 of these species are planktic. Thus they drift through the water column. But the overwhelming majority of foraminifera are benthic, e.g. they live on the seafloor. Benthic foraminifera could either live epifaunal on the surface of the sediments or infaunal inside the sediments. Foraminifera are uniquely adapted to different (partly extreme) environmental conditions. They are distributed everywhere in the ocean from sandmarsh meadows (in extreme +0.5 m above floodwater boundary; Hayward et al., 2011) onto the deepest sea (challenger deep: 10000 m; Gooday et al., 2008). Furthermore they are one of the biggest sources for precipitated calcite. Benthic and planktic foraminifera together produce 1.4 billion tons of calcite a year. This accounts to 25% of the total global calcite production (Langer, 2008). The limestone used to build the Egyptian pyramids consists almost entirely of nummulits. The most primitive foraminiferal test like in *Iridia diaphana* consists only of one chamber which is open to the environment. Also *I. diaphana* is able to leave its test. These primitive test forms most propably developed just to counteract buoyancy of the cytoplasm (Marszalek, 1969). In the evolution more advanced tubes or series of chambers developed as effective barriers against the environment. This includes changes in the chemical as well as in the physical conditions. For example the test form could be optimised to provide time for adaption of the surface to volume ratio of the cell when the osmotic pressure in the surrounding waters changes due to changes in salinity (Marszalek, 1969). Further general test adaptions include the optimisation of the surface to volume ratio of larger foraminifera. Additionally the test in many foraminifera serves most propably as protection against predators. Among the time of their evolution the single foraminiferal species adapted their tests to their habitats in a way that they fit nearly perfectly into the environmental niches they live in. In brackish water or the deep sea for example organic and agglutinated tests are more common then calcitic tests because they are energetically more advantageous when calcium carbonate is undersaturated. On the other hand the organic portion in the test is reduced in shallower waters were calcite is supersaturated (Hallock, P. et al., 1993). Tests in several species are adapted to host algal symbionts (Leutenegger, S., 1984). Solar irradiation could have strong influences on the test structure, too. Porcelanous species for example build their tests out of randomly oriented calcite needles which makes their test appear oparque. This provides protection against mutagenic UV-radiation in shallower waters. Species which host photosynthetic symbionts on the other hand often build more transparent tests to provide enough solar irradiation to their symbionts (Hallock, P. et al., 1993).

Nevertheless, the reason why foraminifera are discussed in such detail is their high importance in paleooceanographic reconstruction. In this work benthic foraminifera were studied as a possible proxy carrier for reconstruction of OMZs. Two features allow foraminifera to preserve informations about the environmental conditions in their habitats. On the one hand the unique mechanism of biomineralisation in laminated rotaliid species provides information about the ambient seawater. These species precipitate their test calcite directly from vacuolized seawater (Erez, 2003) and thus the chemical composition of the test calcite reflects the chemical composition of the surrounding water in their habitats. Different element/Ca ratios are used as proxy for different parameters. Well established is the temperature reconstruction using the Mg/Ca ratio (Nürnberg et al., 1996; Rosenthal et al., 1997; Hastings et al., 1998; Lea et al., 1999; Elderfield and Ganssen, 2000; Lear et al., 2002). But other proxies are utilized, too like the U/Ca ratio for redox state, seawater chemistry and CO_3^{2-} tracing (Russel et al., 1994, 2004; Yu et al., 2008), Zn/Ca ratios for carbonate saturation (Marchitto et al., 2000) and Cd/Ca ratios as phosphate tracer (Boyle and Keigwin, 1985; Boyle, 1988; Bertram et al., 1995, Came et al., 2003). The V/Ca ratio has been suggested as a proxy for redox-conditions, too (Hastings et al., 1996a, b&c). On the other hand the high degree of adaptation of foraminifera facilitates information about the environmental conditions, too. Thus environmental conditions in a habitat could be reconstructed via the taxonomic composition of a assemblage or due to morphological adaptations. A review about proxies based on deep-sea benthic foraminiferal assemblage characteristics is given by Jorissen et al. (2007). An example for reconstruction based on morphological features is that benthic foraminifera with a high test porosity count as an indicator for oxygen depleted environments (Sen-Gupta and Machein-Castello, 1993).

1.6 Methodology for foraminifera analyses

Three major chemical analytical techniques have been used for this work: **E**lectron **m**icro**p**robe x-ray microanalysis (EMP), **S**econdary **i**on **m**ass **s**pectrometry (SIMS) and **q**uadrupole **i**nductively **c**oupled **p**lasma **m**ass **s**pectrometry (Q-ICP-MS). Each of these techniques has its own advantages and disadvantages regarding spatial resolution or required sample sizes, sensitivity and reproducibility. Both EMP and SIMS are using solid samples and are nearly destruction free, preserving the sample for further analyses. For EMP x-ray analysis a JEOL JXA 8200 located at the IFM-Geomar in Kiel was used. The EMP technique uses an electron which is accelerated to an energy between 1 and 50 kev carrying a beam current in the range of 10 pA to 1 µA. This beam is directed onto the surface of the sample

and causes it to emit secondary electrons and x-ray radiation of element characteristic wavelengths. The advantage of this technique is the high spatial resolution and the possibility to use the secondary and backscattered electrons to create scanning electron microscope (SEM) and backscattered electron (BSE) images (Kellner et al., 1998). The volume excited by the JEOL JXA 8200 is nominally about 1 cubic micron in minimum. Thus it is possible to generate element distribution maps of a sample surface in a spatial resolution of about 1 µm. The disadvantage is the relatively low sensitivity which usually allows to quantify elements just above concentrations of 100 ppm. A Cameca ims 6f magnetic sector ion microprobe at the Helmholtz Centre Potsdam was used for SIMS analyses. The SIMS technique is based on the bombardment of the sample surface with an ion beam in the energy range from 0.2-30 eV and the measurement of the emitted secondary ions of the sample material (Kellner et al., 1998). The spatial resolution of the Cameca ims 6f used in this work is with a minimal spot size of about 5 µm diameter worse than of the JEOL JXA 8200. But a much better detection limit allows to quantify elements down to concentrations of about 10 ppb. A connection of these two techniques allows identification of contaminiations on the sample surface via EMP elemental mapping followed by a quantitative analysis at areas of choice which are contamination free. The Q-ICP-MS analyses were performed on an Agilent 7500cx at the IFM-Geomar in Kiel. In Q-ICP-MS the sample is atomized and the atoms subsequently are subsequently ionized in a plasma and a quadrupole mass filter is used for separation of the ions. The plasma gas usually is argon. Due to the very good detection limits (0.5-5 ppt for several elements according to manufacturer) of the Agilent 7500cx it is possible to quantify elements in very low concentrations with a good precision. The problem is that the samples have to be dissolved prior analysis and sample volumes of about 100-200 µl are needed for a single analysis. For example about 40 specimens of the benthic foraminiferal species *Bolivina spissa* have to be dissolved to create enough solution for a single analysis which could not be repeated afterwards. This solution is already diluted to a Ca concentration of about 10 ppm. For solid state analytic techniques like SIMS or EMP only a single specimen is needed and the analyses can be repeated several times. Furthermore the concentrations in the solid material are much higher than in a diluted solution.

A main part in this work was the study of the PD in *B. spissa*. Thus the last part of the introduction (chapter 1.7) is a literature review about the understanding of pore-functionality in benthic foraminifera.

Chapter 1.7

THE FUNCTIONALITY OF PORES IN BENTHIC FORAMINIFERA AND BOTTOM WATER OXYGENATION

A Review

Nicolaas Glock[1,2], Joachim Schönfeld[2] and Jürgen Mallon[1,2]

[1]Sonderforschungsbereich 754, Christian-Albrechts-University Kiel, Climate-Biogeochemistry Interactions in the Tropical Ocean.

[2]Leibniz-Institute für Meereswissenschaften, IFM-GEOMAR, Wischhofstr. 1-3, 24148 Kiel, Germany.

Accepted in Altenbach, A.V., Bernhard, J.M. and Seckbach, J. (eds.), ANOXIA: Evidence for eukaryote survival and paleontological strategies, Springer.

Abstract

This chapter will give a brief review about the present understanding of pores in tests of benthic foraminifera. The interpretation of the pore-function changed through time and a couple of theories were proposed. The research about the functionality of pores recently became of new interest because it seems likely that they are involved in the respiration pathways of some benthic foraminifera. The fact that several benthic species are able to survive anoxia points out the importance for a better understanding of these respiration pathways and which adaptions differentiate these species from species which cannot survive in oxygen depleted habitats. Nitrate respiration seems to be widespread among foraminifera from oxygen depleted habitats and thus knowledge if and in how far the pores are involved in the process of denitrification would help to understand the process of denitrification in eukaryotic foraminiferal cells.

1.7.1 Introduction

Pores are developed in rotaliid calcareous foraminifera and are important morphological features. Their shape, size and density are diagnostic for discerning between several species (Lutze, 1986). But only few publications are discussing the function or the origin of these pores and whether they are or are not important for the survival of benthic foraminifera. With advances in the field of electron microscopy in the early 50´s researchers started to describe the microstructure of the pores and discovered that these pores are often covered by some sieve like microporous organic plates (Jahn, 1953; Arnold 1954a, b). Until the late 70´s other workers (Le Calvez, 1947; Angell 1967; Sliter, 1974; Berthold, 1976, Leutenegger, 1977) observed that the pores in many benthic foraminifera are covered by one or more organic layers but not all of them showed microperforations. Several terms have been given to these structures: “sieve plates”, “pore diaphragms”, “dark discs”, “pore plugs”, and “pore plates”. Only very few experiments have been done to analyse the function of pores and their permeability to dissolved substances into the cytoplasm. It was demonstrated that *Patellina corrugata* is able to take up neutral red dye through the pores (Berthold, 1976) and that *Amphistigina lobifera* takes up CO_2 in a similar way (Leutenegger and Hansen, 1979). Additionally some low-oxygen tolerant species show that their mitochondria, i.e. cell organelles involved in respiration, were more abundant near the pores than in other species from well oxygenated waters. This covariance implies an evolutionary linkage between pores and mitochondria (Leutenegger and Hansen, 1979; Bernhard et al., 2010). These observations

lead to the most widespread interpretation in the literature that the pores in benthic foraminifera promote the uptake of oxygen and the release of metabolic CO_2, the uptake of CO_2 for symbiont bearing foraminifera, the osmoregulation and the intake and excretion of dissolved substances in general. On the other hand it has been suggested that the pores of *Rosalina floridana* are purely an ornamental feature because of the lack of micropores in the pore plates and the thick inner organic lining between cytoplasm and test-walls which seals of the pores (Angell, 1967).

Another term of studies was the variability of morphological features like pore-size and pore-density among several benthic species. In the 60´s it has been found that *Bolivina spissa* from the Californian borderlands show a strong variation in the pore-free area of their test-surface among different water depths (Lutze, 1962). Homeomorphs of *Bolivina spissa* from different time periods at the Santa Barbara Basin, California, show a strong variability in pore-density and -shape (Harmann, 1964). A connection between pore-size and -density and the oxygen concentration of their habitats has been documented for *Hanzawaia nitidula* from the oxygen-minimum-zone (OMZ) in the gulf of Tehuantepec (Perez-Cruz and Machain-Castillo, 1990) and for laboratory cultures of *Ammonia beccarii* (Moodley and Hess, 1992). Furthermore, species with high test-porosity in general may serve as indicator for oxygen depleted environmental conditions (Sen-Gupta and Machain-Castillo, 1993; Kaiho, 1994). The same variation in the pore-density of *Bolivina spissa* among different water-depths that was described by Lutze (1962) was found again for *Bolivina spissa* from the oxygen minimum zone off Peru. But it appears that this variability in pore-density is closely related to the nitrate-concentration in the bottom-water (Glock et al., 2011). So it is speculated whether the pores in *Bolivina spissa* are involved in the mechanism of nitrate respiration. The ability to store nitrate inside the cells and to switch to nitrate respiration in times when no or to less oxygen is available has been recently documented for several benthic foraminiferal species (Risgaard-Petersen et al., 2006; Høgslund et al., 2008; Glud et al., 2009; Piña-Ochoa et al., 2010). The fact that a rod shaped microbial ectobiont of unknown identity and physiology was found to inhabit the outer part of the pore-void in *Bolivina pacifica* while mitochondria are clustered at the inner pore face (Bernhard et al. 2010) gives reason to speculate if and in how far these bacteria are involved into foraminiferal denitrification whether they are symbionts or parasites. The pores in amphisteginids and nummulites are quite obvious adapted for hosting algal symbionts (Hansen and Burchardt, 1977, Lee and Anderson, 1991): The inner surface of the test around the pores is excavated into cup-like pore-rims. The symbiotic diatoms are concentrated along the surfaces of the cytoplasm in cytoplasmic bulges which fit into the pore

rims. Beside all of these evidences the function of pores still remains conjectural and it is unclear in how far the pore-function varies among the different benthic foraminiferal species.

1.7.2 Materials and Methods

Two different data sources were used for this review. First, for the mayor part relevant publications related to the function of pores were compiled (Table 1.1). A few studies concerning the pores in planktonic foraminifera are also listed although they will not be discussed in the progress of this manuscript. Second, sampling material for the pictures in Fig.1 was recovered during Meteor Cruise M77/1. A detailed description of the sampling locations and sampling procedure could be found elsewhere (Glock et al., 2011). All specimens were mounted on aluminum stubs, sputter-coated with gold, and photographed with a CamScan-CS-44 scanning electron microscope (SEM) at the Christian-Albrecht-University in Kiel.

Table 1.1. Publications used as data source for this review.

Author and year	**Results of the study**
Doyle (1935)	Light microscopic observations of *Iridia diaphana* show that this species is able to move mitochondria through its pseudopodia.
Arnold (1954b)	Sieve like plates are covering the pores of several benthic foraminiferal species. These so called “sieve plates” or “pore plugs” contain a large number of micropores in a diameter range of 0.1-0.3 microns. These micropores might restrict the flow of smaller cytoplasmic elements like mitochondria into pore-pseudopodia.
Lutze (1962)	*Bolivina spissa* from the Californian Borderlands show a strong variation in the pore-free area of their test-surface among different water depths. For the explanation of this phenomenon a temperature dependence of different chemical processes is proposed.
Harman (1964)	*Bolivinidae* from the Santa Barbara Basin, California, show morphological variations in response to environmental factors like oxygenation. Additionally there are variations in recent and ancient homogenous sediments. Homeomorphs of *B. spissa* from different time periods show strong differences in pore-density and -shape.
Angell (1967)	The pores of *Rosalina floridana* are filled with organic “pore processes” which are anchored to the inner organic lining. These structures lack micropores and it is speculated that the pores in *R. floridana* are eliminated on purely morphological grounds.

Bé (1968)	Shell porosities of 22 planktonic foraminiferal species are relatively uniform for those co-occurring in same latitudinal belts. Because of this co-variation of porosity and temperature shell porosity in planktonic foraminifera is proposed as climatic index.
Sliter (1970)	Laboratory cultures of *Bolivina doniezi* show variations in pore-morphology and pore density in the clone culture compared to the natural populations.
Hansen (1972)	Freeze dried specimens of living *Amphistigina* show in addition to the apertural pseudopodia other pseudopodia closely connected with the pores.
Frerichs et al. (1972)	Pore density in *Globigerinoides sacculifer, Globorotalia tumida* and *Neogloboquadrina dutertrei* decreases directly with distance from the equator but *Globigerinella siphonifera* and *Globorotalia tumida*show no such relationship. The test porosity however decreases in all five species with distance from the equator. It is speculated that the test porosity is related to the water density, which in turn is related to temperature.
Hottinger and Dreher (1974)	Pores in tests of *Operculina ammonoides* and *Heterostegina depressa* are not covered by pore-plates. The inner organic lining is thickened at pore-rims and thins out over the pore holes while the plasma membrane is differentiated by coarse granules below the pore holes. These observations and the position of the symbionts in the chamber plasma point to a physiological relationship between symbionts and pores.
Sliter (1974)	In contrast to many other foraminiferal taxa *Bolivinitidae* and *Caucasinidae* appear to construct their tests in a monolamellar concept. The studied *Bolivinitidae* show double pore-membranes between consecutive calcitic lamellae.
Berthold (1976)	Experiments on *Patellina corrugata* show that neutral red from ambient water is actively pumped into the cytoplasm through test pores even when the aperture is closed. It is speculated that the pore function is related to osmoregulation, gas exchange or the intake and excretion of dissolved substances.
Hansen and Buchardt (1977)	The inner surface of the test around the pores in amphisteginids and nummulites is excavated into cup-like pore-rims. The symbiotic diatoms are concentrated along the surfaces of the cytoplasm in cytoplasmic bulges which fit into the pore rims.
Leutenegger and Hansen (1979)	Mitochondria are clustered behind the pores of foraminiferal species from low-oxygen habitats. In several foraminiferal species from more oxygenated habitats mitochondria are more uniformly distributed throughout the cytoplasm. Additionally the inner organic lining is disrupted behind the pores of several species from oxygen-depleted habitats. It appears that the pores are related to gas exchange. This includes an uptake of O_2 and an elimination of CO_2 as well as an uptake of CO_2 for photosynthetic symbiont bearing foraminifera like *Amphistigina lobifera* during day time.
Bé et al. (1980)	The mechanism of the formation of pores and pore-plates in planktonic foraminifera is described. Pores

	are formed due to resorption of already precipitated material. There might be differences in pore-formation and function between spinose and non-spinose species.
Bijma et al. (1990)	Laboratory cultures of *Globigerinoides sacculifer*, *Globigerinoides ruber*, *Globigerinoides siphonifera* and *Orbulina universa* show that changes in shell porosity are correlated with changes in salinity and temperature. The highest porosities are attained at higher temperatures and lower salinities.
Perez-Cruz and Machain-Castillo (1990)	*Hanzawaia nitidula* from the oxygen-minimum zone (OMZ) in the gulf of Tehuantepec show more and larger pores than specimens from oxygenated waters.
Moodley and Hess (1992)	Laboratory cultures of *Ammonia beccarii* show an increase in pore-size under low-oxygen-conditions.
Sen Gupta and Machain-Castillo (1993), Kaiho (1994)	Benthic foraminiferal species with high test-porosity are postulated as an indicator for oxygen depleted environmental conditions.
Risgaard-Petersen (2006)	First evidences that foraminiferal species from oxygen depleted habitats switch to nitrate respiration in times when no oxygen is available are discovered.
Høgslund (2008)	Denitrification rates for benthic foraminifera from the Chilean OMZ are measured.
Allen et al. (2008)	Laboratory cultures of the planktic foraminifer *Orbulina universa* show a relationship of pore-density and pore-size to pH but no dependence of temperature.
Glud et al. (2009)	The contribution of foraminiferal denitrification to the nitrogen cycling at Sagami Bay, Japan, is quantified. The production of N_2 was attributed to foraminiferal denitrification in a total amount of 4%. Additionally the nitrate storage in foraminiferal cells was measured for several species. It represented 80% of the total benthic nitrate pool.
Piña-Ochoa et al.(2010)	The nitrate storage among many benthic foraminifera from the Peruvian OMZ was measured.
Bernhard et al. (2010)	The outer part of the pore void of *Bolivina pacifica* in this study is inhabited by a rod-shaped microbial ectobiont of unknown identity and physiology. Again a clustering of mitochondria behind the pores is observed.
Glock et al. (2011)	The pore-density in tests of *Bolivina spissa* from the Peruvian OMZ shows strong locational variations and a relationship to several environmental factors like oxygen- or nitrate concentrations in the bottom-waters. Because of the strong relationship to the nitrate-concentrations in the bottom-waters it gives a reason to speculate if the pores are related to nitrate respiration. Either for the intracellular nitrate uptake or to act as “valve” for the release of waste products like N_2.

1.7.3. The Pore Plates

The pores of many benthic foraminifera are sealed by one or more organic layers (Le Calvez, 1947; Jahn, 1953; Arnold 1954a, b; Angell 1967; Sliter, 1974; Berthold, 1976, Leutenegger, 1977) while some species like *Operculina ammonoides* and *Heterostegina depressa* lack pore-plates (Hottinger and Dreher, 1974). In some species these pore plates are additionally perforated by micropores with a diameter in a range of 0.05 to 0.3 μm depending on the species. These micropores have been described in some unknown nonionid and camerinid species (Jahn, 1953), in *Discorinopsis aguayoi* (Arnold, 1954a) and in *Patellina corrugata* (Berthold, 1976). The pores of *Rosalina floridana* are filled with organic "pore processes" anchored to an inner organic lining and are covered with an organic membrane (Angell, 1967). All of these structures in *Rosalina* lack micropores. Specimens of *Bolivina* and *Coryphostoma* construct their tests in a monolamelar concept and show double pore-membranes between consecutive calcitic lamellae (Sliter, 1974). The surface membrane seems to cover the ultimate chamber completely while a progressive perforation in the pores of successively older chambers could be observed. This results in that the pores of the oldest chambers are open to the surface. If the surface-membrane was intact micropores could be observed only occasionally. These micropores became larger and more common in the penultimate and towards the older chambers. Similar structures exist in *Bolivina spissa*. Most of the pores in the ultimate chamber are covered with several layers of pore plates. The slits in some of the pore-plates are propabely deteriorations caused by the drying process of the samples or by the electron beam of the REM (Fig 1.7.1a and b). In some specimens these pore plates are preserved only in the ultimate chamber while others show well preserved pore plates among several other chambers (Fig 1.7.1c). The pores in the earliest chambers near the proloculus are open to the surface (Fig 1.7.1d).

It was speculated wheather the micropores in some pore-plates could serve as outlet for pore-pseudopodia and selectively control the flow of cytoplasmic elements into and back from the pseudopodia (Arnold, 1954b). Because of the small size of the micropores only very minute cell organelles would be able to pass the pore plates. At least mitochondria are able to move through the cytoplasm and flow into pseudopodia of *Iridia diaphana* (Doyle, 1935). Indeed some thin, thread like structures emerging from pore plates were observed in freeze-dried specimens of living *Amphistigina* which have been interpreted as pore pseudopodia (Hansen, 1972). This is not undisputed since it was discussed that the threadlike extrusions have more similarity to the hyphae of fungi than to granuloreticulose pseudopods (Berthold, 1976).

Observations with the light-microscope on *Patellina* first lead to the conclusion that pores could serve as an outlet for pseudopodia as does the aperture (Myers, 1935). In contrary later investigations found that it is not possible to show a correlation between pores and pseudopods in *Patellina* (Berthold, 1971). Because most of the pores in the tests of the Bolivinitidae and Caucasinidae where sealed completely by a complex of imperforated pore plates Sliter (1974) came to the conclusion that a free exchange of cytoplasm to the test surface is precluded through most of the pores. In summary it could not be proven to date if benthic species indeed could move pseudopodia through some pores or not. But at least for some taxa (*Rosalina*, *Patellina*, Bolivinitidae and Caucasinidae) due to the lack or the very minute size of micropores such pseudopodial movements are not very probable (Angell, 1967, Sliter, 1974, Berthold, 1976).

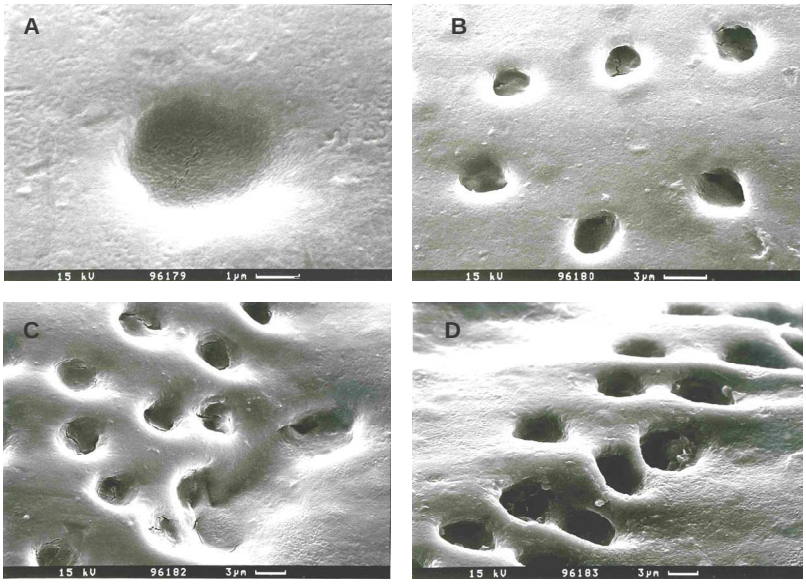

Figure 1.7.1 SEM pictures with close ups of the pores of one specimen of *Bolivina spissa* (oversight shown in Fig.2c). **A** A Pore of the ultimate chamber with a well preserved pore plate. **B** Several pores in the ultimate chamber covered by several layers of membranes (pore plates). Slits in some pore-plates are propabely deteriorations caused by drying process of samples. **C** The pore-plates in this specimen are preserved until the middle chamber. **D** Pores near the proloculus are open to the surface.

1.7.4 Permeability of Pores and the Previous Understanding of Pore-Function

Only few papers describe experiments to test the permeability of pores of benthic foraminifera to dissolved substances in the ambient waters. *Patellina corrugata* could actively pump neutral red dye from surrounding water into the cell through the pores while the aperture was

closed (Berthold, 1976). These results inferred that "the function of pores probably lies in the field of osmoregulation, gas exchange, or the intake and excretion of dissolved organic substances". The pores probably had a special importance during the reproductive phase of a foraminifer because the protoplasm is isolated from the medium and the pseudopodia cannot be extruded through the aperture. Another study on several benthic species from oxygen depleted habitats showed that mitochondria are clustered behind the pores and the inner organic lining is interrupted behind the pores (Leutenegger and Hansen, 1979). Additionally, the same study showed that the symbiont bearing *Amphistigina lobifera* takes up C^{14} labeled CO_2 through the pores while the aperture is closed. Hottinger and Dreher (1974) showed that *Operculina ammonoides* and *Heterostegina depressa* lack pore-plates and the inner organic lining thins out over the pore holes while the plasma membrane is differentiated by coarse granules below the pore holes. These observations and the position of the symbionts in the chamber plasma pointed to a physiological relationship between symbionts and pores. So it seemed obvious that the pores are related to gas exchange. But at least one publication mentions *Rosalina floridana*, where the pores might be built purely as ornamentation or just to provide organic continuity to the test exterior (Angell, 1967). These conclusions were drawn because the pores of *R. floridana* are filled by organic "pore-processes" anchored to the inner-organic-lining and these structures lack micropores. However, no experiments on the permeability of pores in *Rosalina* were performed.

The most widespread opinion today is that the pores in benthic foraminifera are related to the uptake of O_2 and the release of metabolic CO_2. These interpretations were based on observations that foraminiferal species from low-oxygen habitats show a high test porosity. These species were, in turn, used as an indicator for oxygen depleted environmental conditions (Sen-Gupta and Machain-Castillo, 1993; Kaiho, 1994). Furthermore some species show a response in their pore-size and pore–density to variations in oxygen supply. For instance, *Hanzawaia nitidula* from the oxygen minimum zone (OMZ) in the Gulf of Tehuantepec show more and larger pores than specimens from oxygenated waters (Perez-Cruz and Machain-Castillo, 1990). Laboratory cultures of *Ammonia beccarii* show an increase in pore-size under low-oxygen-conditions (Moodley and Hess, 1992). These experimental results were corroborated by field observations from Flensburg and Kiel Fjords. *Ammonia beccarii* showed large pores in Flensburg Fjord, where seasonal anoxia occurred (Nikulina and Dullo, 2008; Polovodova et. al, 2009), and small pores in Kiel Fjord which experiences only a moderate oxygen dropdown during summer (Nikulina et al., 2008). These observations denote the potential of using the pore size and pore-density as a proxy for Recent and past

oxygen variations. A recent study shows a variability in the pore-density of *Bolivina spissa* from the Peruvian OMZ which might be related to oxygen supply (Glock et al., 2011). But this variability of pore-density in *B. spissa* might be more related to the variations in nitrate availability. Three specimens of *B. spissa* from different oxygenated locations are shown in Fig. 1.7.2. At least some foraminiferal species are able to move their mitochondria into their pseudopodia (Doyle, 1935). Because the pseudopodia could extend at to ten times the test diameter of a foraminifer (Travis and Bowser, 1991) it is possible that foraminifera which inhabit an environment with a steep oxygen gradient could use mitochondrial activity in their extended pseudopodia to maintain oxygen supply even when their tests are located in anoxic sediments (Bernhard and Sen Gupta, 2003). In this case an uptake of oxygen through test pores might not be very convincing. But it might be that different species follow different mechanisms of oxygen uptake.

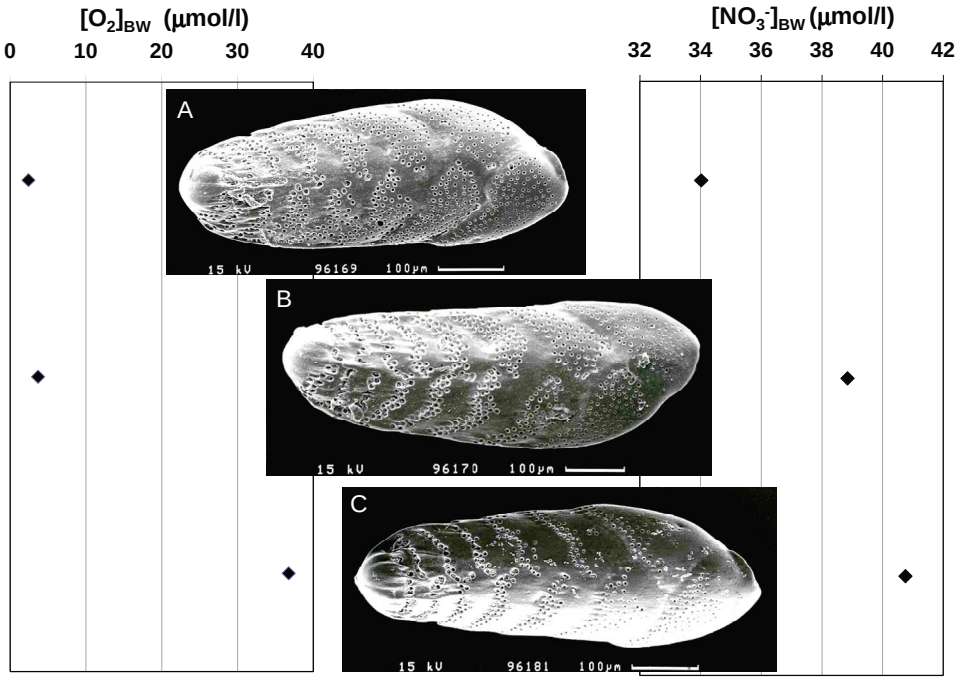

Figure 1.7.2. SEM Pictures of three specimens of *Bolivina spissa* from different locations. The diagram on the right shows the different bottom-water nitrate concentrations and the diagram on the left the bottom-water oxygen concentrations from the different locations. A quantification of these relationships is presented by Glock et. al. (2011). (**A** M77/1-445/MUC-21 (465 m) **B** M77/1-487/MUC-38 (579 m) **C** M77/1-445/MUC-15 (928 m water depth)).

1.7.5. Evidence of Pore Involvement in Nitrate-Respiration Pathways

Recently it has been shown that some benthic species from oxygen depleted habitats respire nitrate via denitrification (Risgaard-Petersen et. al., 2006). This fact in combination with new results which show a strong relationship of the pore-density in *Bolivina spissa* from the Peruvian continental margin to the bottom-water nitrate concentrations (Glock et al., 2011) gives a reason to speculate if and how far the pores might be related to the nitrate-respiration pathways in some benthic foraminifera. If the pores of *B. spissa* are indeed related to the intracellular nitrate uptake an increase of pore-density would optimize their availabilities for nitrate uptake when nitrate is depleted. This would result in a advantage in the competition of nitrate uptake against other foraminiferal and prokaryotic species. These results might open a first window to carry modern knowledge on foraminiferal denitrification into a fossil record and earth history. A study on the nitrogen cycle at Sagamy Bay, Japan, which showed that *Bolivina spissa* have significant intracellular nitrate enrichment (Glud et. al., 2009) supports this assumption. At Sagami Bay intracellular nitrate storage in foraminifera represented about 80 % of the total benthic nitrate-pool. The diagram on the right in Fig. 1.7.2 shows the bottom-water nitrate concentrations in the different habitats of the three specimens of *B. spissa*.

The denitrification process in benthic foraminifera has not been attributed to a specific cell organelle yet (Høgslund et al., 2008). If it is assumed that the pores are directly related to intracellular nitrate-uptake the fact that mitochondria tend to cluster behind the pore plugs, what indeed has been observed from a *Bolivina* at low-oxygen conditions, might imply that mitochondria may also be involved in the mechanism of foraminiferal denitrification. Indeed earlier studies showed that mitochondria are involved in nitrate respiration of the primitive eukaryote *Loxodes* (Finlay et al., 1983). In particular the number of mitochondria became significantly enhanced when *Loxodes* switched from oxygen to nitrate-respiration. The recent observation of microbial ectobionts of unknown identity and physiology inhabiting the pore void of *Bolivina pacifica* (Bernhard et al. 2010) provoke speculations if such ectobionts exist in the pore void of *Bolivina spissa* as well and are indeed denitrifiers. Another possibility would be that these ectobionts act more as parasites. Some Bolivinidae seem to produce N_2O as a product of denitrification instead of N_2 (Piña-Ochoa et al., 2010). Hence it might be that these bacteria cluster in the pore-void of some foraminifera for the uptake of N_2O which is

released as a waste product through the pores. In a reaction, catalyzed by the protein nitrous oxide reductase, N_2O is reduced to N_2 (Zumft, 1997; Riester, Zumft and Kroneck, 1989). The reaction

$$N_2O + 2e^- + 2H^+ \rightarrow N_2 + H_2O \quad (1)$$

is highly exergonic ($\Delta G^{\circ\prime}$ = 340 kJ/mol) and thus a good energy source although N_2O is very inert at room temperature and thus reaction (1) needs an efficient catalyst to occur (Haltia et al. 2003). Some rod shaped bacteria like *Escherichia coli* or *Pseudomonas stutzeri* are known to have the ability to reduce N_2O to N_2 (Kaldorf et al., 1993; Lalucat et al., 2006).

A study of Lutze (1962) on *Bolivina spissa* from the Californian borderland shows that the pore-free area increases with water-depth. This was assumed to reflect decreasing water-temperatures. But later it was shown by comparison to nitrate data from the same study area (Boyer et al., 2009) that the variability in the pore-free area also reflects most probably the nitrate distribution in the water column (Glock et al., 2011). Nitrate is depleted at shallower water-depth due to enhanced primary production on the ocean´s surface. So the habitats of the analysed specimens from shallower water-depths most probably were more nitrate depleted than those from the deeper waters.

1.7.6. Conclusions

Although the pores in tests of benthic foraminifera are an important morphological feature which even is used to distinguish several species, the understanding of the pore-function is very fragmentary. This might be due to the fact that the pore-function differs between the species. Symbiont bearing foraminifera like *Amphistigina lobifera* seem to take up CO_2 through the pores during day time for photosynthesis, while some species from oxygen-depleted habitats probably take up oxygen through the pores (Leutenegger and Hansen, 1979). But also the uptake of dissolved organic substances is possible as shown for *Patellina corrugata* (Berthold, 1976). Recent findings even hint that at least one species, *Bolivina spissa*, takes up nitrate for nitrate respiration through the pores or uses these to release denitrification products like N_2O or N_2 and that they seem to adapt their pore-densities to survive in extreme habitats (Glock et al., 2011). But for a lot of species the pore-function still remains conjectural and it is even speculated that some species just build the pores on purely morphological grounds or just to provide organic continuity to the test exterior (Angell, 1967). A better understanding of the pore-function would help to understand which metabolic adaptations help foraminifera to survive extreme (even anoxic) habitats, because species from

oxygen depleted environments generally show a high porosity. Furthermore it should be tested in how far pore-densities in some benthic species might be used as proxy to reconstruct environmental factors like the oxygen- or nitrate-concentrations.

1.7.7. Faunal reference list:

- *Ammonia beccarii* (Linné) = *Nautilus beccarii* Linnaeus, 1758, p. 710, pl. 1, fig. 1.
- *Amphistegina lobifera* (Larsen), 1976, p.11, pl. 3, figs. 1-5.
- *Bolivina doniezi* (Cushman & Wickenden), 1929, p. 9, pl. 4, fig. 3a-b.
- *Bolivina pacifica* (Cushman & McCulloch) = *Bolivina acerosa* Cushman var. *pacifica* Cushman & McCulloch,1942, p.185, pl. 21, figs. 2, 3.
- *Bolivina spissa* (Cushman) = *Bolivina subadvena* Cushman var. *spissa*, Cushman 1926, p. 45, pl. 6, fig. 8a-b.
- *Discorinopsis aguayoi* (Bermúdez), 1935, p. 204, pl.15, figs. 10-14.
- *Globigerinella siphonifera* (d'Orbigny) = *Globigerina siphonifera* d'Orbigny, 1839, pl. 4, figs. 15-18.
- *Globigerinoides ruber* (d'Orbigny), 1839, p. 82, pl. 4, figs. 12-14.
- *Globigerinoides sacculifer* (Brady), 1877 [type fig. not given], Brady, 1884: p. 604, pl. pl. 80, figs. 11-17.
- *Globorotalia tumida* (Brady) = *Pulvinulina menardii* (d'Orbigny) var. *tumida* Brady, 1877 [type fig. not given], Brady, 1884 pl. 103, figs. 4-6.
- *Hanzawaia nitidula* (Bandy) = *Cibicidina basiloba* Cushman var. *nitidula* Bandy, 1953, p. 178, pl. 22, figs. 3a-c.
- *Heterostegina depressa* (d'Orbigny), 1826, p. 305, pl. 17, figs. 5-7.
- *Iridia diaphana* (Heron-Allen & Earland), 1914, p.371, pl. 36.
- *Neogloboquadrina dutertrei* (d'Orbigny) = *Globoquadrina dutertrei* d'Orbigny, 1839, pl. 4, figs. 19-21.
- *Operculina ammonoides* (Gronovius) = *Nautilus ammonoides* Gronovius, 1781, p. 282, pl. 19, figs. 5, 6.
- *Orbulina universa* (d'Orbigny), 1839, p. 3, pl. 1, fig. 1.
- *Patellina corrugata* (Williamson), 1858, p. 46, pl. 3, figs. 86-89, 89a.
- *Rosalina floridana* (Cushman) = *Discorbis floridana* Cushman, 1922, p. 39, pl. 5, figs. 11, 12.

1.7.8. Acknowledgments

We thank Anton Eisenhauer for helpful general support and the providing of the Ph.D. position of the first author. Volker Liebetrau supported this work with helpful general discussions and organisation. Support in the operation of the SEM at the Christian Albrecht University in Kiel came by Ute Schuldt. The scientific party on R/V METEOR cruise M77 is acknowledged for their general support and advice in multicorer operation and sampling. The "Deutsche Forschungsgemeinschaft, (DFG)" provided funding through SFB 754 "Climate-Biogeochemistry Interactions in the Tropical Ocean".

Chapter 2

Redox sensitive elements in foraminifera from the Peruvian oxygen minimum zone

In review in Biogeosciences

Abstract

Redox sensitive element ratios (Mn/Ca, Fe/Ca) were determined in tests of benthic foraminifera from the Peruvian oxygen minimum zone (OMZ) to test their potential as a proxy for redox conditions. Prior to the determination of the element/Ca ratios element distributions in tests of the shallow infaunal species *Uvigerina peregrina* and *Bolivina spissa* have been mapped with an electron microprobe (EMP). A Fe rich phase which is also enriched in Al, Si, P and S has been found at the inner part of the test walls of *U. peregrina*. This phase most probably represents the inner organic lining. The element distributions of a specimen treated with an oxidative cleaning procedure show the absence of this phase. EMP maps of *B. spissa* show similar success of the oxidative cleaning. Neither in *B. spissa* nor in *U. peregrina* any hints for diagenetic coatings have been found. Mn/Ca and Fe/Ca ratios of single specimens of *B. spissa* from different locations have been determined by secondary ion mass spectrometry (SIMS). Bulk analyses with ICP-MS of samples where enough specimens were available were compared to the SIMS data. The difference between SIMS analyses on single specimens and ICP-MS bulk analyses from the same sampling sites was 14.0 - 134.8 μmol/mol for the Fe/Ca and 1.68 μmol/mol for the Mn/Ca ratios. This accounts to 3 - 29% for the Fe/Ca and 21.5 % for the Mn/Ca ratios of the overall variability between the samples of the different sampling sites. The Mn/Ca ratios were generally relatively low (2.21 – 9.93 μmol/mol) but in the same magnitude as in the pore waters (1.37-6.67 μmol/mol). Comparison with pore water data showed that Mn/Ca in the foraminiferal calcite is proportional to the Mn/Ca ratio in the top cm of the pore water. The lowest Fe/Ca ratio in tests of *B. spissa* (87.0 μmol/mol) has been found at a sampling site which was strongly depleted in oxygen and showed a high, sharp iron peak in the top interval of the pore water. This hints that the specimens already were dead before the Fe flux started and the sampling site just recently turned anoxic due to fluctuations of the lower boundary of the OMZ where the sampling site is located (465 m water depth).

2.1 Introduction

Element ratios in foraminiferal calcite have been widely used to reconstruct chemical or physical properties in the ancient ocean. Due to their mechanism of biomineralisation the calcitic tests of laminated rotaliid foraminifera are directly precipitated from vacuolized seawater (Erez, 2003). The chemical test composition thus directly reflects the chemical and physical conditions in the ambient seawater. Different element/Ca ratios are used as proxy for different parameters. Well established is the temperature reconstruction using the Mg/Ca ratio

(Nürnberg et al., 1996; Rosenthal et al., 1997; Hastings et al., 1998; Lea et al., 1999; Elderfield and Ganssen, 2000; Lear et al., 2002). But other proxies are utilized, too like the U/Ca ratio for redox state, seawater chemistry and CO_3^{2-} tracing (Russel et al., 1994, 2004; Yu et al., 2008), Zn/Ca ratios for carbonate saturation (Marchitto et al., 2000) and Cd/Ca ratios as phosphate tracer (Boyle and Keigwin, 1985; Boyle, 1988; Bertram et al., 1995, Came et al., 2003). Recently a lot attention turned to the analyses of boron isotopes in foraminiferal calcite for pH reconstruction via $\delta^{11}B$ (Spivack et al., 1993; Sanyal et al., 1995; Palmer et al. 1998; Pearson and Palmer, 2000; Sanyal et al., 2001; Palmer and Pearson, 2003; Ni et al., 2007; Foster, 2008; Kasemann et al., 2009; Rollion-Bard and Erez, 2010; Rae et al., 2011). The V/Ca ratio has been suggested as a proxy for redox-conditions (Hastings et al., 1996a, b&c) while the Ba/Ca ratio has been shown to occur in direct proportion to seawater concentration (Lea and Boyle, 1991; Lea and Spero, 1992, 1994). Ba/Ca ratios have already been used to trace deglacial meltwater (Hall and Chan, 2004a) and deep and intermediate water mass circulation (Lea and Boyle, 1989; 1990a&b; Martin and Lea, 1998; Hall and Chan; 2004b).

Diagenetic coatings often contaminate the test calcite of fossile foraminifera. These coatings strongly influence the measured element/Ca ratios and thus sometimes rigorous cleaning techniques have to be deployed. About three decades ago a procedure to remove these contaminants by rinsing crushed tests with distilled water/methanol to remove adhesive clays and removal of metal oxide coatings by reductive cleaning has been developed (Boyle, 1981). Later a procedure was developed to get rid of organic contaminations by using an additional oxidative cleaning step (Boyle and Keigwin, 1985). The influence of the different cleaning steps on the Mg/Ca ratios has been tested and it has been shown that the clay removal step is the most important one while the reductive cleaning step produces a downset of about 10-15% on the Mg/Ca ratios (Barker et al., 2003). Different cleaning techniques and their influence on eight elemental/Ca ratios have also been investigated by Yu et al. (2007). Also there have been experiments of cleaning by using a flow-through system with automated chromatographic equipment (Haley and Klinkhammer, 2002; Haley et al., 2005). In the system contaminant phases are chemically removed from the tests and the cleaned calcite is then dissolved in a stream of weak acid. The advantage of this method is that the different fractions could be collected separately and the measurements of contamination tracers like Fe could show in which fractions only clean dissolved foraminiferal calcite is collected. Furthermore the flow-through system could minimize the problem of readsorption of contaminant rare-earth-elements. As diagenetic contaminant phases Mn carbonates have been

identified as well as Mn and Fe rich oxyhydroxides with laser-ablation-ICP-MS (LA-ICP-MS) and electron microprobe (EMP) mapping (Pena et al., 2005; 2008). Mn/Ca and Fe/Ca ratios therefore have often been used as tracer for diagenetic overprint of the samples. Nevertheless the researcher disagree what is considered an acceptable level of test Mn/Ca from 50 μmol/mol to > 150 μmol/mol (Boyle, 1983; Boyle and Keigwin, 1985; 1986; Delaney, 1990; Ohkouchi et al., 1994, Lea, 2003). But there exist approaches to use Mn/Ca ratios during the obvious absence of diagenetic coatings as a proxy for redox-conditions, too. The Mn/Ca ratio in *Hoeglundina elegans* has been used to trace suboxic conditions during sapropel formation (Fhlaitheartha et al., 2010). Also living stained specimens of *H. Elegans* from the oxygen minimum zone at the Arabian Sea show an increase of the Mn/Ca ratio at the lower boundary of the oxygen minimum zone (Reichart et al., 2003). Culture experiments on *Ammonia tepida* showed that Mn is incorporated into the test calcite in proportion to the concentration in the ambient water (Munsel et al., 2010)

Several analytical techniques have been employed for analyses of element/Ca ratios or isotope systems in foraminiferal calcite. Techniques for multi-element analyses using only small sample volumes have been developed on sector field ICP-MS (Marchitto, 2006) and quadrupole ICP-MS (Yu et al., 2005; Harding et al., 2006). But also microanalytic methods have been deployed. The advantage of the EMP is that single foraminiferal tests can be analysed destruction free after preparation of highly polished sections. This is an important prerequisite for direct comparison with other low trace methods like secondary ion mass-spectrometry (SIMS). Elemental EMP mappings and spot analyses of the test calcite could help to identify contaminant coatings and to analyse the distributions of trace elements inside the foraminiferal calcite for a better understanding for biomineralisation and improvement of the understanding of trace elements as paleoenvironmental proxies (Nürnberg, 1995; Nürnberg et al., 1996; Eggins et al., 2003; 2004; Sadekov, 2005; Toyofoko and Kitazato, 2005; Pena et al., 2008). Also laser ablation techniques on single foraminifera have been used in the recent past (Wu and Hillaire-Marcel, 1995; Hathorne et al., 2003; Reichart et al., 2003; Pena, 2005; Munsel et al., 2010). Another valuable tool for foraminiferal microanalyses is secondary ion mass spectrometry (SIMS). Almost destruction free in the same way as the EMP, SIMS has been used to produce element mappings and determine element/Ca ratios in foraminiferal calcite (Allison and Austin, 2003; Sano et al., 2005; Bice et al., 2005; Kunioka et al. 2006) as well as analyses of $\delta^{11}B$ in single foraminifera (Kasemann et al., 2008; Rollion-Bard and Erez, 2009) and the determination of intratest variability of $\delta^{18}O$ (Rollion-Bard et al., 2008). Even much less distributed but powerful techniques like particle induced x-

ray emission (Gehlen et al., 2004) or μ-synchroton XRF (Munsel et al., 2010) have been used. All these microanalytical techniques have in common that analyses could be deployed even on single foraminiferal specimens while for the wet chemical analyses typically bulk samples of 20-50 specimens are needed which make these methods favourable when there is no sufficient amount of specimens available, or an identification of heterogeneities and a better mechanistic understanding of element incorporation and distribution is required.

In this study the shallow infaunal species *Bolivina spissa* is used for the determination of Fe/Ca and Mn/Ca ratios and the comparison of these ratios to the available pore water data. Studies on the pore density in *Bolivina spissa* showed a morphological adaptation of the test to different environmental conditions (Glock et al., 2011) which makes this species favourable for elemental analyses, too. Because of the relative widespread distribution among the Peruvian OMZ *Bolivina spissa* was available from habitats with a wide range of redox-chemical conditions although at some sampling sites only a small amount of specimens was available. SIMS was used because of the limited availability and compared to ICP-MS data where enough specimens for bulk analysis where available.

2.2 Material and Methods

2.2.1 Sampling procedure

Six short (12-26 cm) sediment cores from the Peruvian OMZ were considered for the present study (Table 2.1). The cores were recovered by using multicore technology during R.V. *Meteor* cruise M77/1 in October and November 2008. Within a couple of minutes after the multicorer came on deck, one tube was chosen from the array, and brought to a laboratory with a constant room temperature of 4°C. Supernatant water of the core was carefully removed. Then the core was gently pushed out of the multicorer tube and cut into 10-mm-thick slices for benthic foraminiferal analysis. The samples were transferred to Whirl-Pak™ plastic bags and transported at a temperature of 4°C.

Table 2.1. Sampling sites. $[O_2]_{BW}$ taken from Glock et al. (2011).

Site	Longitude (W)	Latitude (S)	Water depth (m)	$[O_2]_{BW}$ (μmol/L)
M77/1-421/MUC-13	75°34.82'	15°11.38'	519	-
M77/1-455/MUC-21	78°19.23'	11°00.00'	465	2.42
M77/1-487/MUC-39	78°23.17'	11°00.00'	579	3.7
M77/1-565/MUC-60	78°21.40'	11°08.00'	640	8.17
M77/1-604/MUC-74	78°22.42'	11°17.96'	878	34.23
M77/1-445/MUC-15	78°30.02'	11°00.00'	928	36.77

One core was completely frozen, and later sliced and subsampled at IFM-GEOMAR, Kiel. The samples from these five cores were used to collect the foraminiferal specimens for the analysis.

2.2.2 Foraminiferal studies

The surface sediment samples corresponding to the top centimeter were washed over a 63-µm mesh sieve. The residues were collected in ethanol to prevent corrosion and dried at 50°C. They were further subdivided into the grain-size fractions of 63–125, 125–250, 250–315, 315–355, 355–400, and >400 µm. Specimens of the shallow infaunal species *Bolivina spissa* for ICP-MS and SIMS analysis were picked from the 125–250 µm fraction, specimens of *Uvigerina peregrina* for the EMP analyses were picked from the 355-400 µm fraction.

2.2.3 Cleaning methods

For each ICP-MS analysis a bulk sample of 40 specimens of *B. spissa* was used. The tests were gently crushed between two glass plates. The test fragments were transferred into PE vials and rinsed three times with 18.2 MΩ millipore H_2O (from Elga™ PURELAB Ultra). After each rinsing step the vials were put into a supersonic bath for 20 seconds. Afterwards the vials were rinsed three times with methanol and put into the supersonic bath for 1 minute after each rinsing step. The vials were rinsed again two times with 18.2 MΩ millipore H_2O to remove residual methanol. An oxidative reagent was freshly mixed by adding 100 µl 30% H_2O_2 to 10 ml of a 0.1M NaOH solution. Subsequently 350 µl of this reagent were added to each vial. The vials were put into a waterbath at 92°C for 20 minutes. After another 20 seconds in the supersonic bath the vials were rinsed two times with 18.2 MΩ millipore H_2O to remove residues of the oxidative reagent. The test fragments were transferred into clean vials with a pipette. Into each vial 250 µl 0.001M HNO_3 were added. The vials were put into the supersonic bath for 20 seconds. The extremely low acidic solution was removed and the vials were rinsed three times with 18.2 MΩ millipore H_2O. The samples were dissolved in 300 µl 0.075M HNO_3, centrifuged and transferred into clean vials. Due to the risk of elevated Mn blanks the vials were replaced by Teflon beakers for Mn analyses (except for the cleaning step with 0.001M HNO_3, the sample dissolution and the centrifugation). The cleaning procedure for the microanalyses was in general the same with a few exceptions. The specimens were not crushed and one vial was used for one single specimen. The first three rinsing steps with 18.2 MΩ millipore H_2O were skipped because specimens often lifted to the surface and got lost during the rinsing steps. The specimens were not transferred into a clean vial after the

oxidative cleaning step and were not dissolved. After the last cleaning step the specimens were individual collected over a 125 µm mesh stainless steel sieve.

2.2.4 Microdrilling of the OKA calcite grain

Preparation of a matrix matching standard for direct comparison and established normalization of high resolution methods and ICP-MS analyses. A square of 400 µm edge length was drilled 200 µm deep into a calcite crystal from the OKA carbonatite complex (for which Mg/Ca and Sr/Ca ratios are reported in Gaetani and Cohen, 2006) with a micromill by New Wave Research™. The gouged out powder was collected in a Teflon beaker and dissolved in 2% HNO_3. The OKA was used in this study as reference standard for SIMS after Mn/Ca and Fe/Ca ratios were determined by ICP-MS.

2.2.5 Preparation of crosssections for SIMS and EMP analyses

The crosssection of the *U. peregrina* specimen shown in fig. 2.1 was prepared at the Alfred-Wegener-Institute Bremerhaven. The specimen was embedded under vacuum into Araldite(TM) epoxy resin inside a stainless steel chamber. Afterwards the chamber was set under pressure to collapse air inclusions inside the resin and the resin was hardened at 60°C. The resin was grinded down with alumo-silica grinding paper until the centre of the specimen laid open. Afterwards the surface was polished with different grain sizes of alumo-silica and diamond paste down to 1 µm grain size. After each polishing step the surface was cleaned in a supersonic bath for a few seconds.

All other cross-sections were prepared at the IFM-Geomar in Kiel. The *U. peregrina* specimens shown in fig. 2.2 and 2.3 were not vacuum embedded. They were embedded into epoxy resin. Afterwards they were grinded down by hand on alumu-silica grinding paper till the chambers were opened. Because the chambers were not filled with resin small drops of resin were used to fill the inner part of the chambers. The surface was polished with diamond paste of 5 µm grain size followed by alumo-silica paste of 1 µm grain size by hand on a self-rotating polishing plate. After each polishing step the surface was cleaned in a supersonic bath for a few seconds. All other specimens including all specimens of *Bolivina spissa* were embedded under vacuum into Araldite(TM) epoxy resin using the CitoVac(TM) vacuum embedding system by Struehrs(TM). The resin was grinded down with alumo-silica grinding paper with the Tegra-Pol-21 system by Struehrs(TM) until the centre of the specimen laid open. Afterwards the surface was polished with different grain sizes of alumo-silica and

diamond paste until 1 µm grain size. After each polishing step the surface was cleaned in a supersonic bath for a few seconds.

2.2.6 Electron microprobe mappings

A JEOL JXA 8200 electron microprobe was used to generate element distribution maps for Ca, Mn, Fe, Mg, Ba, Al, Si, S and P within cross-sections of benthic foriminiferal test walls. Each cross-section was carbon coated before the measurements. The microprobe was operated in a wavelength dispersive mode by using different Kα X-ray lines for each element. Up to five spectrometers could be used to measure up to five elements simultaneously. The different spectrometer crystals which were used for the different elements are listed in table 2.2. An acceleration voltage of 15 kV and a beam current of 20 nA was used. The selected areas were mapped by using a step size of 0.5 µm and a dwell time of 500 ms. Results are illustrated as maps of relative measured intensities for the different elements. The JEOL JXA 8200 was also used to generate the secondary electron images of the foraminiferal cross-sections.

Table 2.2. Spectrometer crystals used at the EMP for different elements.

Element	Crystal	Element	Crystal	Element	Crystal
Ca	PETJ	Ba	PETJ	S	PETH
Mg	TAPH	Mn	LIFH	Si	TAP
Fe	LIFH	P	PETH	Al	TAPH

2.2.7 SIMS analyses

The Mn/Ca and Fe/Ca ratio analyses in test cross-sections of *B. spissa* were performed using a Cameca ims 6f magnetic sector ion microprobe at the Helmholtz Centre Potsdam. Each cross-section was cleaned twice ultrasonically in high purity ethanol prior to coating with a 35 nm thick, high purity gold coat.

Analyses used a 200 pA, nominally 12.5 kV, mass filtered $^{16}O^-$ ion-beam which was focused to a diameter of circa 4 µm on the sample surface. Prior to each analysis the analytical location was presputtered for 300 s with the beam rastered over 10 x 10 µm raster followed by a second 3 minutes preburn with a static beam. During the first presputtering the $^{40}Ca^+$ distribution was monitored using the dynamic ion imaging system of the instrument in order to improve the beam targeting on the thin walls of the test being investigated.

The mass spectrometer of the SIMS was operated at a mass resolution $M/\Delta M \approx 6000$ which is needed in order to separate the ^{55}Mn peak from the isobaric $^{54}Fe^1H$ molecule. A 150 µm contrast aperture was used in conjunction with a 750 µm field aperture (equivalent to a 60 µm diameter field of view); no energy offset was employed and a 50 V wide energy window was

used. A single analyses consisted of 30 scans of the sequence 39.95 Da (0.1 s per cycle, used during the spot preburn), ^{40}Ca (2 s), ^{55}Mn (10 s), ^{56}Fe (4 s) and ^{63}Cu (4 s), resulting in a total data acquisition time of roughly 10 min.

The OKA calcite grain was used as a reference material to convert raw Mn/Ca and Fe/Ca count rates into µmol/mol concentration values for which the concentration values of the microdrilled powder determined by ICP-MS were used. WHCG was analysed a total of n = 14 times during our July 2010 analytical session, yielding a 1s repeatability of 1.5% for the observed Mn/Ca, 14.8% for Fe/Ca and 23.2% for Cu/Ca ratios.

The test walls of *Bolivina spissa* are in general relatively thin (about 10 - 20 µm thickness). The test is perforated; however the pores with a diameter of about 6 µm are relatively big and easy to see on secondary electron images of the cross-sections. Each analysis targeted a region of a test wall that had preferably no pores so as to avoid measuring contaminations potentially accumulated inside the pores. Sub sequent to our SIMS session secondary electron images of the cross-sections were made to assess whether that SIMS ion beam was well focused and cantered on the middle of the test wall. Measurements which obviously were done partly on epoxy or at the edge of the test wall or which showed low Ca count rates were not used for the data evaluation. All Cu measurements showed unexpectedly high ^{63}Cu, for which we do not have an explanation. The Cu measurements have not been used in the data evaluation.

2.2.8 Quadrupole ICP-MS analyses

The analyses were performed on an Agilent 7500cx quadrupole ICP-MS. Operation conditions are listed in tab. 2.3. Instrument sensitivity was optimised by using of a 1 ppb Li-Y-Tl-Ce-Mg-Co standard solution before the measurements. For sample introduction a microautosampler (Cetac ASX 100) coupled to a PFA self-aspiration nebulizer fitted to a glass spray chamber was used. Due to the small available sample volume (typically > 500 µl) the low sample uptake rate of the self aspiration system was an important feature during the analyses. The integration times were 0.1 s for ^{48}Ca, 1 s for ^{55}Mn and 2 s for ^{56}Fe with 3 repetition runs. An octopole collision cell flooded with H_2 as reaction gas was used during the ^{56}Fe analyses to minimize interferences with ^{40}Ar^{16}O.

Predilutions were prepared from certified ICP-MS grade stock solutions (10000 ppm for Ca, 1000 ppm for Fe and Mn) by dilution with 2% HNO_3. The working standards were made by mixing the predilutions with 2% HNO_3 to give Ca concentrations of 10 ppm and Fe/Ca and Mn/Ca ratios in the magnitude of foraminiferal calcite. The concentrations for the different standard rows are listed in tab. 2.4. A second standard row with higher Mn concentrations was

prepared for the analyses of the Mn/Ca ratio in the OKA as well as a standard row for determination of Ca concentrations. About 50 µl of the samples were diluted to 250 µl first for the analyses of the Ca content. The remainder was diluted to 10 ppm Ca to overcome matrix effects during the element ratio determinations.

Table 2.3. Operation conditions for Agilent 7500cx.

	value/description
RF power	1500W
Nebulizer	PFA (100µl/min, self aspirating)
Spray chamber	Glass (cooled to 2°C)
Autosampler	Cetac ASX 100
Uptake rate (µl/min)	100
Washout time (s)	90
Uptake time (s)	30
Argon plasma gas flow rate (l/min)	15
Argon auxiliary gas flow rate (l/min)	0,2-0,3
Argon nebulizer gas flow rate (l/min)	0,8-0,9
Sample cone	Nickel (Agilent)
Skimmer cone	Nickel
CeO/Ce and Ba^{2+}/Ba^{+} ratios	<2,5%

2.2.9 Pore-water data

All pore-water data, discussed in this work are taken from Scholz et al. (*in review*).

Table 2.4. Element concentration for the different standard rows used for ICP-MS.

Standard	Ca (ppm)	Fe (ppt)	Mn (ppt)
Row 1 std 1	10	150	5
Row 1 std 2	10	250	10
Row 1 std 3	10	500	15
Row 1 std 4	10	1000	50
Row 1 std 5	10	3000	100
Row 1 std 6	10	5000	150
Row 2 std 1	10	0	10000
Row 2 std 2	10	0	20000
Row 2 std 3	10	0	50000
Row 2 std 4	10	0	75000
Row 2 std 5	10	0	100000
Row 3 std 1	10	0	0
Row 3 std 2	50	0	0
Row 3 std 3	100	0	0
Row 3 std 4	200	0	0

2.3 Results

2.3.1 EMP mappings of *Uvigerina peregrina* tests

Several trace element distribution maps in uncleaned tests of *U. peregrina* and the associated SEM pictures are shown in fig. 2.1-2.3. Strong Mg-bends which are typical for the primary calcite in tests of bilaminated calcitic foraminifera can be seen nicely in fig. 1. The inner parts of the wall are highly enriched in iron. A slight iron enrichment is also present in the pores. The iron rich phase at the inner surfaces of the wall furthermore is enriched in Al, Si, P and S (fig. 2.2&2.3) which hints towards a presence of alumo-silicates (clays) and organic matter. There are accumulations of organic detritus present inside the chambers. These accumulations differ in their chemical composition strongly from the iron rich phase at the inner parts of the wall (less Fe and Ca, more S and P) (fig. 2.2). The chemical composition of two cuts directly through layers of this iron rich phase is shown in fig. 2.3. The element mapping shows nicely the transition from the calcitic test walls into this iron rich phase. A trace element distribution map in a test section of an *U. peregrina* specimen treated with an oxidative cleaning is shown in fig. 2.4. In contrast to the element maps of the uncleaned specimens this specimen does not show an iron rich phase attached to the inner surface of the test.

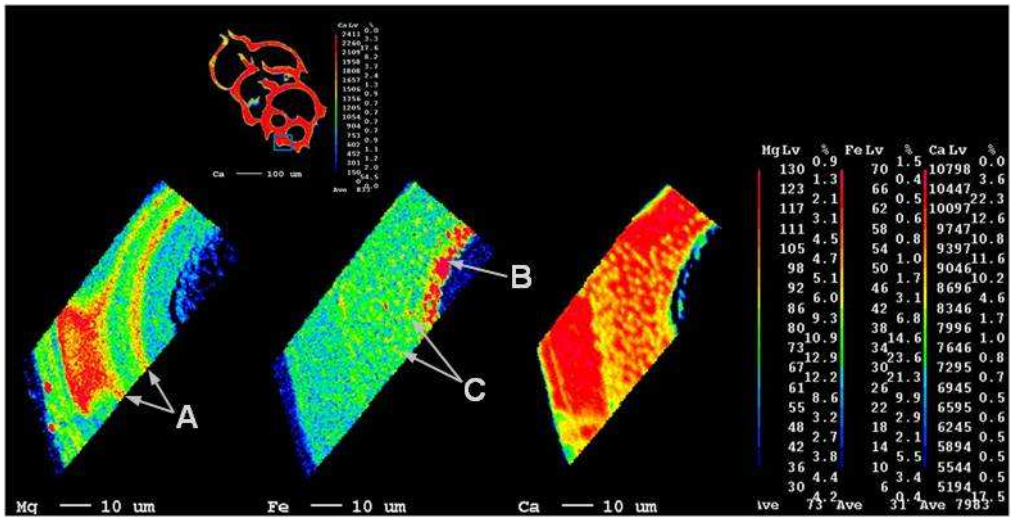

Figure 2.1. EMP elemental mappings for an *Uvigerina peregrina* specimen from 519 m water depth (M77-1-421/MUC-13) on an exposed section of the foraminiferal test. Distribution of Ca, Mg and Fe in the foraminiferal test. All intensity values are expressed in counts per second (cps) as shown in the color bars. **A)** Mg bands **B)** Fe rich phase at inner test surface and pores (**C**).

2.3.2 EMP of *Bolivina spissa* tests

Several trace element distribution maps in tests of *B. spissa* are shown in fig. 2.5-2.7. Maps are shown for uncleaned (fig. 2.5) and cleaned specimens (fig 2.6&2.7). In contrast to *U. peregrina B. spissa* does not show Mg-bands in the test walls. The inner parts of the test wall of the uncleaned specimen (fig. 2.5) are enriched in Fe and also the inner part of the test wall shows a Fe rich spot. These Fe rich phases are absent in the specimens which have been treated with an oxidative cleaning procedure (fig. 2.6&2.7) except in a pore of the specimen from 465 m water depth (fig. 2.7). All Ca distributions show strongly heterogenous patterns. These patterns can be recognized on secondary-electron (SE) and backscattered-electron (BSE) images, too (fig. 2.8). These images have been made after the mappings. The BSE images show that these structures look like some kind of porous bands in the test walls where the Ca maps show higher count rates.

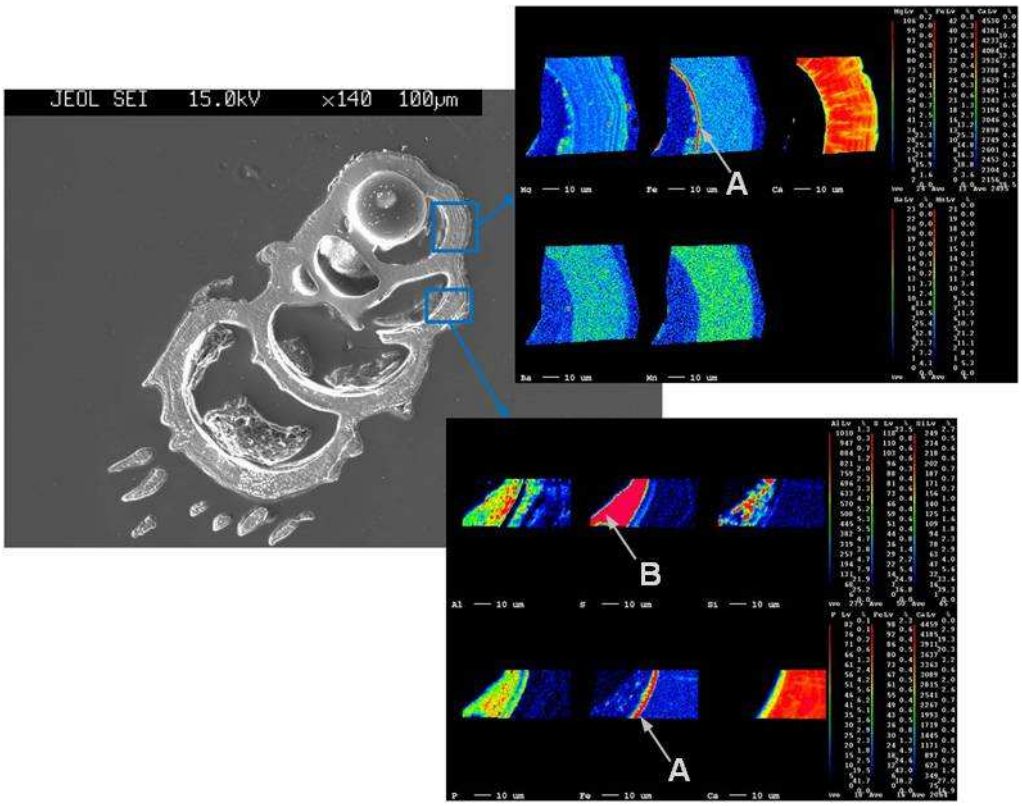

Figure 2.2. EMP elemental mappings and secondary electron image for an *Uvigerina peregrina* specimen from 579 m water depth (M77-1-487/MUC-39) on an exposed section of the foraminiferal test. Distribution of Ca, Mg, Fe, Ba, Mn, Al, S, Si and P in the foraminiferal test. All intensity values are expressed in counts per second (cps) as shown in the color bars. **A)** Fe rich phase at inner test surface **B)** organic detritus inside test chambers.

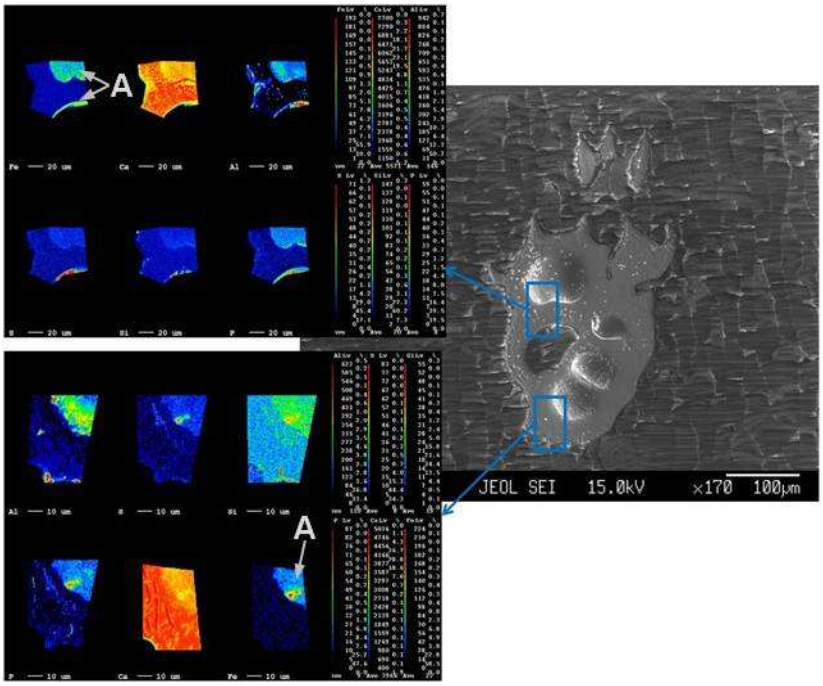

Figure 2.3. EMP elemental mappings and secondary electron image for an *Uvigerina peregrina* specimen from 579 m water depth (M77-1-487/MUC-39) on an exposed section of the foraminiferal test. Distribution of Ca, Mg, Fe, Ba, Mn, Al, S, Si and P in the foraminiferal test. All intensity values are expressed in counts per second (cps) as shown in the color bars. **A)** Fe rich phase at inner test surface

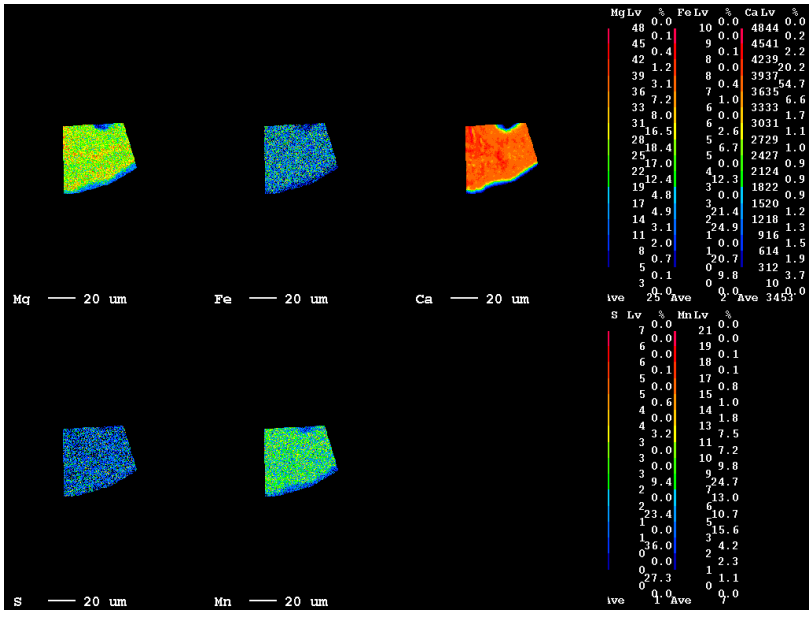

Figure 2.4. EMP elemental mapping of a section from an *Uvigerina peregrina* specimen from 640 m water depth (M77-1-565/MUC-60) on an exposed section of the foraminiferal test treated with an oxidative cleaning procedure. Distribution of Mg, Fe, Mn, S and Ca in the foraminiferal test. All intensity values are expressed in counts per second (cps) as shown in the color bars. Note that no contaminant phases are visible in the Fe distribution.

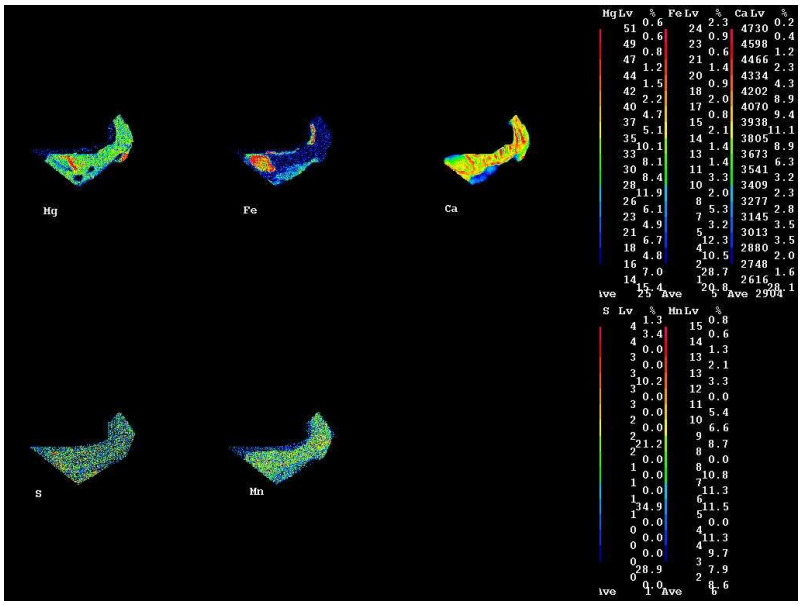

Figure 2.5. EMP elemental mapping of a section from an uncleaned *Bolivina spissa* specimen from 640 m water depth (M77-1-565/MUC-60) on an exposed section of the foraminiferal test. Distribution of Mg, Fe, Mn, S and Ca in the foraminiferal test. All intensity values are expressed in counts per second (cps) as shown in the color bars. Note that the Fe distribution shows a contaminant phase at the inner part of the test walls similar like the uncleaned specimens of *U. peregrina*.

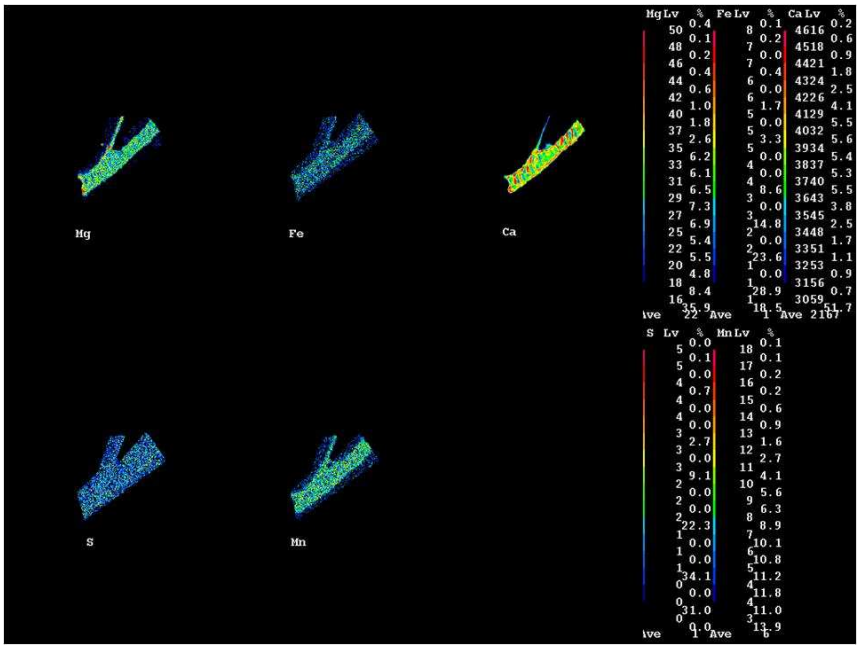

Figure 2.6. EMP elemental mapping of a section from a *Bolivina spissa* from 640 m water depth (M77-1-565/MUC-60) on an exposed section of the foraminiferal test specimen treated with an oxidative cleaning procedure. Distribution of Mg, Fe, Mn, S and Ca in the foraminiferal test. All intensity values are expressed in counts per second (cps) as shown in the color bars. Note that no contaminant phases are visible in the Fe distribution.

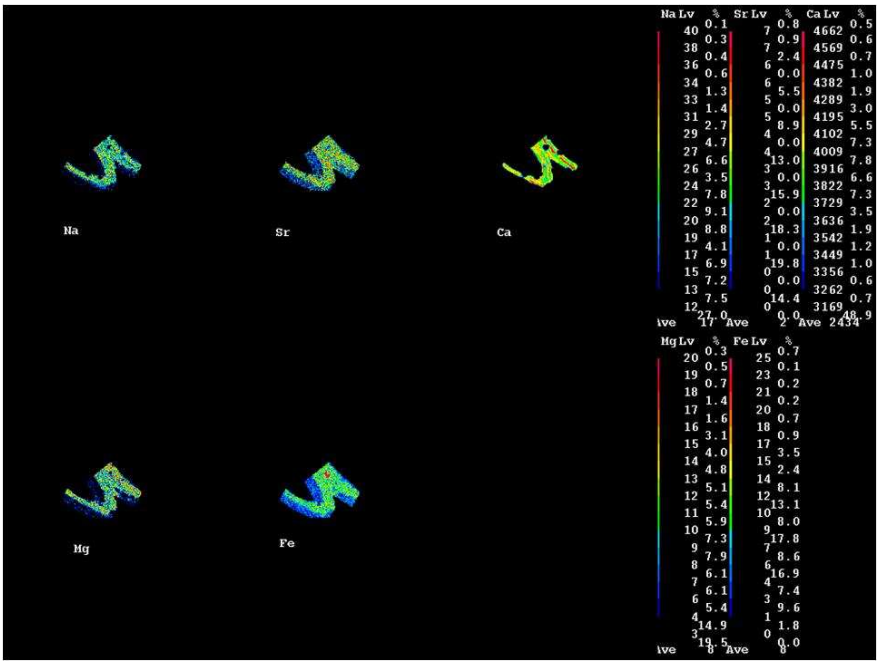

Figure 2.7. EMP elemental mapping of a section from a *Bolivina spissa* from 465 m water depth (M77-1-455/MUC-21) on an exposed section of the foraminiferal test specimen treated with an oxidative cleaning procedure.. Distribution of sodium, strontium, iron, manganese, and calcium in the foraminiferal test. All intensity values are expressed in counts per second (cps) as shown in the color bars. Note that no contaminant phases are visible in the Fe distribution except inside a test pore.

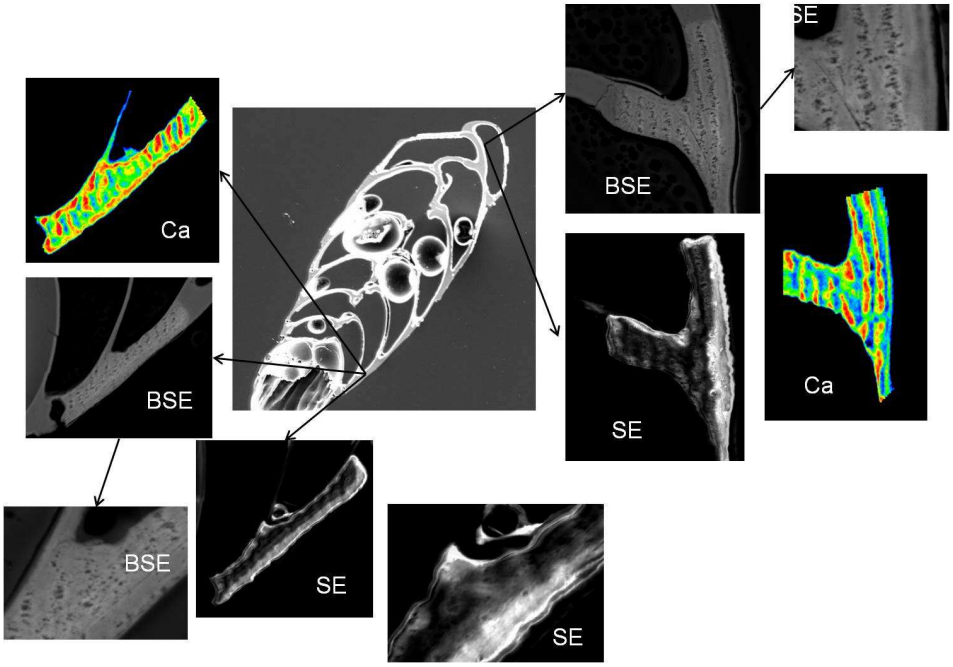

Figure 2.8. Cross section of a *Bolivina spissa* specimen from 640 m water depth (M77-1-565/MUC-60) with a secondary electron overview image in the middle. Close ups of sections of Ca-EMP mappings (Ca) secondary electron images (SE) and backscattered electron images (BSE) are shown. Note that the Ca distribution is reflected by the holey structures seen on the BSE images.

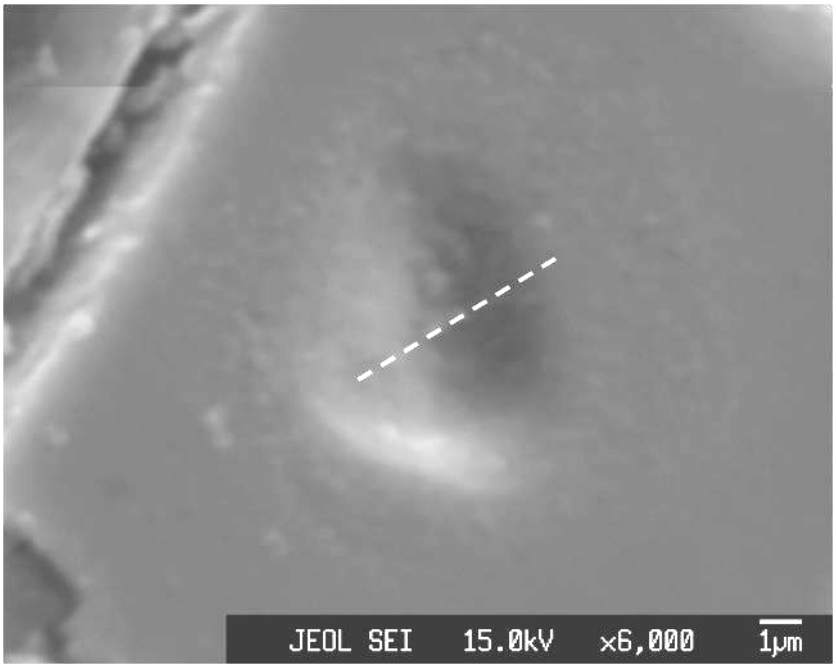

Figure. 2.8. Secondary electron micrograph of a test section from a *Bolivina spissa* specimen after measuring with SIMS. The spot diameter of the ion beam was about 4-5 μm. Data acquisition time was roughly 10 minutes. Estimated depth of the spot ~ 2 μm.

2.3.3 Redox sensitive elements in tests of *Bolivina spissa*

The measured Mn/Ca and Fe/Ca ratios for the Ecrm752, the OKA calcite grain and the tests of *Bolivina spissa* are listed in table 2.5 (ICP-MS), table 2.6 (SIMS) and table 2.7 (mean SIMS). The Ecrm752 solution was used as internal reference standard for the ICP-MS analyses (mean Mn/Ca = 139.30 μmol/mol; mean Fe/Ca = 155.28 μmol/mol). Element ratios for the Ecrm752 showed a sufficiently high reproducibility with standard deviations of 4.02 μmol/mol (Mn/Ca) and 5.18 μmol/mol (Fe/Ca) between the different measurements. The Mn/Ca and Fe/Ca ratios for the Ecrm752 have also been determined in an inter laboratory calibration study (Greaves et al., 2008). The data presented in our study are in accordance to the values reported for the the not centrifuged Ecrm752 where the Mn/Ca ratio ranged from 121-147 μmol/mol and the Fe/Ca ratio ranged from 97-220 μmol/mol between the different laboratories. The mean element ratios for the Oka calcite grain which was used as cross calibration standard for the SIMS analyses was also determined with ICP-MS (mean Mn/Ca = 4930.33 μmol/mol; mean Fe/Ca = 541.33 μmol/mol).

The Mn/Ca and Fe/Ca ratios in tests of *Bolivina spissa* are shown in fig. 2.9. The mean ratios from the SIMS spot analyses for single specimens are plotted as well as the ratios from ICP-MS analyses on bulk solutions of several specimens. The ratios of the bulk samples compared to the microanalyses agree in a maximal differences of 3 - 29% compared to the overall data

range between the different sampling sites, although the Mn/Ca ratio from the bulk analysis is a bit elevated compared to the microanalysis result (3.8 µmol/mol compared to 2.12 µmol/mol). The Mn/Ca ratios range from 2.12 - 9.93 µmol/mol and thus are in general quite low. This falls far below the acceptable level of test Mn/Ca to prove the absence of diagenetic coatings from 50 µmol/mol to > 150 µmol/mol (Boyle, 1983; Boyle and Keigwin, 1985; 1986; Delaney, 1990; Ohkouchi et al., 1994). The corresponding Fe/Ca ratios range from 86.99 – 551.82 µmol/mol. Both element ratios show an increasing trend towards deeper water depths and higher bottom water oxygenation. The standard deviations between the different SIMS spots on single specimens are generally higher among the specimens from the deeper and better oxygenated sampling locations, too. They range from 0.37 – 5.91 µmol/mol for the Mn/Ca and from 23.06 – 392.98 µmol/mol for the Fe/Ca ratio. The Mn/Ca and Fe/Ca ratio for an uncleaned specimen of *B. spissa* is also shown in fig. 9 indicated by a green diamond. Compared to a specimen from the same sampling site, treated with oxidative cleaning, it shows an elevated Fe/Ca ratio and a slightly reduced Mn/Ca ratio.

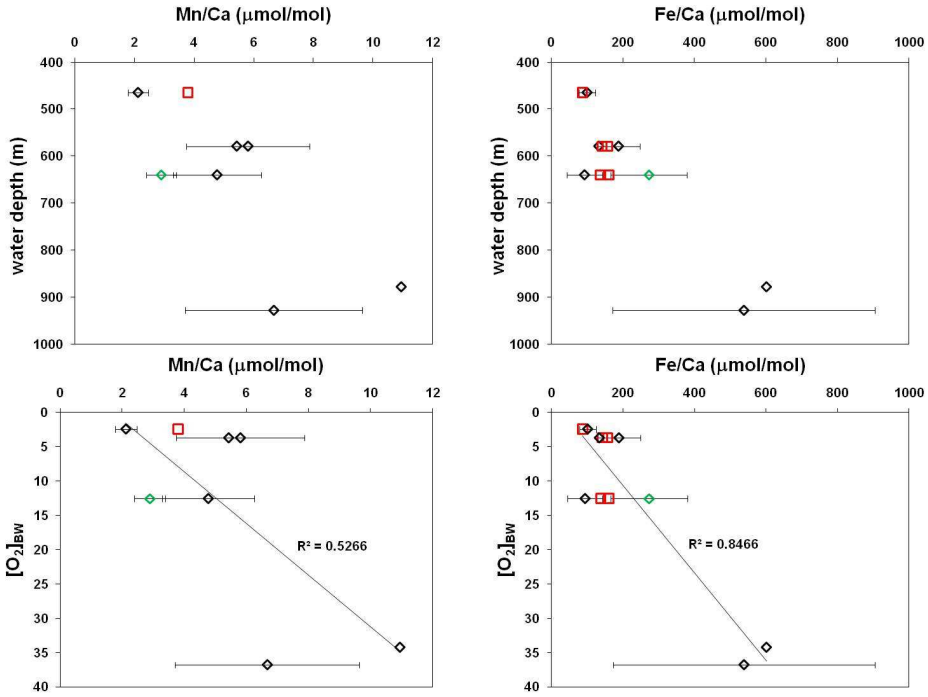

Figure 2.9. Mn/Ca and Fe/Ca ratios in tests of *Bolivina spissa* plotted against water depth and $[O_2]_{BW}$. Red squares indicate data points measured on bulk samples of 40 specimens with ICP-MS while diamonds indicate mean values from single specimens measured with SIMS. The specimens indicated by the black diamonds all have been treated with an oxidative cleaning procedure while the single green diamond represents an uncleaned specimen. Error bars on the SIMS data show the standard deviation between the different spots measured on a single specimen. Diamonds without error bars indicate mean values of only two measurements.

Table 2.5. Element/Ca ratios for different samples determined by ICP-MS.

Material	Mn/Ca (µmol/mol)	1σ (µmol/mol)	Fe/Ca (µmol/mol)	1σ (µmol/mol)
Ecrm752	148.3	10.7	150.1	9.8
Ecrm752	138.2	2.8	150.1	8.0
Ecrm752	137.7	2.1	150.3	7.9
Ecrm752	137.8	1.5	157.3	3.5
Ecrm752	138.3	1.4	157.1	4.5
Ecrm752	138.3	3.7	159.0	5.1
Ecrm752	136.5	1.7	163.1	1.4
OKA	4942.0	57.8	547.7	10.3
OKA	4875.6	181.4	523.1	12.8
OKA	4973.4	54.7	553.2	5.5
B. spissa M77-1-455/MUC-21	3.80	0.06	87.0	3.2
B. spissa M77-1-487/MUC-38			142.0	3.1
B. spissa M77-1-487/MUC-38			157.5	2.1
B. spissa M77-1-565/MUC-60			160.6	3.2
B. spissa M77-1-565/MUC-60			138.1	2.9

2.3.4 Comparison to pore-water data

The correlation between Mn/Ca ratios in the top cm of the pore water and Mn/Ca in tests of *B. spissa* from the same sampling locations are shown in fig. 2.11. The Mn/Ca ratios in *B. spissa* are generally higher at locations where Mn/Ca ratios are higher in the pore-waters.

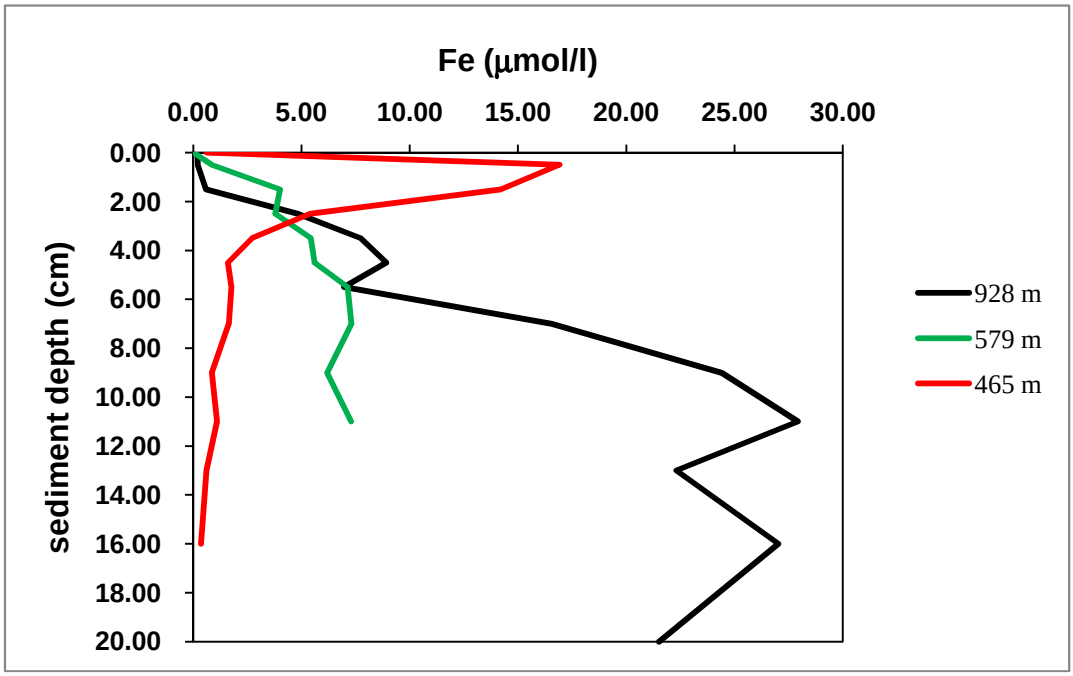

Figure 2.10. Fe pore water profiles for different sampling locations at 11°S off Peru (Red: M77-1-455/MUC-21, 465 m. Green: M77-1-487/MUC-38, 579 m. Black: M77-1-445/MUC-15, 928 m).

Table 2.6. Element/Ca ratios of foraminiferal calcite determined by SIMS.

Material	Mn/Ca (µmol/mol)	1σ (µmol/mol)	Fe/Ca (µmol/mol)	1σ (µmol/mol)
B. spissa M77-1-455/MUC-21	1.68	0.53	108.2	9.7
B. spissa M77-1-455/MUC-21	2.32	0.60	66.9	8.7
B. spissa M77-1-455/MUC-21	2.02	0.61	117.2	10.1
B. spissa M77-1-455/MUC-21	2.46	0.64	111.6	10.2
B. spissa M77-1-487/MUC-38a	5.71	1.01	82.4	8.7
B. spissa M77-1-487/MUC-38a	5.15	0.94	185.0	12.6
B. spissa M77-1-487/MUC-38b	3.48	0.76	227.7	14.3
B. spissa M77-1-487/MUC-38b	6.48	1.02	218.4	14.5
B. spissa M77-1-487/MUC-38b	7.46	1.18	119.2	10.7
B. spissa M77-1-565/MUC-60a	2.82	0.69	48.7	6.1
B. spissa M77-1-565/MUC-60a	4.44	0.81	84.1	6.2
B. spissa M77-1-565/MUC-60a	6.20	0.92	164.1	12.3
B. spissa M77-1-565/MUC-60a	5.61	0.88	78.6	8.3
B. spissa M77-1-565/MUC-60b	2.31	0.58	180.4	12.1
B. spissa M77-1-565/MUC-60b	3.51	0.76	269.8	16.1
B. spissa M77-1-565/MUC-60b	2.76	0.62	423.2	18.5
B. spissa M77-1-565/MUC-60b	3.01	0.63	218.3	12.7
B. spissa M77-1-604/MUC-74	5.29	0.89	216.8	13.2
B. spissa M77-1-604/MUC-74	16.59	2.85	984.4	78.8
B. spissa M77-1-445/MUC-15	9.97	1.23	420.5	21.7
B. spissa M77-1-445/MUC-15	5.57	1.04	853.5	30.0
B. spissa M77-1-445/MUC-15	3.14	0.72	72.1	8.3
B. spissa M77-1-445/MUC-15	8.02	1.17	805.8	91.9

Table 2.7. Mean element/Ca ratios in tests of single *B. spissa* specimens determined with SIMS. Standard deviations are from variability inside single specimens not analytical uncertainties.

Material	Mn/Ca (µmol/mol)	1σ (µmol/mol)	Fe/Ca (µmol/mol)	1σ (µmol/mol)
B. spissa M77-1-455/MUC-21	2.12	0.35	101.0	23.1
B. spissa M77-1-487/MUC-38a	5.15		185.0	
B. spissa M77-1-487/MUC-38b	5.81	2.07	188.4	60.1
B. spissa M77-1-565/MUC-60a	4.77	1.48	93.9	49.3
B. spissa M77-1-565/MUC-60b	2.90	0.50	272.9	106.7
B. spissa M77-1-604/MUC-74	9.93	5.91	551.8	393.0
B. spissa M77-1-445/MUC-15	6.67	2.96	538.0	366.1

The Fe concentrations among the pore water profiles of three sampling locations are shown in fig. 2.10. The core from the shallowest most oxygen depleted sampling site shows a sharp Fe peak with high Fe concentrations in the top 2 cm of the pore waters. In contrast to this profile

the Fe/Ca ratios in tests of *B. spissa* from this location are the lowest found among all samples. The Fe concentration in the pore waters from the deeper sampling locations show a more typical behaviour with increasing concentrations at sediment depths where the Fe reduction starts.

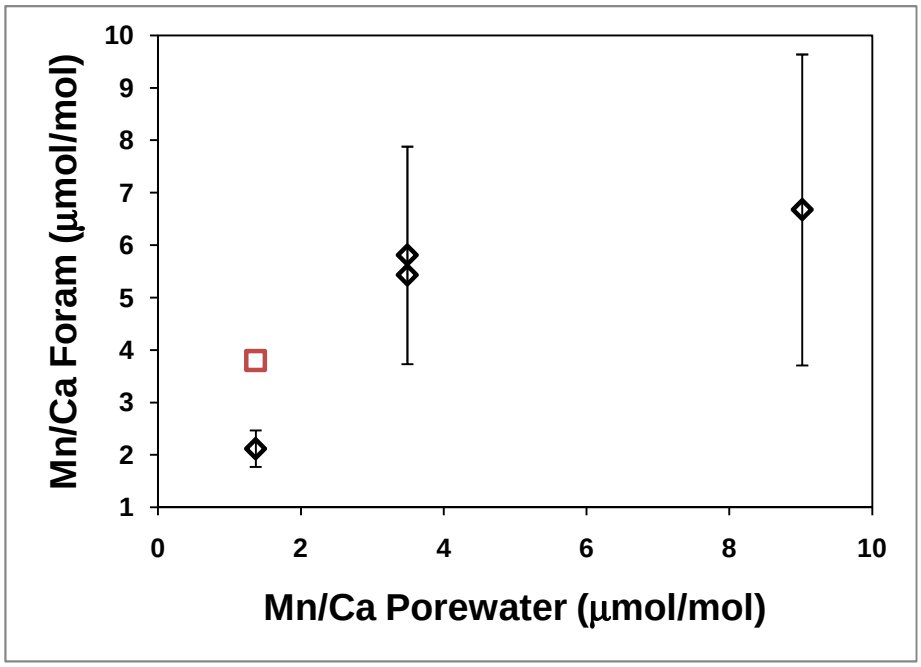

Figure 2.11. Correlation between the Mn/Ca ratio in tests of *Bolivina spissa* to the Mn/Ca ratio in the top cm of the pore water from the same sampling location. Red squares indicate data points measured on bulk samples of 40 specimens with ICP-MS while black diamonds indicate mean values from single specimens measured with SIMS. Error bars on the SIMS data show the standard deviation between the different spots measured on a single specimen. Diamonds without error bars indicate mean values of only two measurements.

2.4 Discussion

2.4.1 Chemical test composition of *Uvigerina peregrina*

The trace element mappings of *Uvigerina peregrina* cross-sections show an iron rich phase which is strongly enriched in different elements. This phase seems to be similar like "coatings" which have been found in the inner chamber walls of *Globigerinoides ruber* (Gehlen et al., 2004). But due to the high organic content (enriched in P and S) it seems like this phase belongs to the inner organic lining of the test and not to a diagenetic coating. The cements in tests of several agglutinated foraminifera and the test walls of several allogromiids

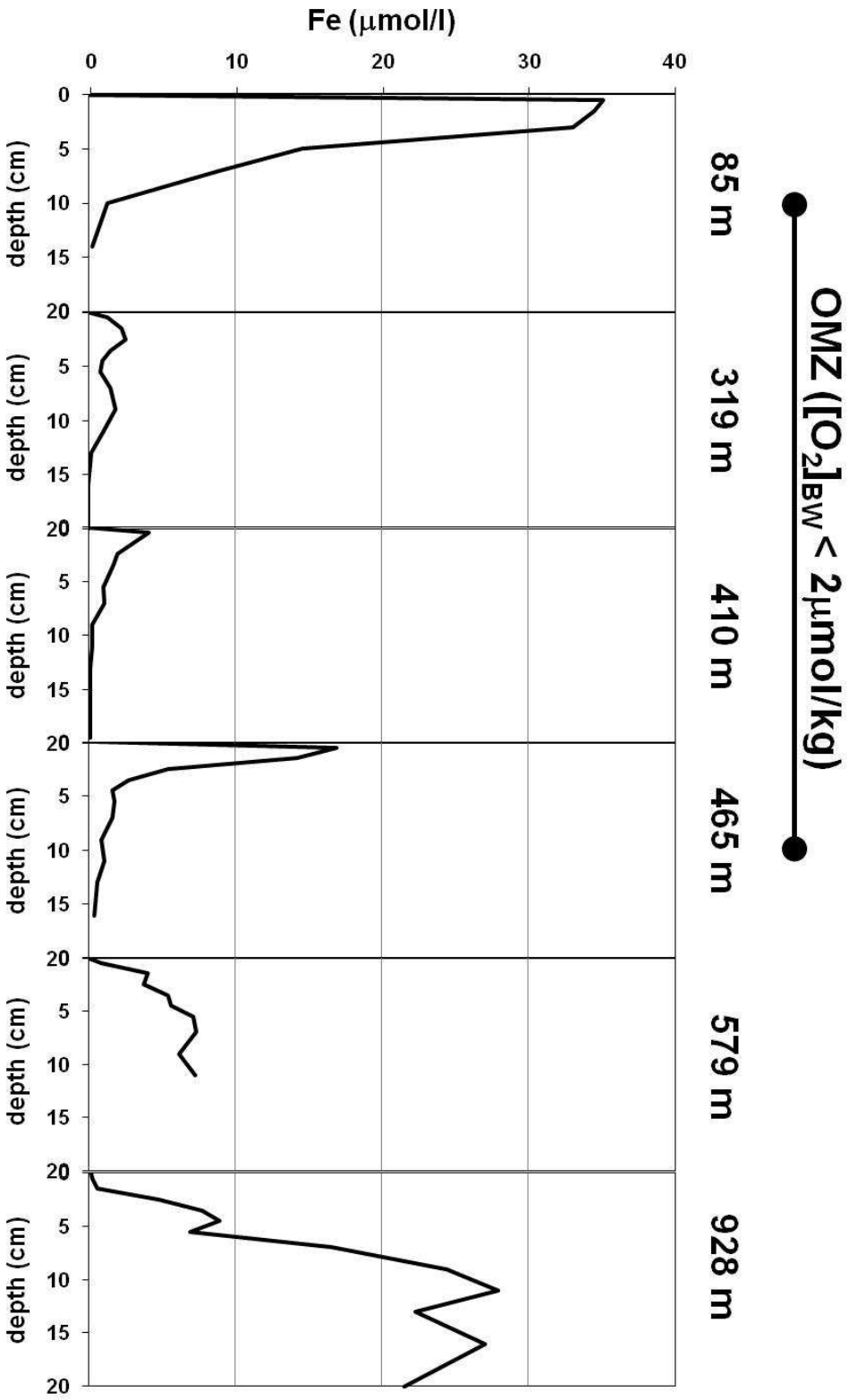

Figure 2.12. Pore water profiles for Fe at different water depths at the Peruvian OMZ. The bracket indicates the boundaries of the OMZ where bottom water oxygen concentrations fall below 2 μmol/kg. Profiles taken from Scholz et al. (*submitted*).

show a similar chemical composition (Bertram and Cowen, 1998; Gooday et al., 2008). Also it is typical that the organic cements of agglutinated foraminifera contain a stabilizing, ferruginous component (Bender, 1989). These similarities in the organic test components of calcareous, agglutinated and allogromiid foraminifera suggest an evolutionary connection between these test components.

The accumulations of organic detritus inside the test walls of the *U. peregrina* specimen shown in fig. 2.2 are most probable remainings of deposit feeding. Deposit feeding and the accumulation of organic detritus in living specimens of *U. peregrina* have been documented by Goldstein and Corliss (1994). The complete difference in the chemical composition of these accumulations compared to the lining inside of the test wall makes the suggestion that this lining consists of remaining clay and other sediment particles from food vacuoles agglutinated to the inner test wall very unreasonable. The elevated Fe concentrations inside the pores also show the presence of this lining. Thus in microanalytical techniques like EMP, SIMS or LA-ICP-MS it should be avoided to measure at the porous parts of the test walls, because the inner organic lining, also present in the test pores, shows, partly due to the presence of clay particles, strongly elevated concentrations in several trace elements, even Mg.

The element mappings show no hints for ferro-manganese-oxide coatings which is most probably related to the highly reducing conditions in the pore waters at the OMZ off Peru. At least for recent samples a reductive cleaning for chemical analyses seems to be not necessarily required. The comparison of the uncleaned specimens with a specimen treated with an oxidative cleaning shows that the oxidative cleaning removes the contaminant Fe rich phase at the inner surface of the test walls. This hints again that this phase represents more the inner organic lining of the test than a diagenetic coating. Also it proofs the value of the oxidative cleaning for the minimization of contaminations inside foraminiferal tests.

2.4.2 Chemical composition of *Bolivina spissa* tests

An iron rich phase present in the uncleaned specimens of *U. peregrina* and *B. spissa* seems to be absent in specimens of *B. spissa* treated with an oxidative cleaning procedure. To minimize contaminations during the microanalysis of foraminiferal tests it is absolutely necessary to use an oxidative cleaning step during sample preparation. But even after intense oxidative cleaning there seem to be still contaminations left inside the test pores. Thus it should be avoided to measure parts of the tests where pores are present. This might be especially complicated during the analyses of foraminifera with a high pore-density with laser ablation

due to the spot diameter (50 - 80 µm) required for low concentration measurements on Q-ICP-MS. Nevertheless the test walls seem to be contamination free after the oxidative cleaning where no pores are present. The element/Ca ratios measured with SIMS in the tests of the cleaned *B. spissa* specimens should therefore represent the element/Ca ratios of the test calcite. This might be more complicated during the presence of diagenetic oxyhdroxide or Mn carbonate coatings. In this case EMP mappings should be used as pre-investigation to locate these coatings and for identification of the measurement spots in the contamination free areas. Additionally the effectivity of a reductive cleaning treatment could be analysed by EMP mapping by comparing cleaned and uncleaned specimens.

The strong Mg-bends present in *U. peregrina* are not visible in *B. spissa*. This might be explained by the fact that bolivinidae construct their tests in a monolamellar concept without a second phase of calcite between the different layers (Sliter, 1974).

Still enigmatic remain the heterogeneous patterns in Ca distribution. The Ca count rates are higher where these holey structures are visuable in the BSE images. This appears to be contradictable because in this case the Ca concentration would be higher at spots of low density. Thus it is probable that the higher Ca count rates in the holey structures are rather artifacts due to topography related analytical problems with. It seems likely that the high energetic X-ray beam pitted the surface of the sample by burning more volatile parts of the test wall.

2.4.3 Redox sensitive elements in pore waters and *Bolivina spissa*

2.4.3.1 Mn/Ca ratios

Reductive dissolution of reactive Mn (oxyhydr)oxides in the surface sediments drive the Mn flux across the benthic boundary (Froelich et al., 1997; Burdige et al., 1993; Pakhomova et al., 2007; Noffke et al., submitted; Scholz et al., submitted). The Mn concentrations and thus the Mn/Ca ratios are relatively low in the pore waters from the OMZ off Peru since most of the Mn delivered to the OMZ is already reduced in the water column (Böning et al., 2004; Scholz et al., submitted).The Mn/Ca ratios in tests of *B. spissa* and the Mn concentrations in the top cm of the pore waters are generally relatively low and show an increasing trend with higher bottom water oxygenation. At a first glance these results appear to be confusing because usually solid MnO_2 is rapidly reduced to soluble Mn^{2+} in oxygen depleted pore waters. Thus it is expectable that Mn concentrations are elevated in the top pore water interval when bottom water oxygen is depleted. Indeed the permanently anoxic OMZ off Peru causes MnO_2

reduction to occur already in the water column, and hence only minor amounts of particulate bound Mn arrive at the seafloor (Böning et al., 2004). Even if the pore water conditions are highly reducing only little Mn can be mobilised due to the absence of particulate MnO_2. At deeper water depths below the OMZ the oxygen concentration starts to rise again and soluble Mn^{2+} can be oxygenated to MnO_2 which again settles down to the seafloor. Thus at the deeper sampling locations the Mn concentrations in the top pore water intervals can be higher due to the higher reservoir in particulate MnO_2 although (or in this case because) the bottom water oxygen concentrations are higher. As already mentioned even the Mn/Ca ratios in *B. spissa* reflect these conditions. These results can be used to interpret downcore profiles of Mn/Ca ratios in benthic foraminifera from the Peruvian OMZ. Elevated Mn/Ca ratios would hint to higher oxygen concentrations during this time due to a higher MnO_2 flux to the ground.

The Mn/Ca and the Fe/Ca ratios both obviously show a higher variability in tests of *B. spissa* from habitats with elevated $[O_2]_{BW}$. Infaunal foraminiferal species are able to migrate vertically in the sediments to where food availability and oxygenation meet their individual requirements (Jorissen et al., 1995; Duijnstee, 2003). At higher $[O_2]_{BW}$ and thus a deeper oxygen penetration depth *B. spissa* might be able to migrate deeper into the sediments. In this case individual specimens would be exposed to a wide range of Mn and Fe concentrations in the pore waters among their lifetime. The comparison between the cleaned and the uncleaned specimen from 640 m water depth (M77-1-565/MUC-60) shows that the uncleaned specimen has an elevated Fe/Ca and a slightly reduced Mn/Ca ratio. The elevated Fe/Ca ratio originates most probably from the contamination of that Fe rich phase which could be seen on EMP mappings of the uncleaned *B. spissa* and *U. peregrina* specimens. The slightly lower Mn/Ca ratio might be more a variability in the lattice bound Mn concentrations between different specimens.

2.4.3.2 Fe/Ca ratios and comparison to the pore waters

The Fe pore water profiles show more typical concentration levels as compared to Mn. However, the interpretation of the Fe/Ca ratios in *B. spissa* is complex in this regard because they appear to contradict the trend of the pore water concentrations: The lowest foraminiferal Fe/Ca ratios were found at 465 m water depth, a location with a strong sharp Fe peak in the pore water next to the sediment surface. Note, no living specimens of *B. spissa* were found at this location during sampling time although a very high amount of dead tests was present. At the two other sampling locations where pore water profiles are available (579 and 928 m water depth) living specimens of *B. spissa* could be found during sampling time (Mallon et

al., in press). In the centre of the OMZ *B. spissa* is completely absent (Glock et al., 2011). This suggests that *B. spissa* needs at least trace amounts of oxygen to survive or enough nitrate for denitrification.

A likely scenario, which can explain all observations and facts outlined above is that the habitat only recently turned anoxic causing the death of high numbers of *B. spissa*. The subsurface peak of Fe is likely the result of enhanced Fe-reduction, which formed after a phase of oxygenation and enhanced deposition and/or precipitation of Fe-(oxyhydr)oxides at the sediment surface (Scholz et al., submitted). The sampling site at 465 m water depth is located at the lower boundary of the Peruvian OMZ where ingression of oxygenated water masses occurs episodically. Overall, this means that the Fe mobilisation in the pore waters most likely started only after their death so that the Fe could not be incorporated into the test calcite anymore. Also the habitat either experienced a long phase of oxygenation short time before or these phases have to occur periodically over, because high amounts of dead *B. spissa* have been found in the top 3 cm of the sediment. These phases of oxygenation have to be at least long enough for *B. spissa* to survive and build up relative big sociations.

Some iron pore water profiles from different water depth at 11°S (taken from Scholz et al., submitted) are shown in fig. 12. The shallowest sampling site at the lower boundary of the OMZ (85 m) shows relatively high Fe concentrations in the pore water which might be partly due to an increased supply of detrital (oxyhydr)oxides from the continent (Suits and Arthur, 2000; Scholz et al., submitted). Very likely another portion of iron supply at this station has been delivered through lateral transport in the water column from deeper sediments in the center of the OMZ and the dissolved Fe is re-oxidized and deposited at the shallower shelf in times of shelf oxygenation. This Fe pool is reduced again when anoxic conditions re-establish and leads to the relatively high pore-water concentrations compared to the stations in the center of the OMZ (Noffke et al., submitted; Scholz et al., submitted). The pore water profiles in the permanent anoxic part of the OMZ (319m, 410 m) show relatively low Fe concentrations while the peak at 465 m water depth again is similar to this one at 85 m although it is not distinctive. Although most probably the continental input is missing at this station it might be that dissolved Fe has been delivered here by lateral transport in the water column from sediments at the centre of the OMZ. In this case as already mentioned oxygen supply from the deeper water masses might have lead to re-oxygenation of the dissolved iron. The new formed (oxyhydr)oxides are reduced again when anoxic conditions re-establish at this sampling site which again leads to these relatively high Fe concentrations in the shallow pore-water. The trend of the higher pore water concentrations with increasing water depth at

the deeper stations (579 m, 928 m) reflects the transition from sulphate reduction to iron reduction. This trend is reflected by the Fe/Ca ratios in *B. spissa*, too.

2.5 Conclusions

An iron rich phase has been found at the inner surface of the test walls and also in the pores of several specimens of *U. peregrina.* This phase most probably represents the inner organic lining. The lining is also enriched in Al, Si, P and S. Similar compositions have been found in test walls of allogromiids and the cements and inner organic lining in the agglutinated tests of textulariids (Bender, 1989; Bertram and Cowen, 1998; Gooday et al., 2008). This points to an evolutionary connection between these test components. The contaminant Fe rich phase could be efficiently removed from the walls with an oxidative cleaning procedure. A similar phase enriched in Fe could be removed from the inner parts of the test walls of *B. spissa* with oxidative cleaning, too. Nevertheless, even after the oxidative cleaning Fe was still enriched in the pores. Thus an oxidative cleaning procedure is essential to minimize the influences of non-lattice bound signatures during the determination of element/Ca ratios even for microanalytical methods. Furthermore it should be avoided to measure at parts of the test wall where pores are present. None of the EMP maps shows any hint for diagenetic coatings. Therefore a reductive cleaning for the determination of element/Ca ratios was not necessary. For minimisation of the whole procedure blank and the loss of sample material it is a good choice to avoid unnecessary cleaning steps.

A comparison of Fe/Ca and Mn/Ca ratios in tests of *B. spissa* determined with SIMS and ICP-MS showed that the results of these two techniques agree in a maximal differences of 3 - 29% compared to the overall data range between the different sampling sites. The low Mn/Ca ratios are in the same magnitude as in the pore waters. The low Mn concentrations in the pore waters originate most propably from the strong oxygen depletion in the water column of the Peruvian OMZ. Most MnO_2 is already reduced in the water column and does not settle down to the sediments. The Mn/Ca ratios in *B. spissa* correlate with the Mn/Ca ration in the top cm of the pore water. Thus Mn/Ca ratios in benthic foraminifera from the Peruvian OMZ could be used to trace the amount of oxygen depletion in the OMZ. In downcore proxy application higher Mn/Ca ratios would indicate a better oxygenation because more MnO_2 settles down to the seafloor, being remobilised in the pore waters. Several observations at a strongly oxygen depleted location, like low Fe/Ca ratios in *B. spissa*, a strong sharp Fe peak in the top interval of the pore water and the presence of a high amount of dead but no living specimens of B. spissa, hint that this site just recently turned anoxic. Therefore the Fe flux out of the sediment

started after the death of *B. spissa* at this site. The sharp peak also might hint that ironoxides, that precipitated in a period of higher oxygen supply, just started to get remobilised when the sediment turned anoxic again.

The fact that the Fe/Ca ratios in *B. spissa* reflect not always the pore water conditions might complicate approaches in paleoreconstruction in contrast to the Mn/Ca ratios which seem to be a very promising tool. Nevertheless, future downcore studies will show the value of these proxies in paleoreconstruction.

Chapter 3

ENVIRONMENTAL INFLUENCES ON THE PORE DENSITY OF *BOLIVINA SPISSA* (CUSHMAN)

Nicolaas Glock[1,2], Anton Eisenhauer[2,4], Yvonne Milker[3], Volker Liebetrau[2], Joachim Schönfeld[2], Jürgen Mallon[1,2], Stefan Sommer[2], and Christian Hensen[2]

[1]Sonderforschungsbereich 754, Christian-Albrechts-University Kiel, Climate-Biogeochemistry Interactions in the Tropical Ocean.

[2]Leibniz-Institute für Meereswissenschaften, IFM-GEOMAR, Wischhofstr. 1-3, 24148 Kiel, Germany.

[3]Institute für Geologie and Paleontologie der Universität Hamburg, , Bundesstrasse 55, 20146 Hamburg, Germany

[4]Correspondence author: E-mail: aeisenhauer@ifm-geomar.de

Published in Journal of Foraminiferal Research, 41, 22-32, 2011.

Abstract

The pore-densities (PD) in the tests of 232 specimens of the shallow infaunal foraminiferal species *Bolivina spissa* from eight locations off the Peruvian continental margin were investigated and compared to different environmental factors as water-depth, temperature, bottom-water oxygen ($[O_2]_{BW}$) and nitrate concentrations ($[NO_3^-]_{BW}$). There is a negative exponential PD-$[O_2]_{BW}$ correlation, but at oxygen-concentrations >10 µmol/l PD approaches a constant value without any further correlation to $[O_2]_{BW}$. The PD-$[NO_3^-]_{BW}$ relationship is better constrained than that for PD-$[O_2]_{BW}$. We hypothesize that the pores in the tests of *B. spissa* largely reflect the intracellular nitrate, and to a smaller extent the oxygen respiration. We also compared PD and porosity (P) of two single *B.spissa* and *B.seminuda* specimens from the same habitat. The comparison showed that P is significantly higher in *B.seminuda* than in *B. spissa* indicating that *B.seminuda* is much better adapted to strong oxygen-depleted habitats than *B. spissa*.

3.1 Introduction

The density and size of pores, developed only in rotaliid calcareous species, are important morphological features. Their shape, size and density are used as diagnostic features for the discernation of several species (Lutze, 1986). In earlier publications it has been suggested that pores promote the uptake of oxygen and the release of metabolic CO_2 (Hottinger and Dreher, 1974; Berthold, 1976; Leutenegger and Hansen, 1979). Some benthic species tolerant of low oxygen show their mitochondria (cell organelles involved in respiration) were more abundant near the pores than in other species from well-oxygenated waters implying an evolutionary linkage between pores and mitochondria (Leutenegger and Hansen, 1979; Sen Gupta and Machain-Castella, 1993). Later observations revealed that mitochondria were also concentrated in apertural cytoplasm (Bernhard and Alve, 1996) and can also move through cytoplasm and pseudopodia (Doyle, 1935). Recent studies performed on *Bolivina pacifica* (Cushman and McCulloch) showed again a clustering of mitochondria at the inner pore face while outer part of the pore void was inhabited by a rod-shaped microbial ectobiont of unknown identity and physiology (Bernhard, Goldstein and Bowser, in press). Other investigations suggested that low metabolic rates in oxygen-depleted habitats decrease the secretion of calcite and thus result in thinner, more-porous, and less-ornamented tests (Hendrix, 1958; Harmann, 1964; Kaiho, 1994). Generally, species of benthic foraminifera from oxygen poor habitats showed relatively high PD and P values as well as pore-size, which has been proposed as morphological low-oxygen indicator (Kaiho, 1994). The influence of

oxygen concentrations on PD and pore size was observed within single foraminiferal species. For instance, *Hanzawaia nitidula* (Bandy) from the oxygen minimum zone (OMZ) in the Gulf of Tehuantepec show more and larger pores than specimens from oxygenated waters (Perez-Cruz and Machain-Castillo, 1990). Furthermore, laboratory cultures of *Ammonia beccarii* (Linné) show an increase in pore-size under low-oxygen conditions (Moodley and Hess, 1992). These observations denote the potential of using the pore size and PD as a proxy for recent and past oxygen variations in their habitats.

Here, we explore the relationship between $[O_2]_{BW}$, $[NO_3]_{BW}$ and PD of the shallow infaunal species *Bolivina spissa* (Cushman) from the OMZ off Peru. Additionally, we will compare the PD relative to each other and with other environmental parameters as to water depth and temperature. The OMZ at the Peruvian continental margin extend from 50–550 m in depth. *Bolivina spissa* was found between 200–1200 m within and below the OMZ (Resig, 1990). The latter species is very tolerant to variations in oxygen concentrations. Ultrastructural analyses show that *B. spissa* possesses peroxisomes to convert H_2O_2 into water and oxygen (Bernhard 2001). Actually *B. spissa* can survive at least some time without oxygen and with increased H_2O_2 concentrations (Bernhard and Bowser, 2008). This makes this specie highly suitable for our investigations.

3.2 Materials and Methods

3.2.1 Sampling Procedure

Seven short sediment cores from the Peruvian OMZ were considered for the present study (Fig. 3.1, Table 3.1). The cores were recovered by using multicore technology during R.V. *Meteor* cruise M77/1 in October and November 2008. One additional core was sampled during R.V. *Meteor* cruise M77/2 in November and December 2008. Within a couple of minutes after the multicorer came on deck, one tube was chosen from the array, and brought to a laboratory with a constant room temperature of 4°C. Supernatant water of the core was carefully removed. Then the core was gently pushed out of the multicorer tube and cut into 10-mm-thick slices for benthic foraminiferal analysis. The samples were transferred to Whirl-Pak™ plastic bags and transported at a temperature of 4°C. One core was completely frozen, and later sliced and subsampled at IFM-GEOMAR, Kiel. The samples from these eight cores were used to collect the specimens for the analysis of PD. Core-doubles from six locations were sampled for supernatant water and pore-water for the analysis of nitrate-concentrations in the same temperature-controlled laboratory like the other cores. Supernatant water was

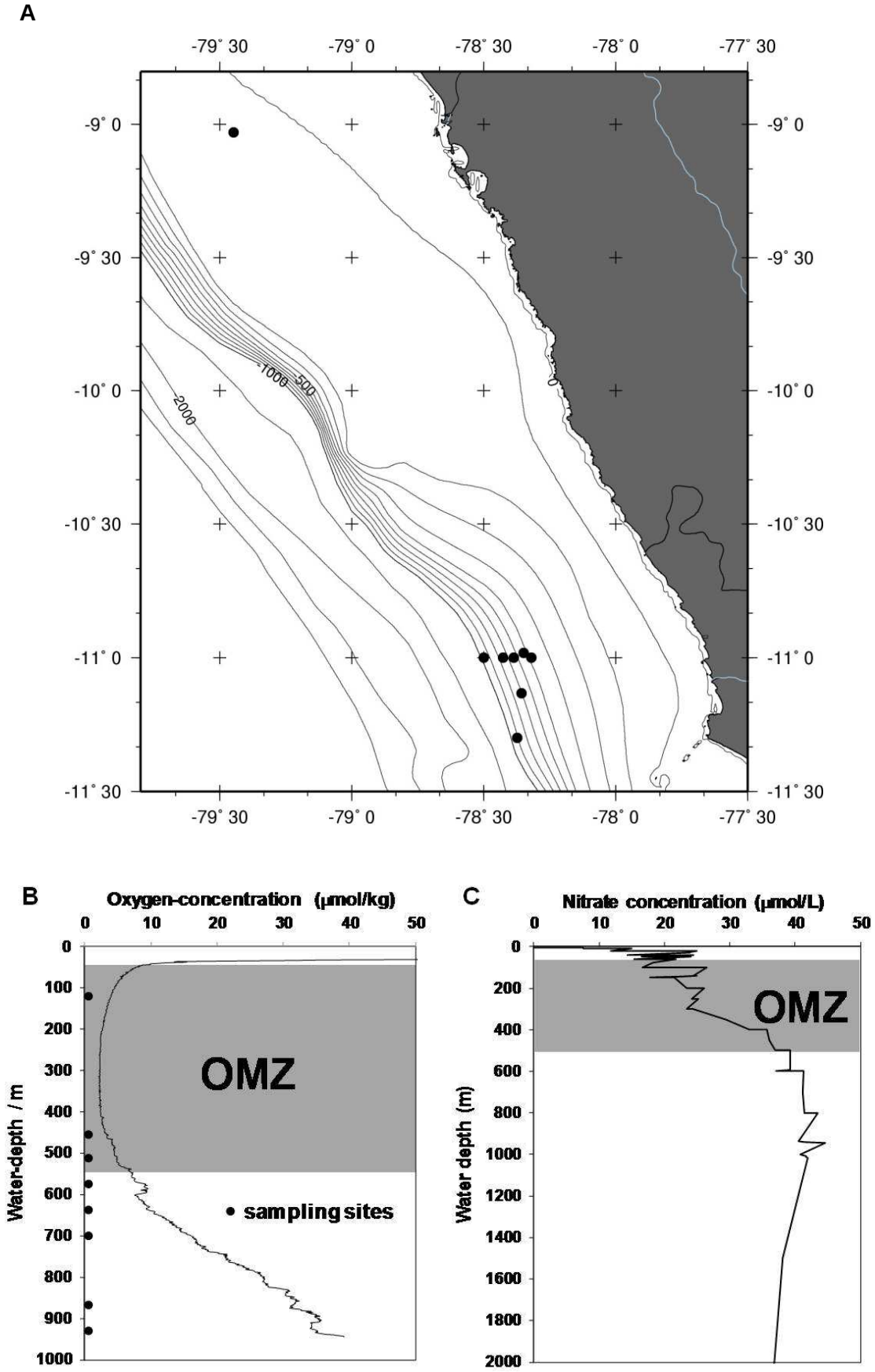

Figure 3.1. **A** Study area and **B** oxygen distribution at 11°S off Peru (water-column oxygen profile from M77/1-424/CTD-RO-9); **C** Nitrate distribution between 10°30' –11°15'S (data from six CTDs at different water depths).

collected with a syringe and filtrated via a syringe filter (0.2-nm cellulose-acetate filters) into a small PTFE-bottle.

The core-tube was placed in a glove bag flooded with argon to preserve pore water from oxygen contamination. The core was pushed out of the multicorer tube and was cut into 10-mm-thick slices and transferred into centrifuge tubules. The pore water was separated from sediments with a cooled centrifuge. The supernatant pore-water was also filtrated with a syringe-filter (0.2 nm cellulose-acetate filters) under argon atmosphere.

For 12 stations one separate multicorer tube was chosen to study benthic foraminifera that were living at the time of sampling (Tab. 3.2). The cores were sliced in 2- or 5-mm intervals from 0–10 mm, in 5-mm intervals from 10–40 mm, and in 10 mm intervals from 40–50 mm sediment depth in order to resolve the microhabitat depth structure. The samples were filled in PVC bottles, stained and preserved with a solution of 2 grams rose Bengal per liter of ethanol. Afterwards the samples were stored and transported at 4°C to IFM-GEOMAR, Kiel.

Table 3.1. Locations sampled for pore-density determination. (* indicates that $[NO_3^-]_{BW}$ was interpolated from the closest measured data points in the profile of $[NO_3^-]_{BW}$.).

Site	Longitude (S)	Latitude (W)	Water depth (m)	$[O_2]_{BW}$ (µmol/L)	$[NO_3^-]_{BW}$ (µmol/L)
M772-031-1 St694	79°26.88'	9°02.97'	114	1.07	18.30
M77/1-455/MUC-21	78°19.23'	11°00.00'	465	2.42	34.02
M77/1-516/MUC-40	78°21.00'	10°59.00'	513	2.40	36.08
M77/1-487/MUC-39	78°23.17'	11°00.00'	579	3.70	38.84
M77/1-565/MUC-60	78°21.40'	11°08.00'	640	8.17	40.10*
M77/1-459/MUC-25	78°25.60'	11°00.02'	698	12.55	40.98
M77/1-604/MUC-74	78°22.42'	11°17.96'	878	34.23	40.82*
M77/1-445/MUC-15	78°30.02'	11°00.00'	928	36.77	40.75

3.2.2 Foraminiferal Studies

The surface sediment samples corresponding to the top centimeter were washed over a 63-µm mesh sieve. The residues were collected in ethanol to prevent corrosion and dried at 50°C. They were further subdivided into the grain-size fractions of 63–125, 125–250, 250–315, 315–355, 355–400, and >400 µm. Up to 40 specimens of the shallow infaunal species *Bolivina spissa* and *B. seminuda* Cushman were picked from the 125–250 µm fraction. The larger fractions were considered when a sufficient number was not found in the 125–250 µm fraction. The 3 specimens shown in Figure 3.4 were mounted on aluminum stubs, sputter-coated with gold, and photographed with a CamScan-CS-44 scanning electron microscope (SEM) at the Christian-Albrecht-University in Kiel. All other specimens were mounted on

aluminum stubs and photographed with a Zeiss™ Leo VP 1455 SEM at the Geological-Palaeontological Institute of Hamburg University. Samples were not coated with a conductive layer to save them for further chemical analyses. To compensate charging effects on the specimens, the SEM was operated in a high pressure mode. Areas on the tests of the specimens were determined with Zeiss™ AxioVision 4.7. The pores from 232 specimens of *B. spissa* were counted on SEM photographs, and the pore diameter was assessed for a single specimen. Only megalospheric specimens were used for the analysis. All visible pores of a specimen were recorded. Because of the spatulate shape of the tests of *B. spissa*, we consider the pores recorded as half of all pores the specimen had. Additionally the PD and P of a single specimen of *B. seminuda* were determined. In this case pores were counted solely in an area of 10,000 μm^2 because of the strong homogeneity of pore distribution and the clavate shape of *B. seminuda*.

The rose Bengal-stained samples were washed on sieves with mesh sizes of 2,000 µm and 63 µm. The 63–2,000-µm size fraction was oven-dried at 50°C and weighed afterwards. The dried residues were divided with an Otto microsplitter until at least 300 well-stained individuals were counted. Specimens were picked onto Plummer cell slides, sorted by species, glued and tallied. The lengths of Living specimens were photographed taken with a MPX2050 CCD-camera from AOS™ coupled with a Navitar™ 6.5× zoom. The lengths of only well-preserved specimens were determined from these images with Zeiss™ AxioVision 4.7.

Table 3.2. Locations sampled for species distribution and test length determinations.

Site	Longitude (S)	Latitude (W)	Water depth (m)
M77-1-449/MUC19	11°26.01’	78°09.97’	319
M77/1-456/MUC-22	11°00.013’	78°19.23’	465
M77/1-459/MUC-25	11°00.03’	78°35.60’	697
M77/1-470/MUC-29	11°00.02’	77°56.60’	145
M77/1-473/MUC-32	11°00.01’	78°09.94’	317
M77/1-482/MUC-34	11°00.01’	78°14.17’	375
M77/1-516/MUC-40	11°00.00’	78°20.00’	511
M77/1-540/MUC-49	11°00.01’	77°47.40’	79
M77/1-553/MUC-54	10°26.38’	78°54.70’	521
M77/1-616/MUC-81	12°22.69’	77°29.05’	302
M77/1-622/MUC-85	12°32.757’	77°34.76’	823
M772-005-1 St.635	12°05.66’	77°40.07’	214

3.2.3 Environmental Parameters

Oxygen concentrations and temperatures in the water column were measured with a CTD-sensor. The oxygen sensor of the CTD was calibrated by Winkler titration of water samples taken during the respective CTD casts. Immediatly after retrieval, the CTD water was carefully subsampled into Winkler (~10 ml) flasks and the oxygen content was fixed immediatlely using 0.1 ml manganese (II) chloride and 0.1 ml alkaline iodide (Grasshoff et al., 1983). Oxygen concentrations were determined within 12 h by Winkler titration.

Nitrate concentrations in pore and bottom waters were measured onboard using a Metrohm 761 compact ion-chromatograph equipped with a Methrom/Metrosep A SUPP5 anion-exchange column (150/4.0 mm) and solution of Na_2CO_3 (3.2 mM) with $NaHCO_3$ (1.0 mM) as eluent. The IAPSO seawater standard was used for calibration. For two sampling sites (M77/1-565/MUC-60 and M77/1-604/MUC-74) $[NO_3^-]_{BW}$ was interpolated from the closest station on the 11°S transect, where $[NO_3^-]_{BW}$ was measured. The nitrate profile (Fig 3.1c) implies an error of ~2 µmol/L for the interpolated data.

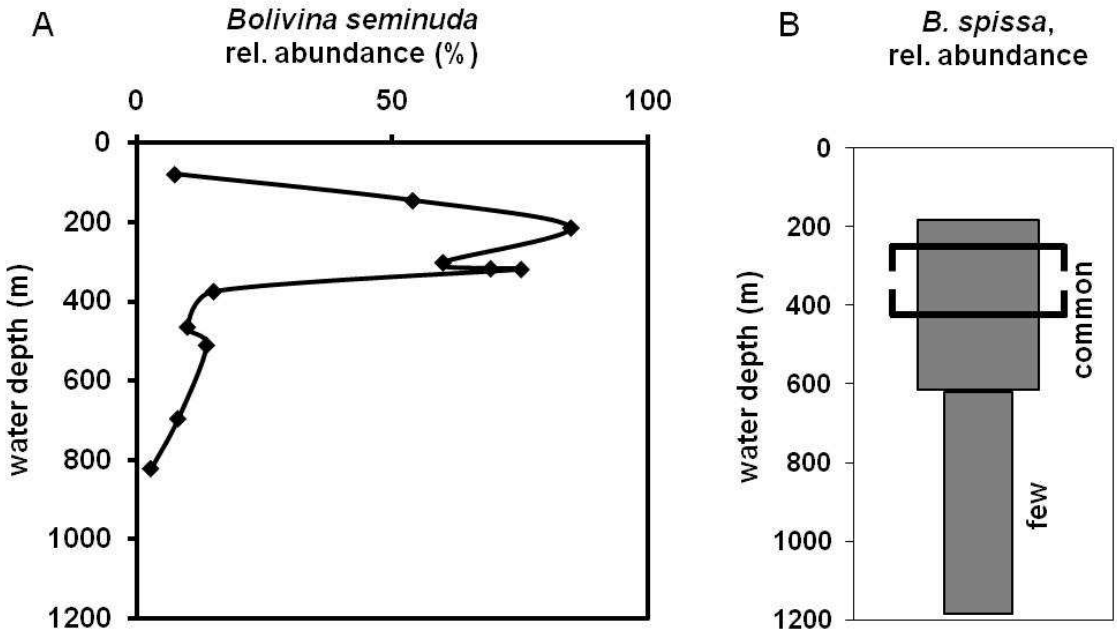

Figure 3.2. **A** Depth distribution of the relative abundance of *Bolivina spissa* in the study area (Resig, 1990). Brackets indicate the center of the OMZ, where no specimens were found in this study; **B** Depth distribution of *B. seminuda* in the study area.

3.3 Results

3.3.1 Species Distribution

Most specimens of *Bolivina seminuda* were found in samples from the central part of the OMZ. *Bolivina seminuda* was rare below the lower OMZ boundary (Fig. 3.2a) and *B. spissa* was missing from the OMZ centre. Living specimens of *B. spissa* could only be found at two sample locations, although dead individuals were present in all samples from 160–1200 m water depth except in the OMZ center from about 200–410 m water depth (Fig. 3.2b). This correlates with the depth distribution of *B. spissa* at the Peru-Chile-trench that was documented by Resig (1990). Empty tests of *B. spissa* were common at the lower boundary of the OMZ and became rare with increasing water depth. The absence of living *B. spissa* may be due to a strong seasonality in the abundance of living individuals, such as that which had been documented for *B. spissa* in the San Pedro Basin of the California Borderland, where its maximum abundance was in July (Silva et al., 1996). At Sagami Bay, Japan, the standing stock of *B. spissa* increased during spring (Nomaki et al., 2006). Furthermore, *B. spissa* is known to selectively ingest certain types of phytodetritus precipitated from the surface waters (Nomaki et al., 2006), indicating that its live cycle is related to phytoplankton blooms.

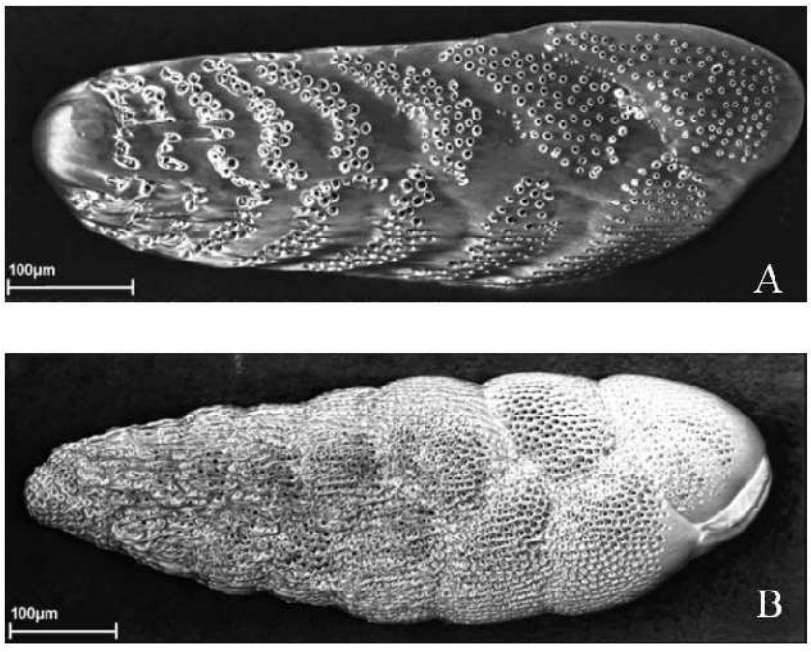

Figure 3.3. Comparison of **A** *Bolivina spissa* and **B** *B.seminuda* from the same location (M77/1-487-MUC-38; 579 m water depth).

3.3.2 Inter-Species Variation in Pore Density and Porosity

The depth ranges of dead *Bolivina spissa* and living *B. seminuda* overlap in the lower part of the OMZ (Fig. 3.2). In order to create a consistent data set of pore properties, we assessed the difference between the species in a sample where both were found (Fig. 3.3). The PD of *B. seminuda* was more than double that of *B. spissa*. Although the pore diameter of *B. seminuda* is slightly smaller than that of *B. spissa*, the P given as void-to-surface ratio is higher in *B. seminuda* (Table 3.3).

Table 3.3. Characteristics of the bolivinids shown in Figure 3.

Species	Number of pores	Surface area (μm^2)	Pore-density (PD)	Mean pore void (μm^2)	Porosity (P)
B. seminuda	178	10000	0.0178	4.47	0.28
B. spissa	649	97133	0.0067	6.23	0.20

3.3.3 Variability of Pore Density in Tests of *Bolivina spissa*

At first glance, an inverse PD-$[O_2]_{BW}$ correlation was recognized for *B. spissa* (Fig. 3.4). The PD decreases from 928 m water depth (Fig. 3.4c) from a PD of 0.00512 μm^2 corresponding to an $[O_2]_{BW}$ of 36.77 µmol/kg to a PD of 0.00801 μm^{-2} corresponding to an $[O_2]_{BW}$ of 2.42 µmol/kg. However, PD also increases within a single foraminiferal test from the early to the later chambers.

The increasing PD from earlier to later chambers is also reflected by a slight correlation of the overall PD with specimen size and total number of chambers (Fig. 3.5). Due to the observation that many specimens do not show more chambers we used the PD of the first ten chambers only relating to an area of about 50,000 to 60,000 μm^2 for the quantification of the PD-$[O_2]_{BW}$ relationship and for the quantification to other environmental parameters (Figs. 3.6 and 3.7). The area calibration was used because sometimes the exact number of chambers was difficult to determine.

3.3.4 PD Correlation with Environmental Factors

The PD of 4–60 individuals of *Bolivina spissa* in each of eight locations was determined. The standard error of the mean value range from 0.00012–0.00044 P/μm^2 corresponding to about 1–4% of the overall variation between all stations. Relationships of the mean PD to the

different environmental factors are presented in Figures 3.6 and 3.7 (also see Appendix 1 for graphic correlation plots of all data points)

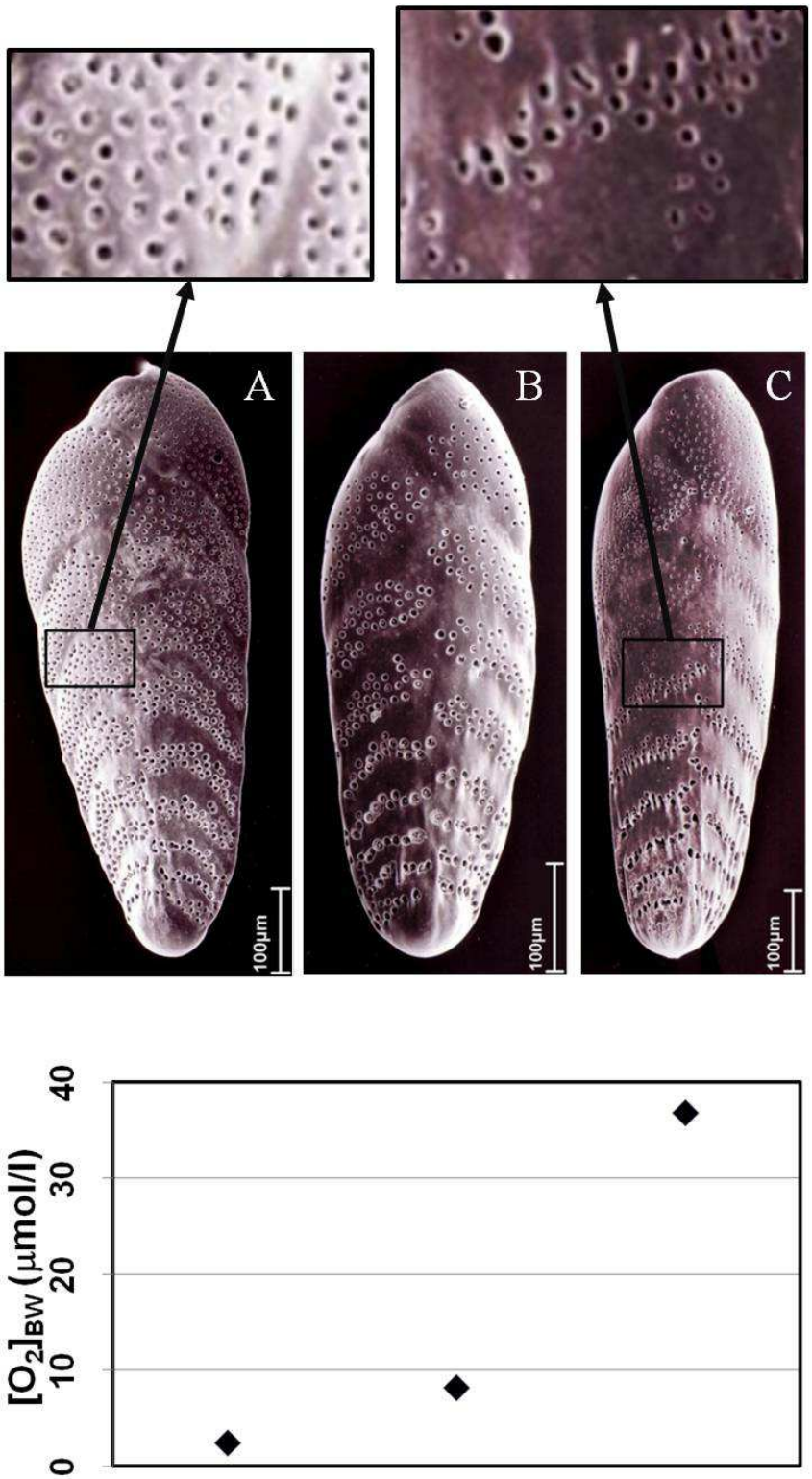

Figure 3.4. Scanning electron micrographs of three *Bolivina spissa* from different depths. The diagram on the right shows the different concentrations of bottom-water oxygen at the three locations: **A** M77/1-445/MUC-21, 465 m; **B** M77/1-566/MUC-59, 640 m; **C** M77/1-445/MUC-15, 928 m).

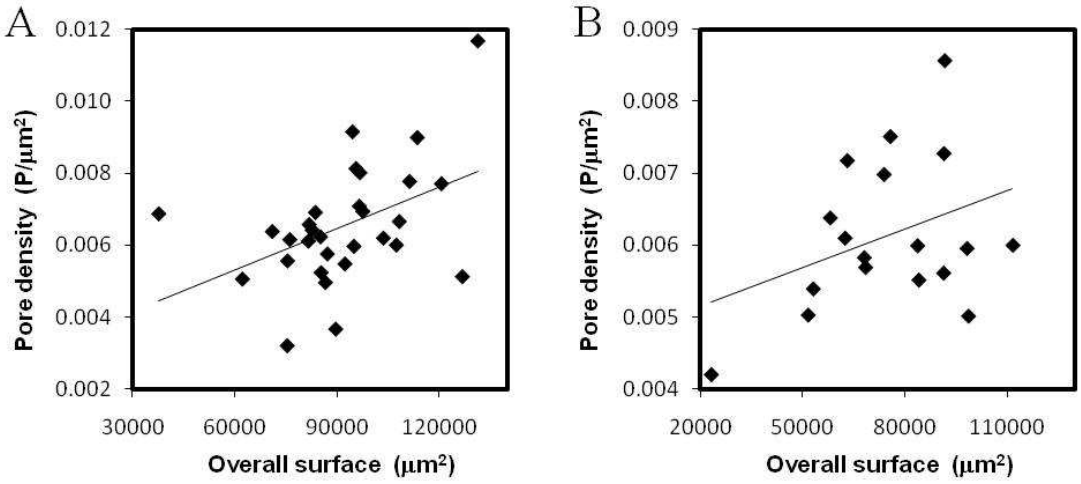

Figure 3.5. Correlation between overall pore density and specimen size of *Bolivina spissa* from two locations: **A** M77-1 445/MUC-15, 928 m; **B** M77-1 604/MUC-74, 878 m. Because PD is progressively greater on each additional (younger) chamber (see Fig. 4A), PD increases with overall test size (growth).

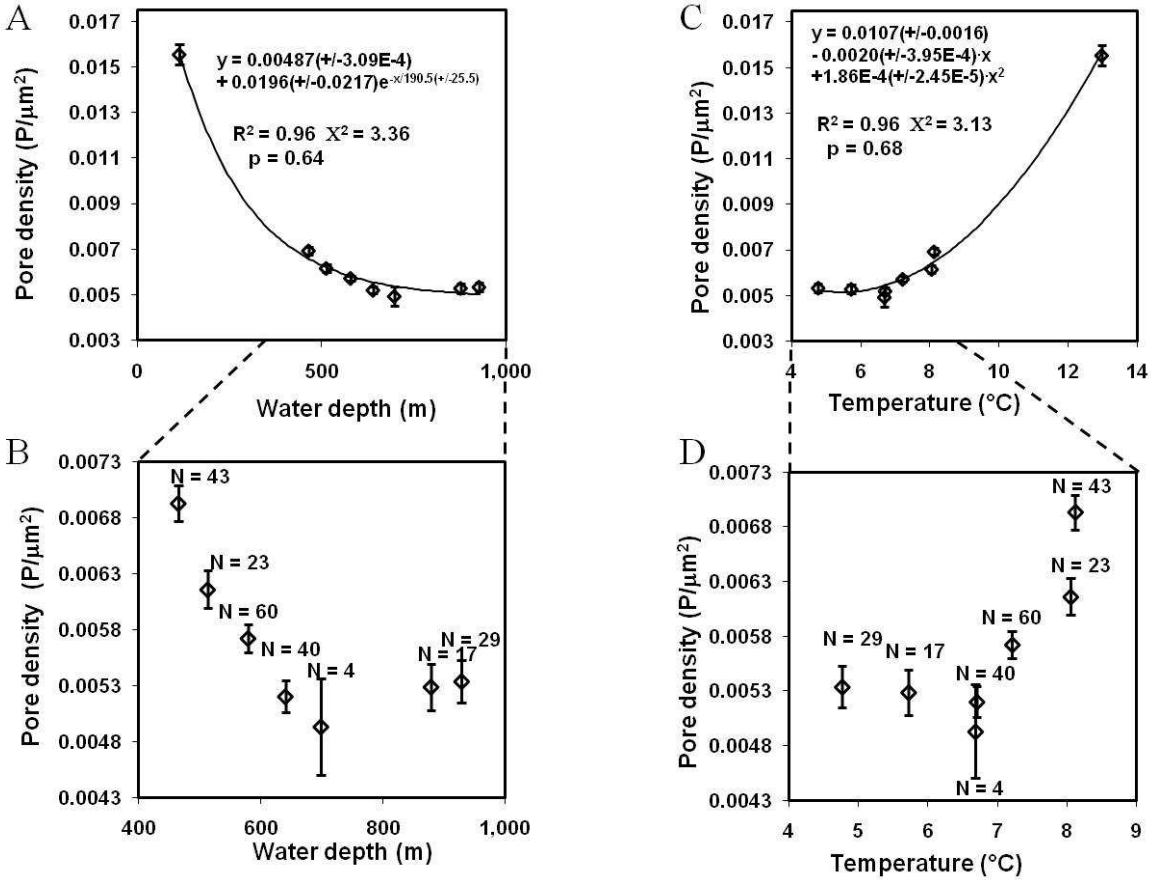

Figure 3.6. Correlations of *Bolivina spissa* pore density with **A, B** water depth and **C, D** temperature. PD of about the first 10 chambers (relates to an area of about 50,000–60,000 µm^2) is plotted. Error bars represent the standard error of the mean. Graphs **B** and **D** represent just the data from the seven deepest stations.

The relationship between PD and water depth is inverse between 114–640 m (Fig. 3.6a). At greater depths, the PD remains more constant, which results in the inverse exponential shape of the approximating function. The PD shows a clear relationship with temperature only above 7°C (Fig. 3.6b).

The PD-$[O_2]_{BW}$ relationship resembles that of PD-water-depth. The main difference between the two is the more abrupt change in slope where PD-$[O_2]_{BW}$ reaches a plateau. Hence, the PD-$[O_2]_{BW}$ dependency is restricted to low $[O_2]_{BW}$ concentrations in the range of 1–10 µmol/l. The highest significance (p = 0.98) was that of the PD-$[NO_3^-]_{BW}$ relationship (Fig 3.7b). This relationship is best approximated by an inverse exponential function.

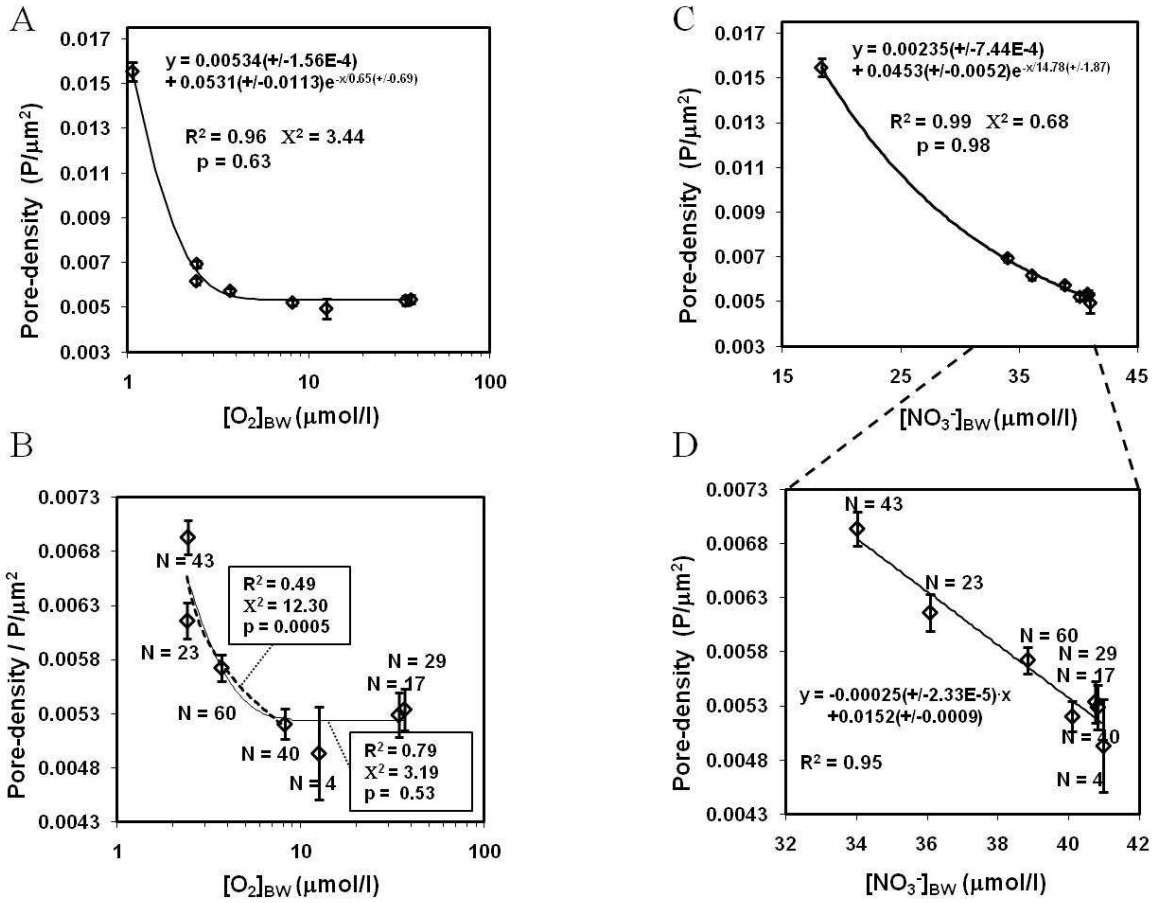

Figure 3.7. Correlations of *Bolivina spissa* pore-density with **A, B** $[O_2]_{BW}$ and **C, D** $[NO_3^-]_{BW}$. PD of about the first 10 chambers (relates to an area of about 50,000–60,000 µm^2) is plotted. Error bars represent the standard error of the mean. Graphs **B** and **D** represent just the data from the seven deepest stations. The dashed line in graph **B** fits only the 4 shallower data points where a correlation between $[O_2]_{BW}$ and PD exists.

3.3.5 Test Size Distribution in the Sediment

We determined the lengths of 92 stained *B. spissa* specimens from 698 m water depth and of 20 stained specimens from 820 m water depth. The length variation with sediment depth was

investigated to determine if there is any ontogenetic variation in the vertical distribution of *B. spissa* within the sediments. Our findings show that the mean length of living *B. spissa* specimens increases with depth in the sediment (Fig. 3.8). Thus, it appears that the juveniles prefer living close to the sediment surface.

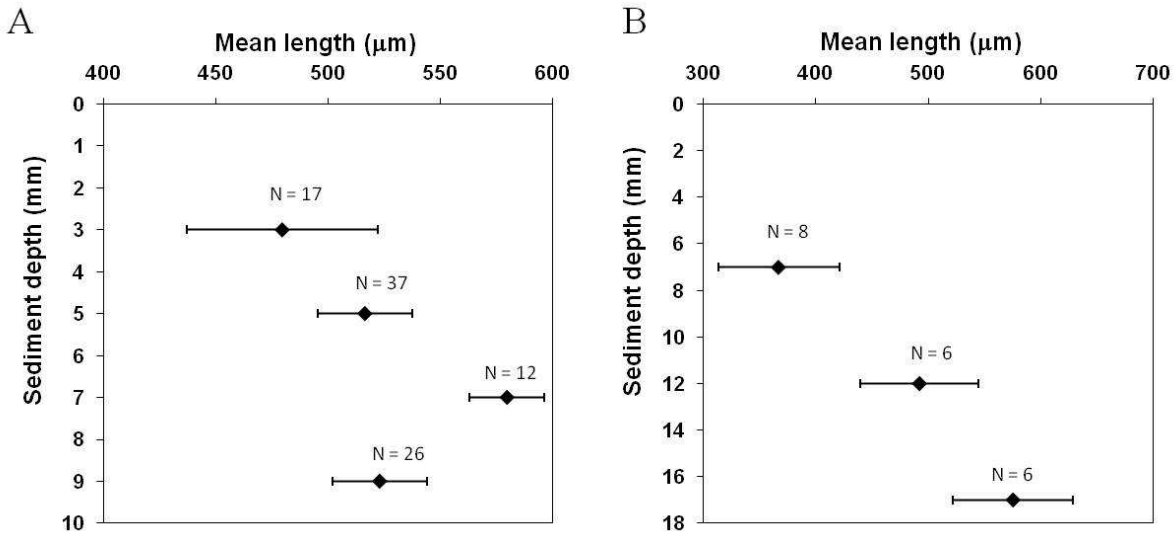

Figure 3.8. Mean length of living specimens at different depths within the sediment. Error bars represent the standard error of the mean. **A** M77-1 459/MUC-25, 698 m; **B** M77-1 621/MUC-85 (820 m).

3.3.6 Comparison between Bottom- and Pore-Water Nitrate Concentrations

The average nitrate concentration in the top centimeter of the pore water ($[NO_3^-]_{PW}$) was analyzed and compared to $[NO_3^-]_{BW}$ values at two stations (Fig. 3.1c). The results show that the average $[NO_3^-]_{PW}$ is significantly lower than $[NO_3^-]_{BW}$ at both stations. Furthermore $[NO_3^-]_{PW}$ show the same trend with water depth as the $[NO_3^-]_{BW}$. At the shallower station (465 m water depth) the $[NO_3^-]_{PW}$ is much lower than at the deeper station (928 m water depth).

3.4 Discussion

3.4.1 Morphologic Comparison of *Bolivina spissa* and *B. seminuda*

Bolivina seminuda is subconical with rounded edges and its lateral surface appears rough. In contrast, *Bolivina spissa* is lanceolate and nearly flat with a relatively smooth surface. In general, the surface-to-volume ratio appears to be higher in *B. seminuda* (Table 3.3) due to its surface texture as well as its P, which probably facilitates mitochondrial oxygen uptake (Leutenegger and Hansen, 1979; Kaiho, 1994).

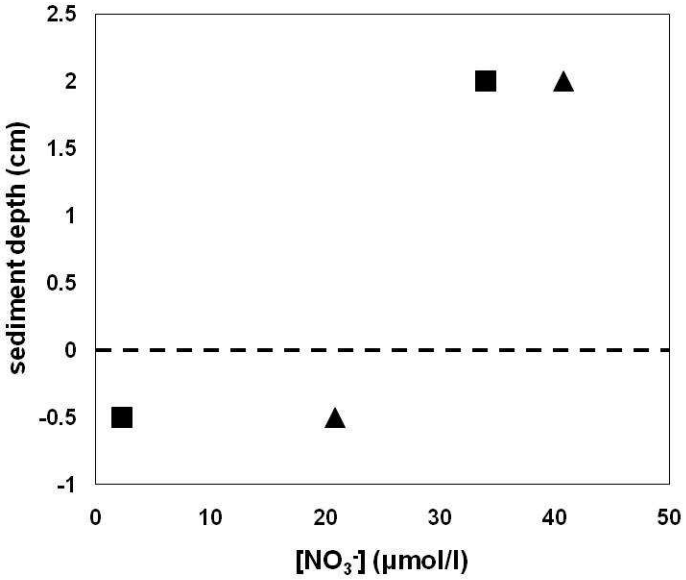

Figure 3.9. Comparison between $[NO_3^-]_{BW}$ (from ~2 cm above the sediment-water interface) and mean $[NO_3^-]_{BW}$ from the first centimeter of the sediment at two locations. The dashed line represents the sediment-water interface Triangles represent locality M77/1-445/MUC-15 (928 m) and squares indicate locality M77/1-455/MUC-21 (465 m).

3.4.2 Variability of Pore Density on Single Tests

On a single test of *B. spissa*, PD increases from the early to the latest chambers. The reason for this PD trend is uncertain and open to speculating several explanations:

1. Presumably, once a new chamber is formed, the entire test is overgrown by a new layer of calcite (Erez, 2003). As the protoplasm expands into the younger chambers, the earlier chambers need less "ventilation", so new calcite layers are allowed to overgrow some of the older pores.
2. Seasonal changes in bottom- or pore-water chemistry influence PD. As previously mentioned, *B. spissa* exhibits strong seasonality in abundance of living specimens (Silva et al., 1996, Nomaki et al., 2006); hence, it is conceivable that individual specimens also record seasonality. This implies that the lifespan exceeds the seasonal duration, and that reproduction occurred before the phytodetritus had reached the seafloor.
3. The surface:volume ratio progressively decreases with test growth so that more pores are needed on the later chambers for sufficient communication between the protoplasm and the external environment.
4. Ontogenetic changes in the vertical distribution of *B. spissa* in the sediment influence PD. The average length of specimens is smaller near the surface (Fig. 3.8) than below,

suggesting that the juveniles live in a shallower pore-water environment that has higher $[O_2]_{BW}$ while the adults tolerate a larger range of pore water $[O_2]_{BW}$ that includes dysoxic levels.

3.4.3 Environmental Influences on Pore Density

The two foraminiferal species largely differed in their PD at one sampling site, but there was also PD variability among the other samples. As previously discussed, we compared the PD of *B. spissa* to several environmental factors (i.e., water-depth, temperature, $[O_2]_{BW}$, and $[NO_3^-]_{BW}$). In the following, we further examine different hypotheses to explain why *B. spissa* may adapt its pore density to external environmental forcing.

Test Strength

A lower PD but thicker test-wall in the deeper core sections (Fig. 3.6a) may reflect an increased ability to withstand greater hydrostatic pressure. However, the tests of foraminifera have openings that would enable the test to equalize its internal pressure with the external environment; hence, it is very unlikely that the bathymetric pressure gradient influences PD.

Another possible reason for increasing test strength as a function of water-depth may involve the sedimentary texture, as documented by Harmann (1964). The shallower stations were characterized by dark mud partly mixed with foraminiferal sand. At stations >640 m, the sediments grade into phosphatic sand. At the deepest station (928 m), the sediment is a coarse sand composed of phosphatic pellets. A thicker test could be advantageous on sands, which are more abrasive than muds and generally indicate higher-energy environments; therefore, in this particular case, thicker-walled *B. spissa* would inhabit the deeper stations. To the contrary, however, there is a strong PD correlation with water-depth at the shallower stations (<640 m) where the sedimentary texture does not show strong variability.

Influence of Temperature on Test Calcification Rate

At the stations studied, temperature decreases with water depth, and pore density correlates with both (Fig. 3.6b). Lutze (1962) proposed temperature dependency of certain chemical processes as a possible explanation for PD variability in *Bolivina spissa*. The only plausible explanation for temperature dependence of PD would be that higher temperatures enable higher metabolic rates and thus generate higher rates of calcite precipitation (Harmann, 1964). This could result in thicker, stronger tests but fewer pores at higher temperatures, which would be contradictory to our observations. However, the influences of carbonate ion

concentrations or pH, which also can influence calcite precipitation rates, were not examined because those parameters had not been measured at the time of sampling.

PD-$[O_2]_{BW}$ Relationship in Bolivina spissa

Based on previous studies, one may speculate that the inverse PD-$[O_2]_{BW}$ correlation shown in Figure 3.7a is due to an increase in mitochondrial oxygen uptake and decrease in oxygen levels. Hence, the PD rises as a function of decreasing oxygen availability. From our data, we may interfere that an $[O_2]_{BW}$ value of ~10 µmol/l represents a minimum threshold for decoupling PD from oxygen availability. At least three explanations for this phenomenon are possible:

1. A minimal pore-density may be necessary for survival, which could explain the uniform pore densities at higher oxygen levels.
2. Oxygen penetration into the sediment is greater below more-oxygenated bottom waters. Shallow-infaunal species may migrate vertically to where food availability and the oxygen level meets their individual requirements (Jorissen et al., 1995; Duijnstee, 2003). The number of examined specimens could therefore include specimens that were living at different levels of pore-water oxygenation.
3. Benthic species in well-oxygenated habitats have their mitochondria more uniformly distributed in the cytoplasm and not clustered near pore terminations (Berthold, 1976; Leutenegger and Hansen, 1979; Sen Gupta and Machain-Castella, 1993). If this applies to *Bolivina spissa* living in oxygenated sediment, the PD would not exhibit a relationship with bottom-water oxygenation.

PD-$[NO_3^-]_{BW}$ Relationship in Bolivina spissa *as Evidence of Nitrate Respiration*

Some species of benthic foraminifera living in disoxic environments recently have been shown to respire nitrate via denitrification (Risgaard-Petersen et al., 2006). Intracellular nitrate-stores are used for denitrification as augmented energy sources when there is insufficient oxygen. Our data support this observation because the PD-$[NO_3^-]_{BW}$ relationship shows a significant correlation ($p = 0.98$; Fig. 3.7b).

The influence of foraminiferal denitrification on the local nitrogen budget has recently been documented in deep-sea sediments of Sagami Bay, Japan (Glud et al., 2009). Intracellular nitrate storage represented ~80 % of the total benthic nitrate-pool. *Bolivina spissa* shows significant intracellular NO_3^- enrichment. However, the minimum $[O_2]_{BW}$ level at Sagami Bay of 55–60 µmol/kg is still significantly higher than at our sampling sites off Peru that have

$[O_2]_{BW}$ values of 1–37 µmol/l. It is conceivable that the dependency of shallow infaunal species to nitrate-respiration may be much higher at bottom-water oxygen concentrations that are lower than those in Sagami Bay.

The denitrification process in benthic foraminifera has not been attributed to a specific cell organelle yet (Høgslund et al., 2008). In the light of our results. it may be anticipated that the pores are directly related to nitrate-uptake or may act as a kind of "valve" for N_2 release. From the observation that foraminiferal mitochondria tend to cluster behind the pore plugs, as observed from a *Bolivina* in low-oxygen conditions, the mitochondria may also be involved in the mechanism of denitrification. This is supported by the observations of Finlay (1983) who showed that the number of mitochondria became significantly enhanced in the primitive eukaryote *Loxodes* when it switched from oxygen to nitrate-respiration. The recent observation of microbial ectobionts of unknown identity and physiology inhabiting the pore void of *B. pacifica* (Bernhard et al., 2010) provoke speculations on whether ectobionts also exist in the pores of *B. spissa*.

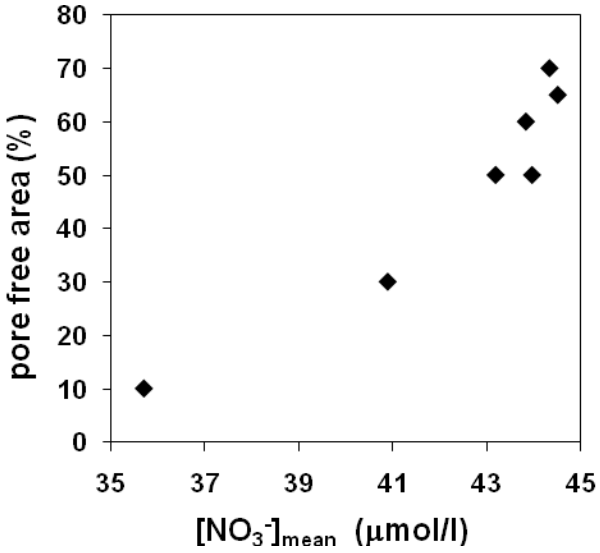

Figure 3.10. Correlation between the pore-free area of *Bolivina spissa* from the California Borderland (from Lutze, 1962) and the mean nitrate concentration from similar water depths at the same study area $[NO_3^-]_{mean}$ as recorded in the World Ocean Atlas 2009 (Boyer et al., 2009). All available nitrate data from the region between 31.5–33.5°N and 121 –119°W were used. Mean values where calculated from every datapoint at the same water depth ±20 m.

An early study on *B. spissa* (Fig. 3.10) from the Californian Borderland shows that the pore-free area increases with water depth (Lutze, 1962), which was thought to reflect decreasing

water-temperatures. Alternatively, and following our arguments above, this may also reflect nitrate distribution in the water column. Nitrate is depleted in shallower water due to enhanced primary production on the ocean's surface. So the habitats of the analyzed specimens from shallower water- most probably were more nitrate-depleted than those from deeper waters. Also, the specimens from shallower water had broader tests with more costae. Higher length:width increases the surface:volume ratio, which could enhance its uptake of nitrate. Figure 3.10 shows a strong inverse correlation between the proportion of the test that is pore-free (from Lutze, 1962) and the mean nitrate concentration later recorded from similar water depths in the same study area (Boyer et al., 2009).

Nitrate microprofiles were not available for our sampling locations, so it was not possible to quantify the nitrate concentration directly from where the nitrate uptake by the foraminifera occurred. However, nitrate microprofiles from the OMZ off Chile indicated intense nitrate consumption at the sediment–water interface (Høgslund et al., 2008). A comparison of $[NO_3^-]_{BW}$ and mean pore water nitrate concentrations from the first centimeter of sediment revealed that the nitrate concentration in a hypothetic zone of nitrate-uptake was significantly lower than in the bottom water (Fig. 3.9). This infers that an adjustment of the foraminiferal microhabitat, which may influence the PD, is important for nitrate uptake. Nevertheless, changes in $[NO_3^-]_{PW}$ reflect changes in $[NO_3^-]_{BW}$, although there are secondary factors in the spatial and temporal variations of $[NO_3^-]_{PW}$ that superimpose this relationship (see Fig. 3.9). However, the smaller specimens apparently prefer shallower depths in the sediment (Fig. 3.8). Since we used just the first ten chambers for PD determination, the PD signature may represent more shallow pore-water environments that are closely related to the bottom-waters. We hypothesize that foraminifera optimize their abilities for nitrate uptake in nitrate-depleted habitats by increasing their pore density to achieve a competitive advantage over other prokaryotes.

It is possible that foraminifera take up nitrate for respiration inside seawater vacuoles. *Bolivina pacifica* has several seawater vacuoles near its mitochondria that are clustered at the pores (Bernhard, et al., 2010). Foraminifera could migrate upwards in the sediment to where much nitrate is available in order to fill their vacuoles so they can survive deeper in the substrate. This assumes that the pores are not involved in intracellular nitrate uptake but rather act as valves for the removal of N_2 from the cytoplasm. However, it would difficult to explain why the pore density should increase if less nitrate is available. If there is more nitrate available, more nitrate is likely to be consumed; therefore, more pore "valves" would be needed for N_2 removal. Instead, the foraminifer might optimize its denitrification abilities by

accumulating more mitochondria to efficiently use the remaining nitrate when less nitrate is available, and this could result in higher PD.

Interaction of Multiple Factors

More than one factor might influence PD, such as both the oxygen and nitrate concentrations. Perhaps *Bolivina spissa* switches stepwise from oxygen to nitrate respiration when oxygen concentrations draw down substantially. Whereas the primitive eukaryote *Loxodes* increases its number of mitochondria when it switches to nitrate-respiration (Finlay, 1983), *B. spissa* may do likewise to increase the number of mitochondria, which implies that the number of pores would also increase stepwise. If it switched completely to nitrate respiration, the nitrate concentration might become the controlling factor, and if nitrate levels drop, the PD would increase to optimize its uptake.

3.5 CONCLUSIONS

In this study, we found a strong correlation between PD-$[O_2]_{BW}$ and PD-$[NO_3^-]_{BW}$ in *Bolivina spissa*. The higher significance of the PD-$[NO_3^-]_{BW}$ correlation suggests that PD is more sensitive to $[NO_3^-]_{BW}$ than to $[O_2]_{BW}$. Although interactions between multiple parameters (e.g., O and N) may also influence PD, we propose that foraminifera in nitrate-depleted habitats optimize their nitrate uptake by increasing PD.

The clustering of mitochondria behind the pore plugs of several foraminiferal species is probably an adaptation to oxygen-depleted habitats (Leutenegger and Hansen, 1979; Bernhard et al., 2010) that may be involved in nitrate respiration. A comparison of PD, P, and shape of *B. spissa* and *B. seminuda* suggests that *B. seminuda* is better adapted to live in disoxic environments. Future studies will examine the potential use of pore density in *B. spissa* as a proxy for present and past nitrate concentrations.

3.6 Acknowledgments

We thank Anna Noffke, Florian Scholz, Bettina Domeyer, Meike Dibbern, and Renate Ebinghaus for performing bottom- and pore-water nitrate measurements, Sonja Kriwanek for calibrating oxygen concentrations and Ute Schuldt for support in the operation of the SEM at the Christian Albrecht University in Kiel. The scientific party on R/V METEOR cruise M77 is acknowledged for their general support and advice in multicorer operation and sampling.

The "Deutsche Forschungsgemeinschaft, (DFG)" provided funding through SFB 754 "Climate– Biogeochemistry Interactions in the Tropical Ocean."
Received 28 September 2009

APPENDIX 3.1

Correlations of *Bolivina spissa* pore density with **a** water depth; **b** temperature; **c** bottom-water oxygen concentrations, and **d** $[NO_3^-]_{BW}$ concentrations. PD of about the first ten chambers (surface area of about 50000–60000 μm^2) is plotted. Data of all examined specimens was used. This figure can be found on the Cushman Foundation website in the JFR Article Data Repository (http://www.cushmanfoundation.org/jfr/index.html) as item number JFR-DR20110001.

APPENDIX 3.2

Pore-densities and data for pore-density determination. This table can be found on the Cushman Foundation website in the JFR Article Data Repository (http://www.cushmanfoundation.org/jfr/index.html) as item number JFR_ 20110001.

SUPPLEMENTARY APPENDIX A3.3

(Ultrastructural observations on *Bolivina spissa* cells)

This part is ***not published in the original manuscript***. But since the results presented here are directly linked to the previous results of this chapter this work is presented here. It connects the results of the morphological observations directly to the cell biology of *Bolivina spissa* and describes ultrastructural observations on thin sections of *B. spissa* cells.

A3.3.1 Material and methods

A3.3.1.1 Sampling procedure

One short sediment core (SO206-43; 568 m water depth; 8°52.27’ S; 84°14.10’ W) from the Pacific continental margin off Costa Rica was considered for the present study. The core was recovered by using multicore technology during R.V. *Sonne* cruise SO206 in June 2010. This core was taken for cell fixation experiments. Just before the cores were coming on deck a fresh solution of 5% Glutaraldehyde and 0.1 M cacodylate buffer were mixed out of 1 part 25% Glutaraldehyde, 2.5 parts 0.2 M cacodylate buffer, pH 7.2, and 1.5 parts of distilled water. Within a couple of minutes after the multicorer came on deck, one tube was chosen from the array, and brought to a laboratory with a constant room temperature of 4°C. In less then one hour after the cores were recovered they were cut into 10 mm thick slices and 15-16 ml of sediment were transferred into 50 ml centrifuge tubules. These tubules were filled up with the fixative and mixed sufficiently without rigorous shaking and stored at 4° C.

A3.3.1.2 Preparation for ultrastructural investigations

Samples were processed for embedding in the Woodshole Oceanographic Institute. A few ml of concentrated Rose Bengal solution were added to the samples and they were incubated in a refrigerator overnight. Small amounts of the fixed sediment were wet sieved with 0.1 M cacodylate buffer. Stained specimens of *Bolivina spissa* were wet picked from 0.1 M cacodylate buffer and decalcified in a 50 mM EDTA/0.1 M cacodylate buffer solution in 10 ml glas vials for five hours in a refrigerator. Maximal five specimens were transferred into one vial. Examples for the used specimens of *B. spissa* are shown in fig. A3.3.1. The samples were rinsed 3 times with 0.1 M cacodylate buffer. The vials were filled with 2-3 ml of a chilled 0.5% OsO_4/0.1 M cacodylate buffer and transferred into a darkened, ice filled bucket. The samples were incubated for 1 hour and rinsed 4 times with chilled distilled water afterwards. Afterwards the specimens were taken through a series of ethanol dehydrations (30%, 50%, 70%, 90% twice, 100% twice). Each dehydration step lasted for 15 minutes. The

Figure A3.3.1: Specimens of *Bolivina spissa* fixed in glutaraldehyde/cacodylate buffer and stained with Rose Bengal. SO206-43; 568 m water depth.

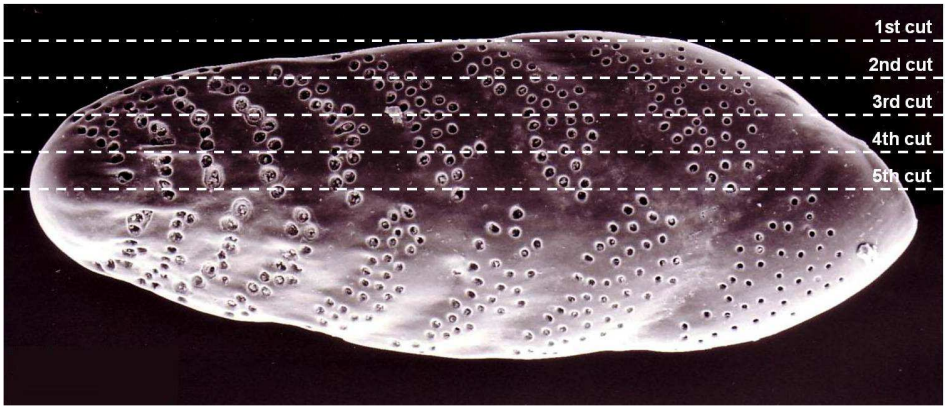

Figure A3.3.2: SEM micrograph of *Bolivina spissa* showing how a specimen was cut to yield five thin-sections.

dehydration was finished with acetonitrile. The specimens were transferred into another glass vial filled with 1:1 mix of acetonitrile and uncatalyzed Epon-Araldite resin and left overnight. Specimens again were transferred into a fresh glass vial filled with uncatalyzed resin, placed in a rotator and left for 24 hours. Finally the specimens were transferred into embedding molds and placed in oven temperature (70°C) for 12 hours. The single specimens were cut out of the main part of the resin. Due to their spatulate shape the embedded specimens settled down in the resin and stayed lying down on one of the flat sides. In this study most attention is paid on the pores in *Bolivina spissa*. The pores are located on the flat sides up and down the test. Thus to include the pores in the thin sections the cuts have to be made from the upper part to the lower part of the specimen (see fig. A3.3.2). Therefore after cutting out of the main part of the resin, the specimen was reembedded to assure that it is completely surrounded by

resin. Afterwards it was sectioned to approximately 90 nm thick sections and placed on slot grids. Sections on grids were stained with uranyl acetate. The specimen was divided in five sections. The first one at the peripheral side and four more in equidistant steps to the middle of the specimen (see fig. A3.3.2). Three replicates have been done from each section (in 90 nm distance). The grids were viewed at a FEI 208 S transmission electron microscope (TEM).

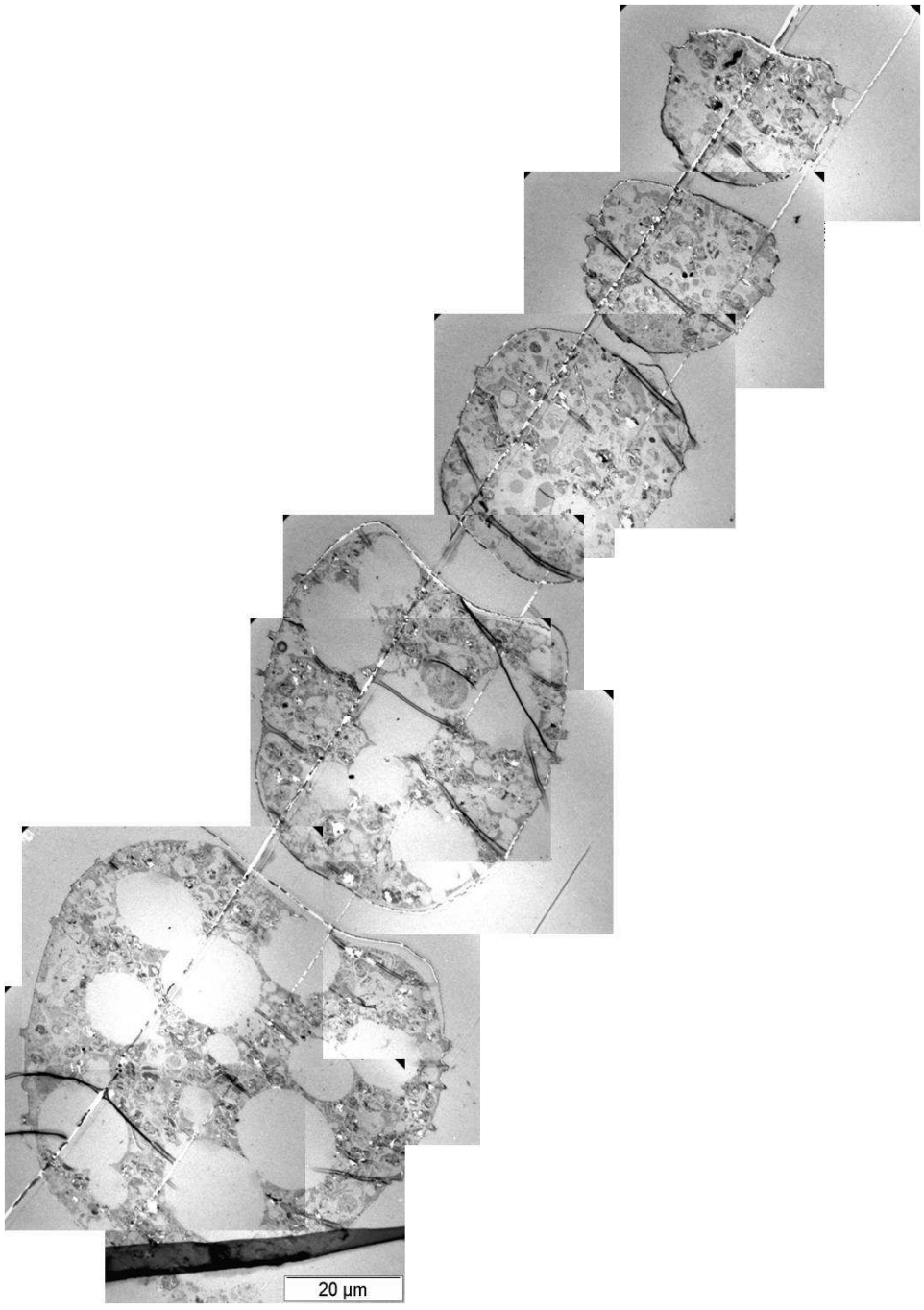

Figure A3.3.2: Collage of TEM micrographs from a thin section of a *Bolivina spissa* cell which reconstructs the whole section. Note that seawater vacuoles are frequent in the youngest two chambers while absent in the older chambers.

A3.3.2 Results

A3.3.2.1 Ultrastructural observations in *Bolivina spissa*

A collage of TEM micrographs reconstructing one whole section from the middle part of *Bolivina spissa* (5^{th} cut) is shown in fig. A3.3.3. A lot of seawater vacuoles are clustered in the last two chambers while there are no visible seawater vacuoles in the older chambers. Food vacuoles for deposit feeding can be found in every part of the cell although they appear to be more often in the younger chambers. Several TEM micrographs from pores in *B. spissa* are shown in fig. A3.3.4. Mitochondria (m) are clustered behind almost every pore (p) (also in the pictures which are not shown). In many pores some parts of the inner organic lining (IOL) which would be located at the inner part of the pores (piol) is still at least partially preserved. Actually in the pore shown in fig. 3.3.4 **d)** the whole inner organic inside the pore is preserved and the pore is still covered by a pore plate (pp). Also in this pore still some bacteria seem to be preserved. Food vacuoles (fv) with ingested detritus are present everywhere in the cell from the periphery (fig. 3.3.4 **d)**) to the inner parts of the cell (fig. 3.3.5 **a)**&**b)**) and even in the proloculus (fig. 3.3.5 **c)**). No visible mitochondria have been found in other parts of the cell except the ones clustered behind the pore terminations. Unfortunately sometimes the mitochondria are not exactly discernible. Thus a quantification of mitochondria clustered behind the pores is not possible. In some of the inner cell parts peroxisomes (po) are present (fig. 3.3.5 **b)**) while in the proloculus parts of an endoplasmatic reticulum have been found (fig. 3.3.5).

A3.3.3 Discussion

A3.3.3.1 Ultrastructural observations in *Bolivina spissa*

Although their quantification was not possible it seems like that the mitochondria in the analysed specimen of *B. spissa* are solely clustered behind the pore-terminations because they have not been found in any other parts of the cell. Similar observations have been done in cells of several other foraminiferal species from oxygen depleted environments including some Bolivinidae, too (Leutenegger and Hansen, 1979; Bernhard et al., 2010). The pores in *B. spissa* are supposed to be adapted to the intra-cellular nitrate uptake for nitrate-respiration (Glock et al. 2011a&b). The denitrification process in benthic foraminifera has not been attributed to a specific cell organelle yet (Høgslund et al., 2008). Since it seems like the pores are directly related to intracellular nitrate-uptake the fact that mitochondria tend to cluster behind the pore plugs in *B. spissa* might imply that mitochondria may also be involved in the mechanism of foraminiferal denitrification. Indeed earlier studies showed that mitochondria

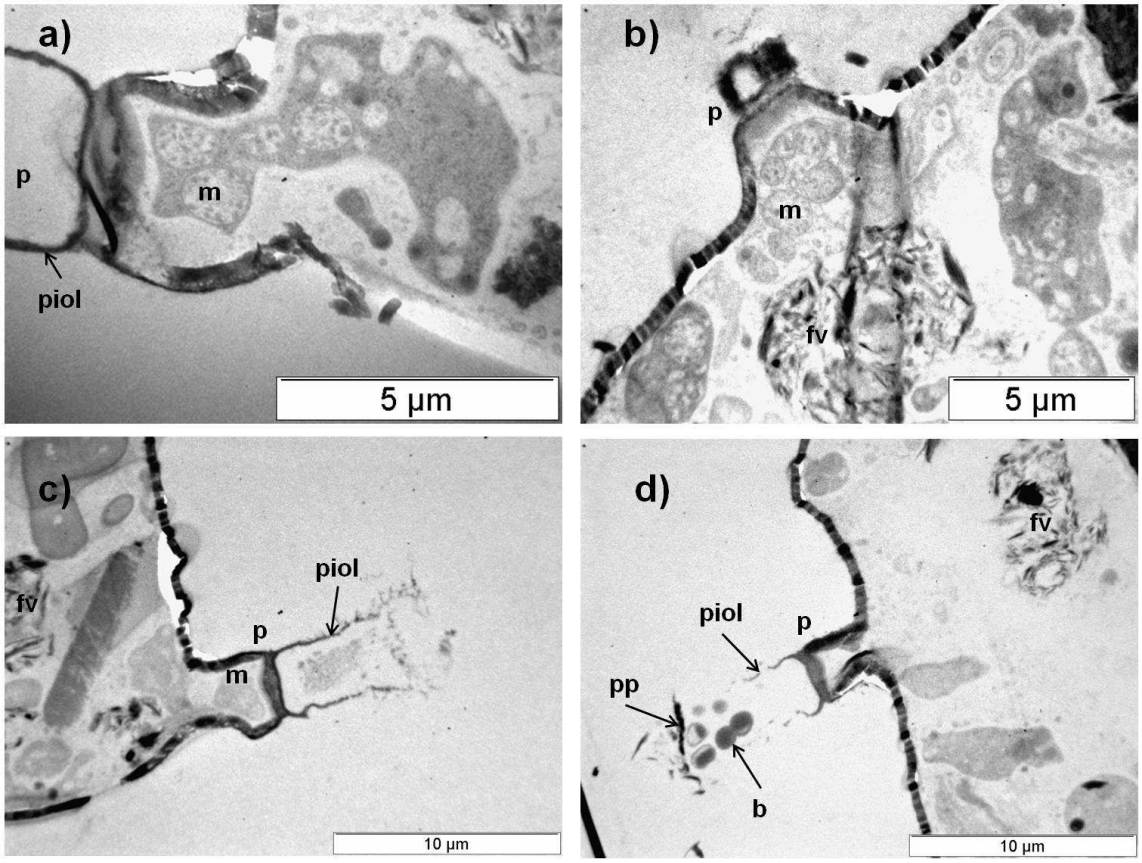

Figure A3.3.4: TEM micrographs showing the pores (p) in *Bolivina spissa*. Mitochondria (m) are present in nearly every pore (**a**-**c**). Often the inner organic lining from the inner part of the pores (piol) is at least partitially preserved (**a**, **c**&**d**). The pore in **d** is still covered by a pore plate (pp) and seems to be inhabitated by bacteria (b). On several micrographs food vacuoles for deposit feeding (fv) are present.

are involved in nitrate respiration of the primitive eukaryote *Loxodes* (Finlay et al., 1983). In particular the number of mitochondria became significantly enhanced when *Loxodes* switched from oxygen to nitrate-respiration. Since the pore density in *B. spissa* is inverse proportional to the nitrate availability (Glock et al., 2011a) and mitochondria are clustered behind pore terminations it is reasonable to assume that mitochondria in cells of *B. spissa* are inversely correlated to the nitrate availability, too. As much more there is a reason to speculate if mitochondria are at least involved inside the foraminiferal denitrification process. The recent observation of microbial ectobionts of unknown identity and physiology inhabiting the pore void of *Bolivina pacifica* (Bernhard et al. 2010) provoke speculations if such ectobionts exist in the pore void of *Bolivina spissa* as well and are indeed denitrifiers. Indeed some bacteria have been found inside the pore void of *B. spissa*.

Another point of interest is that the seawater vacuoles seem to be present only in the youngest chambers of *Bolivina spissa*. This might explain why fixed specimens of several foraminiferal species often show a much stronger coloration in the older chambers, especially the

proloculus, when they have been stained. Among other things foraminifera use seawater vacuoles to adapt their surface to volume ratios to osmotic changes in the surrounding seawaters. It might be that in the older chambers the cytoplasm is better isolated against the environment and does not need seawater vacuoles for the adaption against osmotic changes. Additionally laminated calcareous foraminifera use seawater in vacuoles as a reservoir for the precipitation of calcite (Erez, 2003). When a new chamber grows all old chambers are covered by a new layer of calcite, too. The vacuoles are transported through the cytoplasm surrounding the whole test to the outer part of the test. The transport of the seawater vacuoles from the older chambers to the outside would consume much more energy than the transport from the newest chambers which are located near the aperture. The presence of food vacuoles filled with detritus for deposit feeding in benthic foraminifera (Goldstein and Corliss, 1994) and the presence of peroxisomes in the cytoplasm of *B. spissa* (Bernhard et al., 2001) are well documented in previous studies.

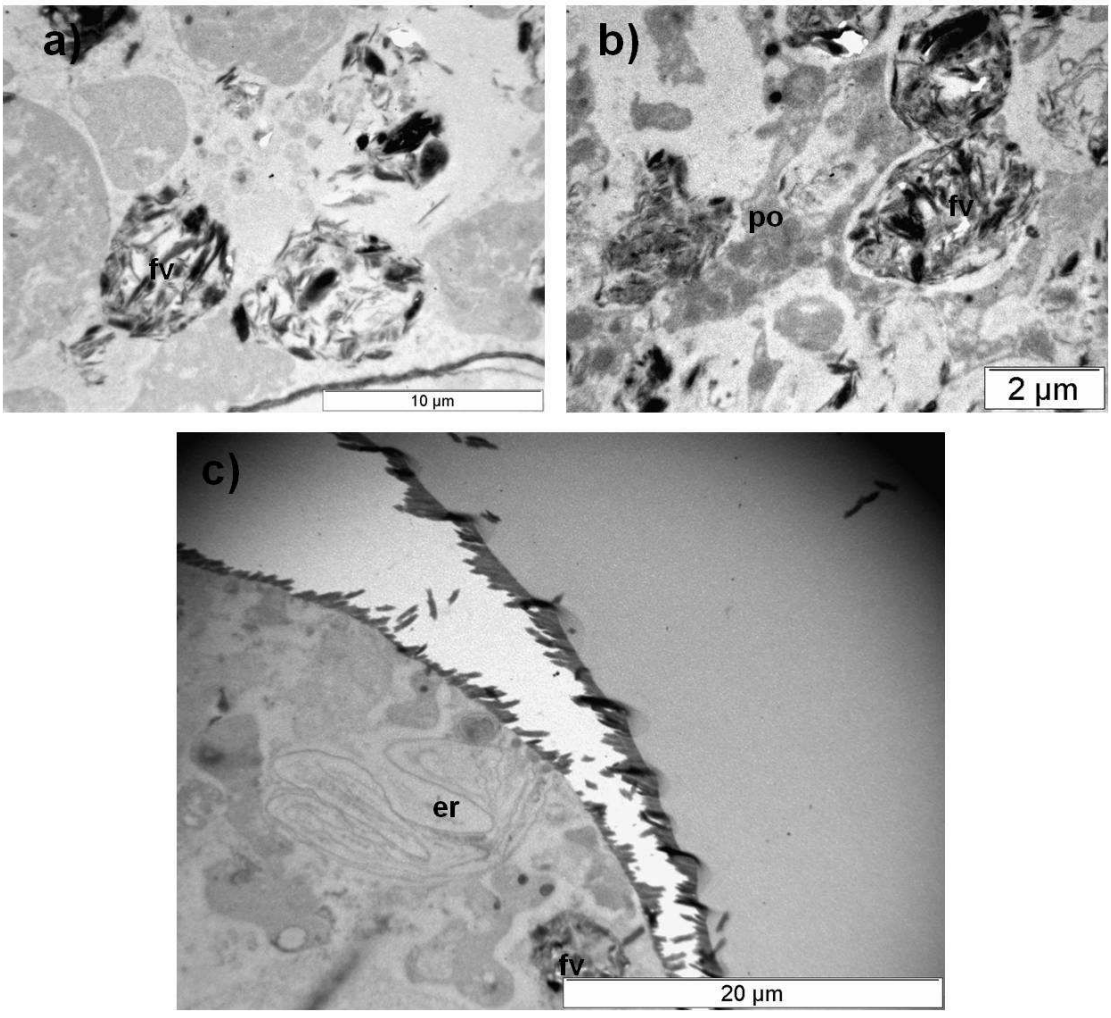

Figure A3.3.5: TEM micrographs showing the inner part of the cell and the proloculus of *Bolivina spissa*. Food vacuoles (fv) are very frequent (**a**-**c**). In some parts of the cell peroxisomes (po) can be found (**b**). Note the presence of an endoplasmatic reticulum (er) in the proloculus (**c**).

Chapter 4

APPLICATIONS FOR THE USE OF THE PORE DENSITY IN BOLIVINA SPISSA AS ENVIRONMENTAL PROXY

Abstract

Previous studies showed that the pore density of the shallow infaunal benthic foraminiferal species *Bolivina spissa* is closely related to the nitrate availability in their habitats. In this study first applications of this new developed proxy are presented. Samples were collected in the Peruvian oxygen minimum zone. We considered one short core which covers the end of the Little Ice Age and a long core which covers segments from the Holocene into the last glacial. Furthermore specimens collected during a strong El-nino were compared to specimens from non-El-nino conditions. The pore density of the El-nino specimens is significantly elevated compared to specimens from non-El-nino conditions at a location were nitrate was depleted during that El-nino. No significant variation of the pore density has been found among that short sediment core although there is a slight minimum at the end of the Little Ice Age where there was a rapid shift in the biogeochemical conditions at the Peruvian oxygen minimum zone. However the pore density downcore the long core shows significant variations. There is a strong shift towards higher pore densities at the beginning of the last glacial. These results indicate lower nitrate availability during the last glacial compared to the Holocene. The nitrate depletion at this sampling site might either arise from changes in upwelling and thus the biogeochemical conditions, due to the lower sea level during that time or an interaction of both. In summary, the pore-density of *B. spissa* seems to be a valuable proxy for nitrate availability at least on millennial time scales.

4.1 Introduction

In the Peruvian upwelling area the hydrography is dominated by the oxygen rich, equatorward Peru-Chile Current (flowing in depths between 0-100 m) and the oxygen deficient, nutrient-rich, poleward Peru-Chile undercurrent (flowing between ~100-350 m) (Brockmann et al., 1980; Shaffer et al., 1995; 1997; Hill et al., 1998, Böning et al., 2004, Díaz-Ochoa et al., 2009). The definition and extension of the oxygen minimum zone (OMZ) of Peru is a bit contradictory in literature. For the definition of the OMZ authors either quote oxygen concentrations < ~5 µM (Brockmann et al., 1980; Böning et al., 2004) or < 8.7 µM (Helly and Levin 2004; Díaz-Ochoa et al., 2009). For the extension water depths either between 50 m and 650 m (Emeis et al., 1991; Lückge and Reinhardt, 2000; Böning et al., 2004) or between ~75 m and ~310 m (Helly and Levin 2004; Díaz-Ochoa et al., 2009) are quoted. The upper boundary can sink to ~200 m during El-nino (EN) events (Helly and Levin 2004). In the Peruvian OMZ the upwelling is perennial and wind-driven (Suess et al., 1986; Böning et al., 2004).

Biogeochemical variability in the Eastern Tropical South Pacific, modulating bioproductivity and oxygen concentrations, is mainly caused by seasonal and interannual changes of the Intertropical Convergence Zone (ITCZ) and the trade winds (Barber and Chávez, 1983; Pennington et al., 2006; Gutiérrez et al., 2009). There are several studies about biogeochemical variability in the OMZ off Peru during the Late Quaternary. Fish scales were used as a proxy for fish abundance together with phosphorous from fish remains and combined the analyses of redox sensitive elements in the sediments as a proxy for redox conditions (Díaz-Ochoa et al., 2009). Other studies on laminated sediments from the OMZ off Peru included X-ray digital analyses, mineralogy, inorganic contents and organic geochemistry (Sifeddine et al., 2008) while Gutiérrez et al. (2009) used a massive multiproxy approach on box cores off Calao (~12° S) and Pisco (~14° S). All these studies conclude that there was a massive shift in the biogeochemical conditions at the OMZ off Peru during the beginning of the 19th century. These changes included an increase in bioproductivity and a strong depletion in oxygen concentrations. This rapid shift towards the end of the Little Ice Age was interpreted to be driven by a northward migration of the ITCZ and the South Pacific Subtropical High, combined with a strengthening of Walker circulation (Gutiérrez et al. 2009).

Studies about changes in the biogeochemical conditions in equatorial and coastal upwelling areas during the glacial are a bit contradictory. On the one hand it has been suggested that upwelling was reduced during the last glacial resulting in lower flux of organic material through the OMZ and thus lower denitrification (Ganeshram et al., 1995; Falkowsky, 1997; Ganeshram et al., 2000). This is supported by model simulations, which predict a weakening of upwelling winds off Peru due to a weaker subtropical-high pressure system in the South Pacific during the LGM (Kutzbach et al., 1993) and by several studies at 11° S off Peru, which hint to a lower bioproductivity during the Last Glacial (Wefer et al., 1990; Schrader and Sorkness, 1990). On the other hand there are several authors who came to the exactly opposite conclusions: Upwelling and thus bioproductivity in equatorial and coastal upwelling areas was strengthened during the glacials (Pedersen, 1983; Pedersen et al., 1988; Lyle, 1988; Lyle et al., 1988; Rea et al., 1991; Ohkouichi et al., 1997; Patrick and Thunnel, 1997; Perks and Keeling, 1998; Wolf, 2002), which might be related stronger trade winds due to higher latitudinal temperature gradients (Mix et al., 1986).

In this study first applications of a new developed proxy, the pore density in the benthic foraminiferal species *Bolivina spissa*, are presented, using a several sediment cores from the Peruvian OMZ and comparing specimens from EN and non-EN conditions. The pore density

in *B. spissa* is supposed to be inversely correlated mainly to the nitrate availability although the influence of different factors like oxygen concentration could not be excluded (Glock et al., 2011a). A detailed review about the understanding of the pores in benthic foraminifera can be found in Glock et al. (2011b).

4.2 Material and Methods

4.2.1 Sampling Procedure

Three short and a long sediment core from the Peruvian OMZ taken during R.V. *Meteor* cruise M77/1 and M77/2 in October and November 2008 and two short cores from a strong EN were considered for the present study (table 4.1). The long core (M772 47-2) was recovered by using pistoncore technology. When the pistoncorer came to deck the sediment filled plastic tube was cut into segments of one meter length which were stored and transported at 4°C. The core was subsampled in Kiel with 10 ml syringe corers for the samples which were used only for pore density determination. Whole 2 cm broad slices were taken for the samples which were used for ^{14}C dating on planktic foraminifera. Surface samples were taken from a short core of the corresponding multicore station (M772 47-3). The sampling procedure and treatment of the samples from non-EN conditions, including the sampling of benthic foraminifera (except for the piston core), the oxygen determination and the nitrate profiling is described in detail in Glock et al. (2011a).

Table 4.1. Sampling sites. Sites marked with a * were sampled during a strong EN (1997-1998).

Site	Type	Longitude (W)	Latitude (S)	Water depth (m)
M77/1-487/MUC-39	MUC	78°23.17'	11°00.00'	579
M77/1-622/MUC-85	MUC	77°34.76'	12°32.76'	823
M77/2-47-2	Piston-Core	80°31.36'	7°52.01	623
M77/2-47-3	MUC	80°31.36'	7°52.01	623
*	MUC	77°29.58’	12°32.54’	562
*	MUC	77°34.76’	12°32.76’	830

The EN samples were provided by E.M. Perez. These samples were collected during the Panorama Expedition, Leg 3a, aboard the RV *Melville* by using the multicorer technology. The sampling sites are located at the lower boundary of the Peruvian OMZ at 562 m water depth (12°32.54’S, 77°29.58’W) and below the OMZ at 830 m water depth (12°32.76’S, 77°34.76’W). From one core at each site the top cm of each core was sampled and then sliced in 0.5 cm-intervals from 1-3 cm and in 1 cm-intervals from 3-10 cm. Samples were preserved

in 10% formalin, using procedures described by Shepherd (2007). 65 ml of Rose Bengal solution (1 g/l 10% formalin) was added to each preserved sample in a laboratory and allowed to stain for at least one week before processing.

4.2.2 Foraminiferal Studies

The sediment samples were washed over a 63-µm mesh sieve. The residues were collected in ethanol to prevent corrosion and dried at 50°C. They were further subdivided into the grain-size fractions of 63–125, 125–250, 250–315, 315–355, 355–400, and > 400 µm. Specimens of the shallow infaunal species *Bolivina spissa* were picked from the 125–250 µm fraction. The EN samples were wet-sieved and split into manageable volumes for examination using a modified OTTO microsplitter. Specimens of *Bolivina spissa* were picked from the >150 µm fraction.

All specimens from core M77-1 487/MUC-39 were mounted on aluminum stubs and photographed with a Zeiss™ Leo VP 1455 scanning electron microscope (SEM) at the Geological-Palaeontological Institute of Hamburg University. Samples were not coated with a conductive layer to save them for further chemical analyses. To compensate charging effects on the specimens, the SEM was operated in a high pressure mode. All other specimens were mounted on aluminum stubs and sputter-coated with gold. The EN specimens and specimens from core M77-1 622/MUC-85 were photographed with a CamScan-CS-44 SEM of the institute for paleonthology and historical geology at the Christian-Albrecht-University in Kiel. Specimens from cores M772 47-2 and M772 47-3 were photographed with a Zeiss DSM 940 SEM of the central microscopy at the Christian-Albrecht-University in Kiel.

Areas on the tests of the specimens were determined with Zeiss™ AxioVision 4.7. The pores in the first 10 chambers (contributes to an area of about 50000-60000 µm^2) of *B. spissa* were counted on SEM photographs. Only megalospheric specimens were used for the analysis. All visible pores of a specimen were recorded. The results of the mean pore density of each sample are listed in table 2.

4.2.3 Core Chronology

^{210}Pb

The analysis of ^{210}Pb excess in the sediment was used to determine a chronological model for the short core (M77-1 487/MUC-39). The isotopes ^{210}Pb, ^{137}Cs and ^{226}Ra were determined with gamma-ray counting using a low-background coaxial Ge(Li)detector. The samples were

analysed in the Labor für Radioisotope am Institut für Forstbotanik, University of Göttingen. ^{210}Pb was measured via its gamma peak at 46.5 keV, ^{137}Cs via its gamma peak at 661 keV and gamma peak of ^{226}Ra via the granddaughter ^{214}Pb at 352 keV.

^{14}C

To determine a chronological model for the pistoncore (M77-2 47-2) the radiocarbon isotopes were measured in tests of bulk samples from *Neogloboquadrina dutertrei* and *Neogloboquadrina pachyderma* by accelerated mass spectrometry at Leibniz-Laboratory for Radiometric Dating and Stable Isotope Research at the University of Kiel.

Prior to the analyses organic surface coatings and detrital carbonate were removed with 30% H_2O_2 in a supersonic bath followed by a cleaning step with 15% H_2O_2 in a supersonic bath. The cleaned samples were acidified with 100% phosphoric acid in an evacuated, flame sealed quartz tube. The produced CO_2 was reduced to graphite with H_2 on an iron catalyst. The resulting powder consisting of graphite and iron was pressed into aluminium studs for accelerator mass-spectrometer (http://www.uni-kiel.de/leibniz/index.htm).

4.3 Results

4.3.1 Comparison of nitrate-profiles through the water column of the Peruvian OMZ between EN and non-EN conditions

A comparison between the nitrate profiles through the water column of the Peruvian OMZ between EN and non-EN conditions is shown in fig. 4.1. The non-EN profile was taken from Glock et al. (2011a) while the EN profile was taken from Levin et al. (2002). The EN profile generally shows slightly lower nitrate concentrations. Especially near the water surface where primary production occurs nitrate seems to be much more depleted during EN. In water-depths between 500-600 m the nitrate concentrations are quite similar while at lower water depths until 800 m there is again a distinct gap between the EN/non-EN nitrate concentrations.

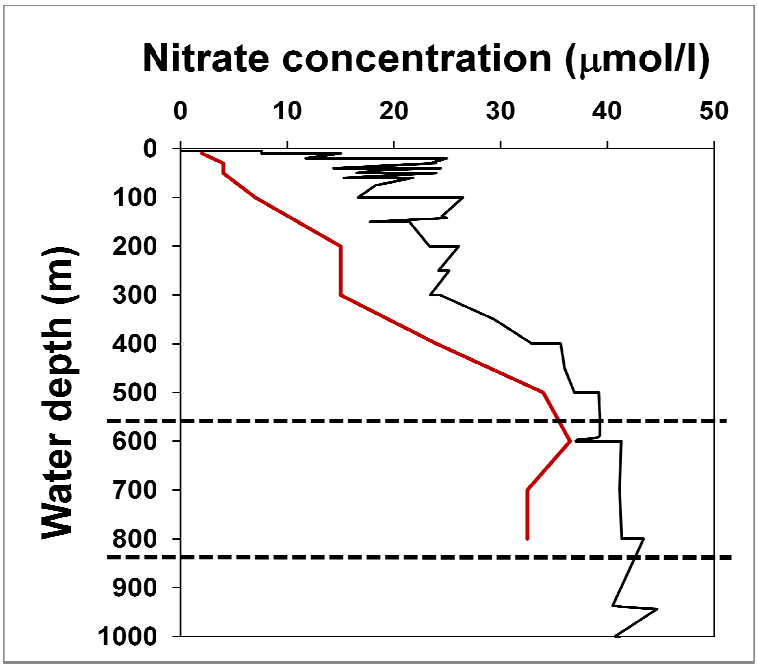

Figure 4.1. Comparison of nitrate distributions during non-EN conditions between 10°30´-11°15` S (Taken from Glock et al., 2011) (black line) and EN conditions at 12°00´ S (Taken from Levin et al., 2002) (red line).

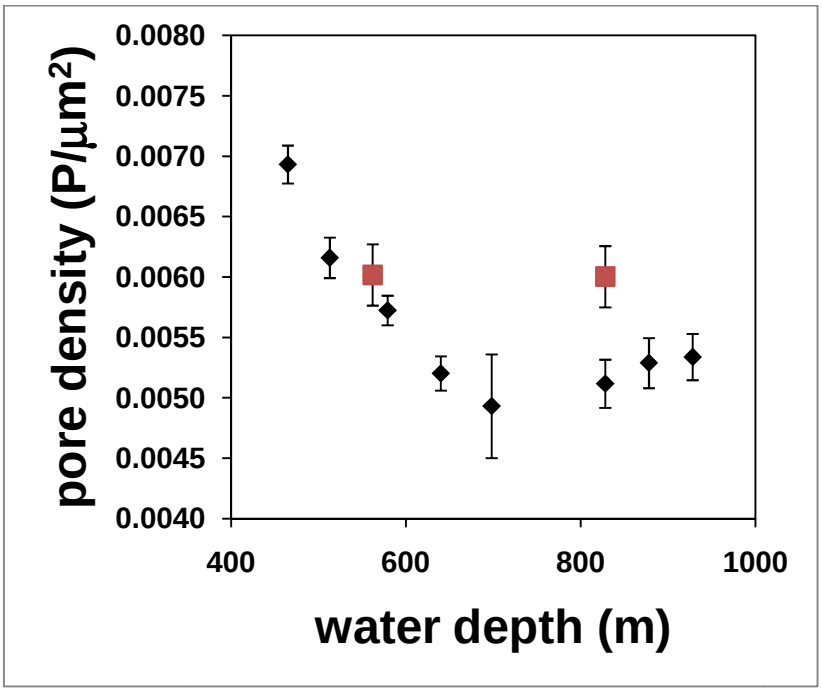

Figure 4.2. Correlation of *Bolivina spissa* pore density with water depth. Comparison between specimens from a strong EN (red squares) and non-EN conditions (black diamonds). Error bars represent the standard error of the mean.

Table 2. Pore density results.

Core	Depth (cm)	Mean pore density (P/μm^2)	SEM (P/μm^2)	Specimens counted
M77-1 487/MUC-39	0-1	0.00574	0.000123	57
M77-1 487/MUC-39	1-2	0.00557	0.000125	42
M77-1 487/MUC-39	2-3	0.00561	0.000156	36
M77-1 487/MUC-39	3-4	0.00571	0.000143	40
M77-1 487/MUC-39	4-5	0.00572	0.000137	42
M77-1 487/MUC-39	5-6	0.00547	0.000140	42
M77-1 487/MUC-39	6-7	0.00549	0.000116	43
M77-1 487/MUC-39	7-8	0.00540	0.000171	41
M77-1 487/MUC-39	8-9	0.00564	0.000157	38
M77-1 487/MUC-39	9-10	0.00554	0.000200	23
M77-1 487/MUC-39	10-11	0.00552	0.000243	14
M77-1 487/MUC-39	11-12	0.00558	0.000165	36
M772 47-3	1-2	0.00498	0.000134	22
M772 47-2	5	0.00479	0.000180	22
M772 47-2	110	0.00507	0.000199	20
M772 47-2	200	0.00548	0.000195	20
M772 47-2	314	0.00543	0.000174	19
M772 47-2	400	0.00536	0.000159	26
M772 47-2	514	0.00531	0.000225	21
M772 47-2	600	0.00458	0.000143	24
M772 47-2	710	0.00538	0.000169	24
M772 47-2	910	0.00499	0.000148	25
M772 47-2	914	0.00519	0.000170	26
M772 47-2	1110	0.00532	0.000159	25
M772 47-2	1205	0.00503	0.000181	24
M772 47-2	1287	0.00514	0.000236	24
M77-1 622/MUC85	0.5-1	0.00512	0.000199	10
EN (562 m)	0-1	0.00602	0.000253	6
EN (830 m)	0-2	0.00600	0.000300	6

4.3.2 Comparison of *B. spissa* pore density during EN and non-EN conditions

A comparison of the pore densities in tests of *Bolivina spissa* specimens from an intense EN (1997-1998) to specimens from non-EN conditions and their correlation to water depth are shown in fig. 4.2. All samples are from the Peruvian OMZ (in this case from 11°-12°S). Both the EN and non-EN samples from 830 m water depth were sampled at the same coordinates. All the 10 analysed non-EN specimens from the 830 m site were alive during sampling time (staining with rose-bengal). From the EN samples at the 830 m site at least the three specimens from 0-1 cm sediment depth were alive. Also at least three EN specimens from the 562 m site were alive during sampling time.

Whereas the pore density at the 830 m site is elevated during EN, the pore density of the EN specimens from 562 m water-depth fits well into the correlation between pore density and water-depth during non EN conditions (fig. 4.2). The pore densities at the 830 m site differ significantly between EN and non-EN conditions (P = 0.031) while there is no significant difference between the pore densities at the 562 m site during EN and the 579 m site during non-EN conditions (P = 0.471). Significance was calculated by using unpaired two sample student´s t-tests (significance level 0.05). A comparison of the pore-densities of the single analysed specimens between EN and non-ell-nino conditions is shown in fig. 4.3.

In fig. 4.4 the pore densities of the EN and non-EN specimens are plotted against **a)** $[NO_3^-]_{BW}$ and **b)** $[O_2]_{BW}$. $[NO_3^-]_{BW}$ during EN was intrapolated for the depths of the sampling sites from the nitrate profile shown by Levin et al. (2002) in fig. 2b. $[O_2]_{BW}$ at the sampling sites during EN was provided by E.M. Perez (pers. comm.). The EN pore density at the 562 m site fits well into the pore density/$[NO_3^-]_{BW}$ correlation during non-EN conditions while the pore density at the 830 m site seems to be too low to fit. On the other hand the pore density at both EN sites is to high to fit into the pore density/$[O_2]_{BW}$ correlation during non-EN conditions, since $[O_2]_{BW}$ was higher during the EN at similar water depths compared to non-EN conditions.

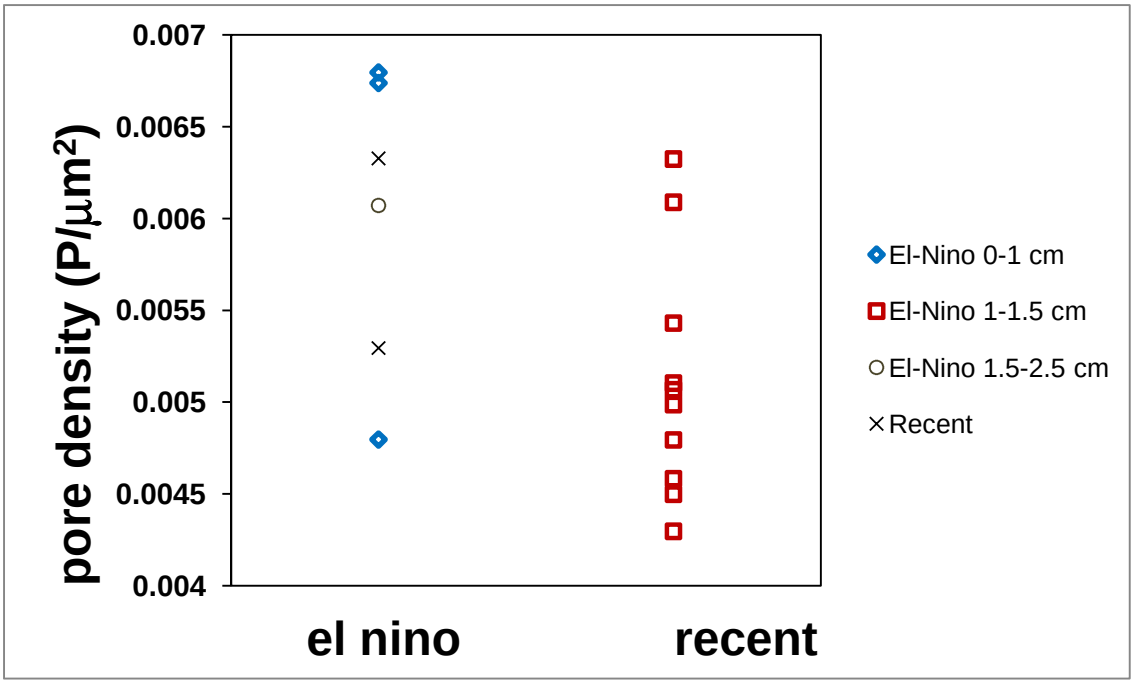

Figure 4.3. Comparison of *Bolivina spissa* pore densities of single analysed specimens from the 830 m site between EN and non-EN conditions.

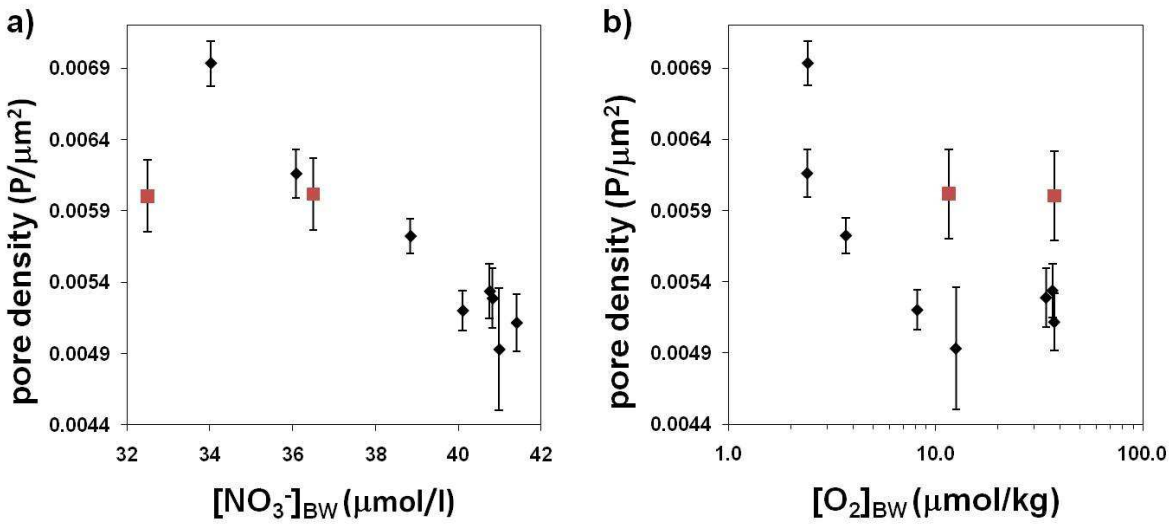

Figure 4.4. Correlation of *Bolivina spissa* pore density with **a)** $[NO_3^-]_{BW}$ and **b)** $[O_2]_{BW}$. Comparison between specimens from a strong EN (red squares) and non-EN conditions (black diamonds). Error bars represent the standard error of the mean.

4.3.3 Pore density variability in *Bolivina spissa* among the last 300 years

The variability of the pore-density in *Bolivina spissa* among the sediment depth of the 12 cm long core M77-1 487/MUC-39 (579 m water depth) is shown in fig. 4.5. The dashed line on the left side represents the mean core top pore density of the next deeper sampling location (M77-1 565/MUC-60; 640 m) while the dashed line on the right represents the mean core top pore density of the next deeper sampling location (M77-1 516/MUC-40; 513 m). Both core top pore densities were taken from Glock et al. (2011). Thus the pore density variation among the 12 cm sediment depth is relatively low compared to the variability in between the core top pore densities from different sampling locations. The standard errors of the mean (SEM) range from 0.000116 to 0.000243 P/µm^2. This represents 34.1 – 71.3% of the maximum variation among this core. Although the overall variability is quite small there is a minimum in the pore density in the segment between 5 and 8 cm sediment depth.

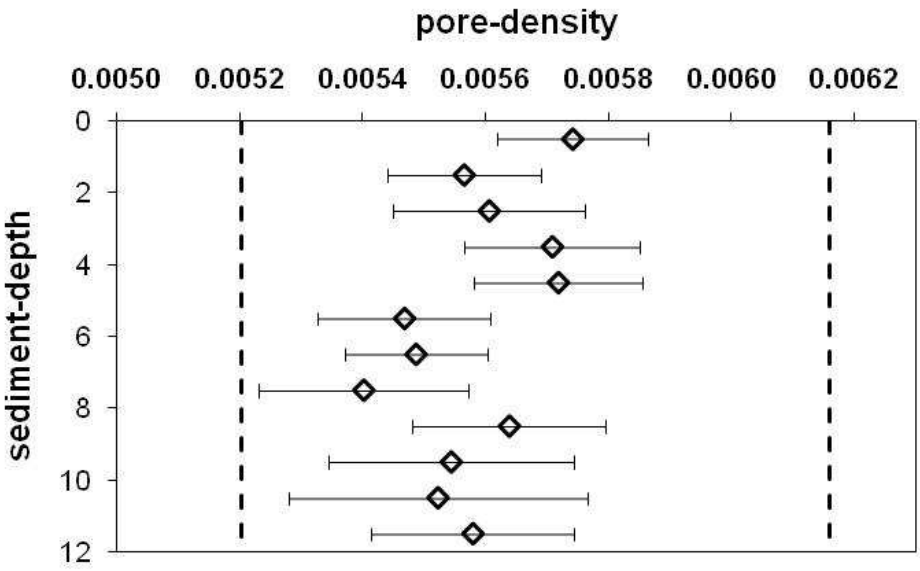

Figure 4.5. Downcore variability of the pore density in tests of *Bolivina spissa* along the core M77-1 487/MUC-39 (579 m water depth). The error bars are the SEM. The dashed line on the left side represents the mean core top pore density of the next deeper sampling location (M77-1 565/MUC-60; 640 m). The dashed line on the right represents the mean core top pore density of the next deeper sampling location (M77-1 516/MUC-40; 513 m).

The pore density is plotted against the relative age of the sediment for core M77-1 487/MUC-39 in fig. 4.6 a) including the ^{210}Pb core chronology. Pore densities were converted into $[NO_3^-]_{BW}$ by using the equation shown in fig. 7 D in Glock et al. (2011a). The calculated $[NO_3^-]_{BW}$ are plotted against the relative age of the sediment in fig. 4.6 b). The minimum in the pore density and the maximum in the $[NO_3^-]_{BW}$ respectively which appears in the depth interval between 5 and 8 cm corresponds to a time interval from about 1858-1915. A one way ANOVA over the pore density data of the whole core with a significance level of 0.05 shows that the pore density in the different depth intervals do not distinguish significant ($P = 0.88$). Even a unpaired two sample student´s t-test (significance level 0.05) between the minimal and maximal pore density among this core shows that there is no significant difference between this two data points ($P = 0.12$) although these points are clearly divided by their SEMs.

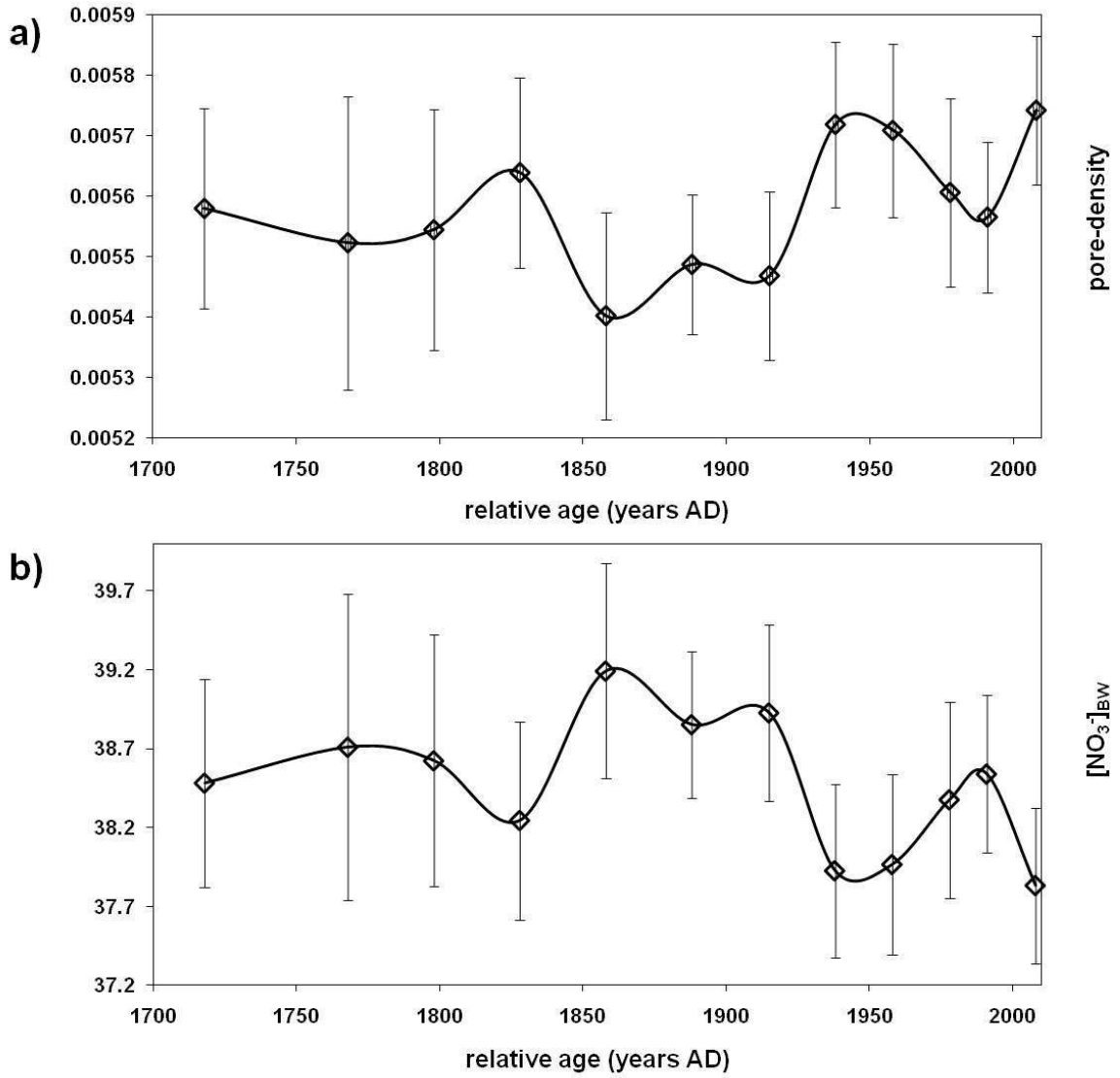

Figure 6. Relative age of the core M77-1 487/MUC-39 plotted against **a)** the pore density in tests of *B. spissa* and **b)** $[NO_3^-]_{BW}$ calculated out of the pore density by using the equation shown in fig. 7 D in Glock et al. (2011a). The error bars are the SEM.

4.3.4 Pore density variability in *Bolivina spissa* from Holocene into the last Glacial

The variability of the pore-density in *Bolivina spissa* among the sediment depth of the 13 m core M772 47-2 (626 m water depth) is shown in fig. 4.7. The standard errors of the mean (SEM) range from 0.000134 to 0.000235 P/µm^2. This represents 14.8 – 25.9% of the maximum variation among this core. The pore density increases from the surface of the core to 2 m sediment depth. Afterwards the pore density tends to decrease slightly with sediment depth. Noticable is the strong pore density minimum at the depth of 6 m.

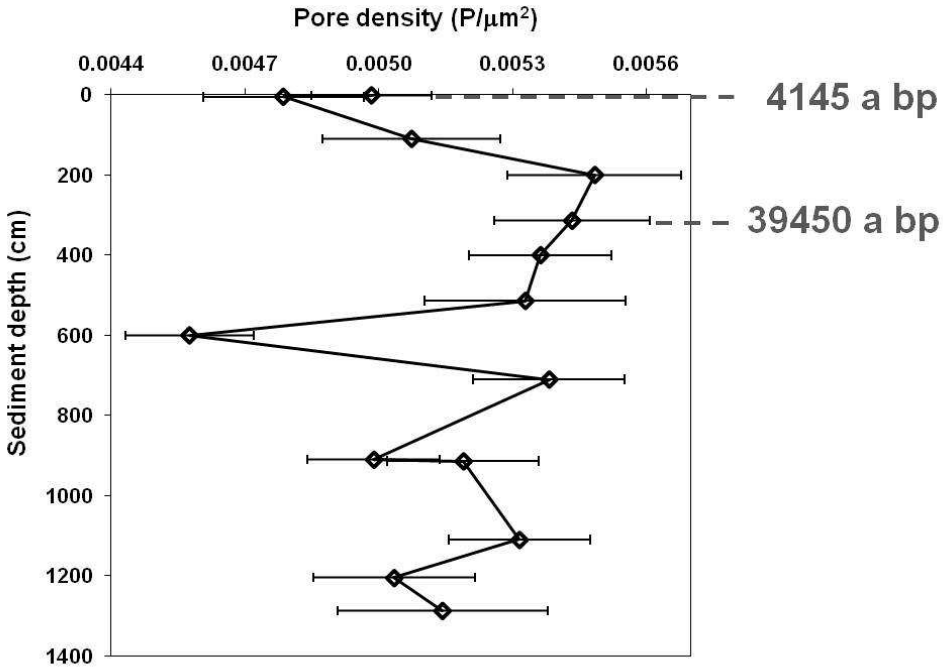

Figure 4.7. Downcore variability of the pore density in tests of *Bolivina spissa* along the core M772 47-2 (626 m water depth). The error bars are the SEM. Dashed lines indicate the depths where ^{14}C ages are available.

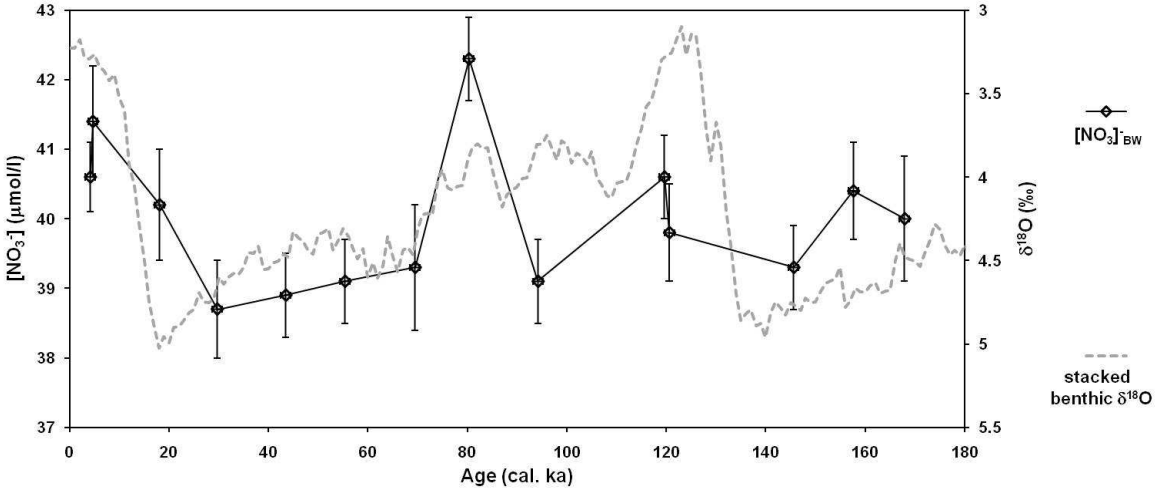

Figure 8. Calendar age of the core M772 47-2 plotted against $[NO_3^-]_{BW}$ calculated out of the pore density by using the equation shown in fig. 7 D in Glock et al. (2011a). The error bars are the SEM. The age model was constrained by using the 2 available ^{14}C ages and fitting the curve onto the stacked benthic $\delta^{18}O$ curve (grey dashed line) from Liesicki and Raymo (2005). By courtesy of Joachim Schönfeld.

Pore densities were converted into $[NO_3^-]_{BW}$ by using the equation shown in fig. 7 D in Glock et al. (2011a). The calculated $[NO_3^-]_{BW}$ for core M772 47-2 are plotted against the calendar age of the sediment in fig. 4.8. The grey dashed line represents the stacked $\delta^{18}O$ curve from Liesicki and Raymo (2005). There seems to be a strong increase in the pore density and thus a

decrease in nitrate availability during the transition from the Holocene into the Last Glacial. A one way ANOVA over the pore density data of the whole core with a significance level of 0.05 shows that the pore density in the different depth intervals do distinguish significant (P = 0.018).

4.4 Discussion

4.4.1 Comparison of *B. spissa* pore density during EN and non-EN conditions

As shown in the results (4.3) the EN pore density at the 562 m site fits well into the correlation between pore density and water depth during non-EN conditions while the pore density at the 830 m site is elevated during EN compared to the pore density during non-EN conditions at the same sampling site (fig. 4.2). This might be explained by the progress of the nitrate profiles through the water column during EN and non-EN conditions (fig. 4.1). At a water depth of about 560 m the nitrate concentrations during EN and non-EN conditions are quite similar whereas the nitrate concentrations at about 800 m seem to be depleted during EN. Since the pore density is inversely correlated to nitrate availability (Glock et al. 2011a) this might be an explanation why the pore density was elevated at 830 m during EN. On the other hand the pore density at this site is still too low to fit into the pore density/$[NO_3^-]_{BW}$ correlation from the recent (non-EN) samples (fig. 4.4). This might be caused by several reasons:

- The correlation is shown for $[NO_3^-]_{BW}$ or for intrapolated values from the water column at similar water depths like the sampling sites. But *Bolivina spissa* is living shallow infaunal in sediments and thus indeed it depends on the nitrate availability in the pore water. Nitrate usually is depleted in the pore water compared to the bottom water due to diffusion, denitrification and several other factors. Since $[O_2]_{BW}$ and thus the oxygen penetration depth into the sediment was higher during EN it might be that there occurred less denitrification in the pore water. So there was comparable more nitrate in the pore water.
- For the EN samples $[NO_3^-]_{BW}$ was intrapolated from the nitrate profile shown in Levin et al. (2002). Since the profile ends at 800 m water depth it had to be extrapolated from this profile for the 830 m site. Thus it might be that the "real" $[NO_3^-]_{BW}$ at this water depth is slightly different.
- Nobody knows how fast *B. spissa* adapts its pore density to environmental changes. ENs are only short time events and it might be that *B. spissa* did not have enough time to completely adapt to the massive environmental changes during EN. But since the

differences in the pore density of the EN specimens to the non-EN specimens from the 830 m site were significant it is highly propable that there was an adaption.

- The sample size of the EN specimens was limited and thus quite small. The mean pore density might still change with more samples. Nevertheless, it should not change more than the range of the SEM and thus the results would not change distinctively.

In both EN samples the mean pore density is too high to fit into the pore density/$[O_2]_{BW}$ correlation during non-EN conditions. Indeed the pore density at the 830 m site is higher during EN although $[O_2]_{BW}$ was higher, too. The pore density and $[O_2]_{BW}$ were supposed to be inversely exponential correlated (Glock et al., 2011a). Thus it is not very probable that the pore density in *B. spissa* is solely correlated to the oxygen availability.

4.4.2 Pore density variability in *Bolivina spissa* among the last 300 years

The variation of the pore density along the 12 cm core M77-1 487/MUC-39 is very low. The variation in between the different core top samples from the next deeper and shallower sampling location is much higher than any variation along that single core over the last 300 years. There does not even seem to be a statistical difference between the different sampling depths. Several factors could have caused these results. It might be that the dominating environmental factor that influences the pore density (propably nitrate availability) did not change distinctively over the last 300 years at this location. Thus the differences in the nitrate availability were much higher between the different sampling locations than in the different time intervals at the same sampling site at 579 m water depth. Alternatively it might be that the evolutionary adaption of the pore density in *Bolivina spissa* is quite slow and that the big difference of the pore density between the different sampling locations developed over a much longer time than the last 300 years. Finally the sedimentation rate at this sampling site is relatively low and a slice of 1 cm covers ca. 30 years. Additionally *B. spissa* lives infaunal and thus is able to migrate vertically in the sediment column. It is possible that specimens migrate 1 or even up to 2 cm into the sediments and recent specimens in *B. spissa* are found in 60 years old sediment. In this case it is possible that one slice of the core contains a mix of *B. spissa* specimens from a time period of 60-90 years. Any variation in the nitrate availability on a short time scale could not be detected anymore due to the low time resolution in the slices.

But even with these low variations it is possible to discuss the progress of the pore density among this core. It is very conspicuous that the minimum of the pore density appears in the middle of the nineteenth century since there were intense changes in the environmental

conditions at the Peruvian OMZ during the end of the little ice age in the 1830´s (Guitierrez, 2009). It has been shown that at the end of the little ice age there was a rapid expansion of the nutrient rich and oxygen depleted subsurface waters which resulted in a higher bioproductivity, including pelagic fish. Among others this shift was likely driven by a northward migration of the Intertropical Convergence Zone (Guitierrez et al., 2008). The minimum in the pore density and thus a maximum in nitrate availability seem to appear simultaneously with this mayor regime shift. A bit contradictory is that oxygen depletion often is correlated to nitrate depletion due to higher denitrification rates. But maybe the mix of higher nutrient availability, bioproductivity and thus remineralistion rates due to the stronger upwelling result in higher nitrate concentrations in the water column and this factor dominates over the influence of the higher denitrification rates. A more propable explanation could be that the northward migration of the Intertropical Convergence Zone results in more saline and thus nitrate enriched water masses. Over the time the higher denitrification rates seem to become more dominant which results again in a higher pore density (lower nitrate availability) in the 1940´s till now. The relative progress of the pore density follows exactly the same trend as the content of P in fish remainings in the sediments at 12° S and 179 m water depth off Peru and the number of anchovy landings off Peru (Díaz-Ochoa et al., 2009). Since the pore density is inversely proportional to the nitrate availability there was less nitrate available in times of higher occurance of pelagic fish. Thus it might be that the bioproductivity of pelagic fish (in this case especially anchovies) is inversely coupled to the nitrate availability in a water depth of about 579 m. Higher occurance of pelagic fish is most propably caused by higher food availability and thus a higher general bioproductivity. This could lead to a more massive nitrate depletion in the shallower waters which might influence the nitrate availability in the deeper waters, too. Additionally a higher bioproductivity results usually in a stronger oxygen depletion due to higher remineralisation rates which on the other hand leads to higher denitrification rates which could explain the lower nitrate availability at 579 m water depth in times higher pelagic fish productivity.

Since the variations in the pore density among the analysed core are not statistically significant it is hard to make solid statements about the interpretation of the results. But it is to conspicuous that the minimum of the pore density occurs exactly during that time, where there was a mayor regime shift in the sampling area (Guitierrez et al., 2008) and that the pore density follows exactly the same trend like the productivity of pelagic fish (Díaz-Ochoa et al., 2009).

4.4.3 Pore density variability in *Bolivina spissa* from Holocene into the last Glacial

There are significant variations in the pore density of *B. spissa* from the Holocene into the last glacial. The pore density shows a maximum during the last glacial which corresponds to a minimum in nitrate availability during that time. It has been suggested that during glacial times nitrate was enriched in the global ocean due to a decrease in denitrification (Ganeshram et al., 1995; Falkowsky, 1997; Ganeshram et al., 2000). This glacial decline in denitrification propably origins in reduced upwelling and flux of organic material through the OMZ (Ganeshram et al., 2000). Indeed general circulation model simulations predict a weakening of upwelling winds off Peru due to a weaker subtropical-high pressure system in the South Pacific during the LGM (Kutzbach et al., 1993). Additionally several studies at 11° S off Peru hint to a lower bioproductivity during the last llacial (Wefer et al., 1990; Schrader and Sorkness, 1990). At a first glance it seems to be contradictory that the pore density in *B. spissa* indicates lower nitrate availability at 623 m water depth off Peru during the Last Glacial because due to the decreased denitrification during this time nitrate is supposed to be enriched. But on the other hand the Pacific Intermediate Waters which occupy the deeper water masses (below 600 m) at the OMZ off Peru at 8°S. This is beneath the intense denitrification zone (Ganeshram et al., 2000). These water masses distinguish clearly from the overlying waters in salinity as well as in nutrient characteristics (Wyrtki, 1967). Due to its deeper position in the water column the Pacific Intermediate Waters should only be weakly affected by effects on denitrification by ventilation changes. Thus depletion of nitrate in this depth might be caused by lower remineralisation rates due to lower bioproductivity and thus a lower flux of organic material through the OMZ.

On the other hand there are several studies which hint to a strengthening in upwelling and thus bioproductivity in equatorial and coastal upwelling areas during the glacials (Pedersen, 1983; Pedersen et al., 1988; Lyle, 1988; Lyle et al., 1988; Rea et al., 1991; Ohkouichi et al., 1997; Patrick and Thunnel, 1997; Perks and Keeling, 1998; Wolf, 2002). An increase of upwelling might be related to stronger trade winds due to higher latitudinal temperature gradients (Mix et al., 1986) which contradicts the conclusions of Kutzbach et al. (1993). If there was indeed higher upwelling during the last glacial at the Peruvian OMZ nitrate depletion, predicted by the pore density in our study, might just be related to a general increase in denitrification.

Another explanation for nitrate depletion at this site might be the lower sea level during the last glacial. Nitrate is usually depleted at shallower waters due to primary production near the

water surface. Due to remineralisation of organic matter nitrate concentrations rise with water depth. After Fairbanks (1989) the sea level during the LGM was about 120(+/- 5) m below the present. Other studies proclaim that the global sea level was 60-90 m below the present during the last 50000 years (Yokoyama et al., 2001; Lambeck et al., 2002; Siddal et al., 2003; Yokoyama et al., 2007). There is a difference of 0.0005 P/μm^2 between the maximum pore density value at 200 cm sediment depth (last glacial) and the pore density of the surface sample (4145 a bp). This corresponds exactly to the difference in the pore density between two surface sample from 640 m (0.00520 P/μm^2) and 579 m (0.00572 P/μm^2) water depth at 11°S off Peru (Glock et al., 2011a). These results imply that the water level at 8°S off Peru was about 60 m lower during the last glacial then during present. An interaction of several factors like a lower water level during the last glacial and changes in upwelling intensity and thus productivity, denitrification and flux of organic material could not be excluded. Thus it might be that the water level indeed was 120 m lower but the pore density was also superimposed by a reduced upwelling in during this time which would correlate with lower denitrification and a bit elevated nitrate levels. The fact that the pore density seems to follow the stacked $\delta^{18}O$ record in benthic foraminifera shows that this proxy is sensitive to climatic changes and might serve as an invaluable archive for climate reconstruction. But since only two ^{14}C ages are available at the moment, the relation to the stacked $\delta^{18}O$ record has to be treated with care. A disturbance of the stratigraphy in this core cannot be excluded by now.

4.5 Conclusions

In this study the variability of the pore density in *B. spissa* from the Peruvian OMZ was analysed on different time scales. Short time variations were considered by comparing the pore densities from EN specimens and specimens from non-EN conditions. Downcore observations on a short and a long core investigated the pore density variability on a centennial and a millennial time scale. Three mayor results come out of this study:

- Comparison of recent specimens with specimens from the strong EN (1997-1998) from the same area at the Peruvian continental margin showed that there are significant differences in the pore densities of specimens from 830 m water depth between EN and non-EN conditions. Nitrate profiles through the water column off Peru showed that in this water depth nitrate was depleted during that EN compared with the non-EN conditions when we took our samples. No significant difference was found between the pore densities at a 562 m site during EN and a 579 m site during

non-EN conditions. These results hint also that the pore density variability during EN is mostly uncoupled from oxygen variations during this time.

- The short core covers a time span of about the last 300 years. Although the pore densities did not differ significantly in the several depth intervals of that core there is a slight minimum in the pore density at the end of the Little Ice Age in the beginning of the 19th century when there were mayor shifts in the biogeochemical conditions at the OMZ off Peru (Gutiérrez et al., 2009).
- The pore densities in the several depth intervals of the long core on the other hand show significant differences. There seems to be a strong shift to higher pore densities during the last glacial maximum (LGM). The higher pore densities indicate nitrate depletion during the LGM which either might origin from changes in the upwelling intensity of Peru during that time and the related biogeochemical shifts or the lower sea level or even an interaction of these factors.

These results imply that the pore density in *B. spissa* might be a valuable proxy for nitrate availability at least on millennial time scales. Further investigations will show if this proxy could be used in a higher resolution on centennial time scales, too, on different sampling locations.

Chapter 5

SUMMARY AND OUTLOOK

5.1 Summary and conclusions

First studies have been done in this work on the value of Mn/Ca and Fe/Ca ratios in benthic foraminifera from the Peruvian OMZ as proxy for the reconstruction of past redox-conditions. The most widespread species along the Peruvian continental margin, *Bolivina spissa*, was used for this work. Furthermore a new proxy for nitrate availability, the PD in *B. spissa*, has been developed and first applications of this proxy have been tested.

Elemental distribution maps of test cross-section from recent benthic foraminifera collected at the Peruvian OMZ show the absence of diagenetic coatings like Mn carbonates or Mn and Fe rich (oxyhydr)oxides. The Mn/Ca in *B. spissa* ratios are relatively low (~2.12-9.93 µmol/mol) but in the same magnitude as in the pore waters. Indeed the permanently anoxic OMZ off Peru causes MnO_2 reduction in the water column and only minor amounts of particulate bound Mn arrive the seafloor. Nevertheless Mn/Ca ratios in *B. spissa* reflect the trend in the pore waters. The interpretation of the Fe/Ca ratios in *B. spissa* is a bit more complicated, because the lowest Fe/Ca ratios have been found at a sampling site, where the pore water profile shows a distinctive and sharp Fe peak at the shallower pore water intervals. The sampling site at 465 m depth is located at the lower boundary of the anoxic Peruvian OMZ. The absence of living but presence of a lot of dead *B. spissa* specimens indicates that the pore water at this site just recently turned anoxic. This caused ironoxides, which precipitated during a previous period of higher oxygen supply, to remobilise. The trend of the higher pore water concentrations with increasing water depth at the deeper stations again is reflected by the Fe/Ca ratios in *B. spissa*.

- The Mn/Ca ratios in benthic foraminifera could be a good tool for the reconstruction of oxygen depletion along the Peruvian OMZ. Higher Mn/Ca ratios would indicate a better oxygenation because more particulate bound Mn would reach the seafloor and be remobilised in the pore waters. Additionally the presence of Mn an Fe rich coatings in fossile specimens would indicate longer periods of higher oxygen supply, because short time fluctuations would cause the coatings to dissolve again in anoxic periods.
- The Fe/Ca ratios in *B. spissa* seem to be superimposed by more factors then the pore-water concentrations. The value of use as a paleoproxy has to validified by further studies.

The PDs in tests of *B. spissa* specimens from eight locations at the Peruvian OMZ show a negative exponential correlation between the PD and $[O_2]_{BW}$. Nevertheless the relationship between the PD and $[NO_3^-]_{BW}$ is much better constrained. This indicates an adaption for the

intracellular nitrate uptake for nitrate-respiration through the pores. These results are supported by the finding that mitochondria (cell organelles involved in respiration) are clustered behind the pores of thin sections of a living fixed *B. spissa* cell.

- The PD in *B. spissa* seems to be very sensitive to $[NO_3^-]_{BW}$ and might prove as an invaluable proxy for nitrate availability. This proxy bears a very good resistance against diagenetic overprinting.
- The fact that mitochondria are clustered behind the pores of *B. spissa* indicates that mitochondria are at least involved in the process of foraminiferal denitrification. Nitrate respiration in benthic foraminifera has not been attributed to a specific cell organelle before.

First applications of the new knowledge about the PD in *B. spissa* have been done by analysing the PD variability on different time scales. Short time variations were considered by comparing the pore densities from EN specimens and specimens from non-EN conditions. Downcore observations on a short and a long core investigated the pore density variability on a centennial and a millennial time scale:

- Specimens from a strong EN (1997-1998) have significant elevated PDs, compared to specimens from non-EN conditions, at a sampling site where nitrate was depleted during the EN. On the other hand the PD shows no significant differences between EN and non-EN conditions at a water depth where the nitrate concentrations were nitrate concentrations were similar during both sampling times. These results also hint that the PD variability during EN is mostly uncoupled from oxygen variations during this time.
- The short core covers a time span of about the last 300 years. PDs did not differ significantly in the several depth intervals of that core. But there is a slight minimum in the pore density at the end of the Little Ice Age in the beginning of the 19th century when there were mayor shifts in the biogeochemical conditions at the OMZ off Peru.
- The pore densities in several depth intervals of the long core on the other hand show significant differences. The PDs were elevated during the LGM. The higher pore densities indicate nitrate depletion during the LGM which either might origin from changes in the upwelling intensity of Peru during that time and the related biogeochemical shifts or the lower sea level or even an interaction of these factors.

These results imply that the PD in *B. spissa* might be an invaluable proxy for nitrate availability at least on millennial time scales. Together with information from Mn/Ca and

Fe/Ca ratios changes in oxygen and nitrate availability might be traced during the last glacial. This might give a much more complete picture about changes in the biogeochemical conditions in the Peruvian OMZ during this time.

5.2 Outlook

In this work first studies have been done on the variability of redox-sensitive elements in benthic foraminifera from the Peruvian OMZ. Additionally with the PD of *B. spissa* a new proxy for nitrate concentrations has been developed. Only first applications have been done so far with this new proxy. Future work should definitely include the consequent analysis of Fe/Ca and Mn/Ca downcore on different cores from the OMZ off Peru. These studies could analyse short time fluctuations on a centennial timescale as well as fluctuations on a millennial timescale. Higher Mn/Ca ratios would indicate times of more oxygen supply and the presence of Mn and Fe rich coatings would hint to even longer periods of higher oxygenation. A combination of this geochemical proxy with the PD-proxy on cores with a good stratigraphy would give a much better understanding about the biogeochemical conditions at the OMZ off Peru during different time periods (Little Ice Age, LGM). Application of other proxies for oxygen-supply like the micropaleontological proxy, working with foraminiferal assemblages, from Mallon et al. (*in press*) would complete this picture.
Since the PD proxy is newly developed a lot of work has to be done in this field. Culture experiments with *B. spissa* or other benthic foraminiferal species which adapt their PD to different environmental conditions could give a much better understanding about the processes which govern the PD in these species. Incubations under controlled conditions with different oxygen- and nitrate-concentrations, temperatures, salinities, etc. would help to identify the dominating factor which influences PD although by the moment it seems to be nitrate availability. Also there are possibilities to proof if oxygen uptake and denitrification is really governed via the pores. Previous work already proofed that *Patellina corrugata* actively pumps neutral red die through its pores (Berthold, 1976) and that Amphistigina lobifera takes up ^{14}C labelled CO_2 through its pores (Leutenegger and Hansen, 1979). For both studies the apertures of the specimens have been closed with silicon grease and a drop of paraffin oil. The apertures of cultured *B. spissa* could be closed in a similar way. Afterwards oxygen-respiration and denitrification rates could be measured with microsensors and compared to cultures with an open aperture. The methods for measuring denitrification and oxygen respiration rates of foraminifera wirh microsensors have already been developed (Pina-Ochoa

et al., 2010, Geslin et al., 2011). Presence of respiration and denitrification in the cultures with the closed aperture could finally proof the function of pores in these species. In this field of work also the distribution of mitochondria in *B. spissa* cells could be investigated more closely. Monoclonal antibodies specific for oxidative phophorylisation might be used to stain mitochondria in fixed *B. spissa* specimens. Mitochondria could be quantified that way in respect to different environmental conditions (like nitrate availability) and their location in the cell. If it would be shown that mitochondria in this species are just located behind the pores the involvement of mitochondria in foraminiferal denitrification might be proofed finally. Our knowledge about the PD in benthic foraminifera is restricted to *B. spissa* from the Peruvian OMZ at the moment. Future studies should definitely include different sampling areas and different species. The PD of *Planulina limbata* seems to be very sensitive on environmental influences, too. The sampling should be done at sites with very well known environmental parameters. For example *in situ* oxygen- and nitrate-microprofiles would have been of great support for this work.

Acknowledgements

First I would like to thank Toni Eisenhauer for supervision of my thesis and his support during the last three years. Volker Liebetrau helped me a lot during this time with organisational issues and had always an open door to discuss results or any problems. Without Joachim Schönfeld this work would not have been possible. Based on his passion for benthic foraminifera he tought me a lot about these amazing eukaryoths.
The close collaboration with Jürgen Mallon who also worked with benthic foraminifera from the Peruvian OMZ was very fruitful for my work. He, as well as my other officemates Patricia Grasse and Claudia Ehlert tolerated my untidiness which is not self-evident. So thanks to all of you! It was nice to work with you ;)
Furthermore I wanted to thank Elena Perez because she tought me about the taxonomy of benthic foraminifera in the Peruvian OMZ and provided the El-Nino samples discussed in chapter 4. From Gernot Nehrke I learned a lot about the preparation of cross-sections for microanalytical techniques like SIMS and EMP. Christian Horn introduced me into the cleaning techniques of foraminifera for ICP-MS analyses while Nadine Gehre always gave support when problems occurred in this lab. A big thank you is entitled to Joan Bernhard who spent a lot of time teaching me the fixation techniques and embedding of fixed foraminiferal cells for the preparation of cell thin sections. Also thanks to Ana Kolevica, Micheal Wiedenbeck and Mario Thöner for their help with operation with the Q-ICP-MS, SIMS and EMP. Without you the chemical analyses would not have been possible. The cross-calibration standards for these analyses were provided by Ed Hathorne. The electron microscope pictures in this work were recorded at several places. Thus I want to thank all the people who helped by the operation of these devices: Ute Schuldt, Yvonne Milker, Meike Dibbern, Marita Beese and Maria Mulisch.
Andy: Thank you for the helpful tips and corrections you gave me for my thesis! Also to Chistian: Thank you for your help by the comparison of the foraminiferal element ratios with the pore water profiles! The crew and scientific party on R/V METEOR cruise M77 and Sonne cruise SO-206 is acknowledged. In this case a special thanks to Andrea, Phillip, Stefan, Andy, Jürgen, Christian (both of them), Anna, Thomas, Tebke, Dirk, Bettina, Meike, Anke, Andre, Cyrus, Florian and everybody else I forgot who made these cruises unforgettable. Many colleagoes I didn´t mention, yet gave me during the last three years a nice working climate. So thanks to Guillaume, Kristin, Elfi, Roland, Anna, Björn and everybody else I forgot to mention in this acknowledgements. It was not for purpose ;) And also I´m grateful to Martin Frank for consenting to be the co-referee of this work.
Finally I wanted to thank my family and all my friends and for being what and who they are. Especially my flatmates Hannes and Timo who survived the last time with me and together with Dorian give the musical compensation for the work in science. And Usch: I´m deeply thankful for your endurance and patience with me which was not easy for you in the last time!

The “Deutsche Forschungsgemeinschaft, (DFG)” provided funding through SFB 754 “Climate– Biogeochemistry Interactions in the Tropical Ocean.”

References

Allen, K. A., Hoenisch, B., James, K. M., Eggins, S. M. and Spero, H. J.: Effects of pH and temperature on calcification of the planktonic foraminifer *O. universa*: insights from culture experiments, Eos Transactions, AGU, Fall Meeting Supplement, 89, Abstract PP51C-1519, 2008.

Allison, N. and Austin, W. E. N.: The potential of ion microprobe analysis in detecting geochemical variations across individual foraminifera tests, Geochem. Geophys. Geosyst., 4(2), 8403, 2003 doi:10.1029/2002GC000430.

Angell, R. W.: The Test Structure of the Foraminifer *Rosalina floridana*, Journal of Protozoology, 14, 299, 1967.

Arnold, Z. M.: *Discorinopsis aguayoi* (Bermudez) and *Discorinopsis vadescens* Cushman and Brönnimann: A study of variation in cultures of living Foraminifera, Contributions from the Cushman Foundation for Foraminiferal Research, 5, 4-13, 1954a.

Arnold, Z. M.: A Note on Foraminiferan Sieve Plates, Contributions from the Cushman Foundation for Foraminiferal Research, 5, 77, 1954b.

Arrigo, K. R.: Marine microorganisms and global nutrient cycles, Nature, 437, 349–355, 2005.

Bandy, O. L.: Ecology and paleoecology of some California foraminifera, Part 1 - The frequency distribution of Recent Foraminifera off California, Journal of Paleontology, Tulsa, Oklahoma, 27, 2, 1953.

Bange, H. W., Naqvi, S. W. and Codispoti L. A.: The nitrogen cycle in the Arabian Sea, Prog. Oceanogr. 65, 145 (2005).

Barber, R. T. and Chavez, F. P.: Biological consequences of E1 Nino, Science, 222, 1203-1210, 1983.

Barker, S., Greaves, M. and Elderfield H.: A study of cleaning procedures used for foraminiferal Mg/Ca paleothermometry, Geochem. Geophys. Geosyst., 4(9), 8407, 2003.

Baturin, G. N.: Some unique sedimentological and geochemical features of deposits in coastal upwelling regions, *in* Suess, E. and Thiede, J. (eds.), Coastal upwelling – its sediment record, Part B: Sedimentary records of ancient coastal upwelling, Plenum Press, NY, 11-27, 1983.

Bé, A. W. H.: Shell Porosity of Recent Planktonic Foraminifera as a Climatic Index, Science, 161, 881-884, 1968.

Bé, A. W. H., Hemleben, C., Andersen, O. R. and Spindler, M.: Pore structures in planktonic foraminifera: Journal of Foraminiferal Research, 10, 117-128, 1980.

Bender, H.: Gehäuseaufbau, Gehäusegenese und Biologie agglutinierter Foraminiferen (Sarcodina, Textulariina). Jahrb. Geol. Bundesanst., 132(2): 259-347, 1989.

Berger, W. H., Smetacek, V. S. and Wefer, G.: Ocean productivity and paleoproductivitiy – an overview, *in* Berger, W. H., Smetacek, V. S. and Wefer, G. (eds.), Productivity of the Ocean: Present and Past, Dahlem Workshop Reports, Wiley-Interscience Publ., Chichester, 1-34, 1989.

Bermudez, P. J.: Foraminiferos de la Costa Norte de Cuba, Memorias de la Sociedad Cubana de Historia Natural, La Habana, Cuba, 9, 129-224, 1935.

Bernhard, J. M., and Alve, E.: Survival, ATP pool, and ultrastructural characterization of foraminifera from Drammensfjord (Norway): response to anoxia, Marine Micropaleontology, 28, 5–17, 1996.

Bernhard, J. M., Buck, K. R., and Barry, J. P.: Monterey Bay cold-seep biota: assemblages, abundance, and ultrastructure of living foraminifera, Deep-Sea Research I, 48, 2233–2249, 2001.

Bernhard, J.M. and Sen Gupta, B. K.: Foraminifera of oxygen-depleted environments, *in* B. K. Sen Gupta (ed.), Modern Foraminifera, Kluwer Academic Publishers, New York, Boston, Dordrecht, London, Moscow, pp. 201-216, 2003.

Bernhard, J. M., and Bowser, S.: Peroxisome proliferation in foraminifera inhabiting the chemocline: An adaptation to reactive oxygen species exposure?, Journal of Eukaryotic Microbiology, 55, 135–144, 2008.

Bernhard, J.M., S.S. Bowser and Goldstein, S.: An ectobiont-bearing foraminiferan, *Bolivina pacifica*, that inhabits microxic pore waters, Cell-biological and paleoceanographic insights: Environmental Microbiology, 12, 2107-2119, 2010.

Berthold, W.-U.: Untersuchungen über die sexuelle Differenzierung der Foraminifere *Patellina corrugata* Williamson mit einem Beitrag zum Entwicklungsgang und Schalenbau, Archiv für Protistenkunde, 113, 147-184, 1971.

Berthold, W.-U.: Ultrastructure and function of wall perforations in *Patellina corrugata* Williamson, Foraminiferida, Journal of Foraminiferal Research, 6, 22-29, 1976.

Bertram, M. A. and Cowen J. P.: Biomineralization in Agglutinating Foraminifera: An Analytical SEM Investigation of External Wall Composition in Three Small Test Forms, Aquat. Geochem., 4, 455-468, 1998.

Bertram, C. J., Elderfield, H., Shackleton, N. J. and MacDonald, J. A.: Cadmium/calcium and carbon isotope reconstructions of the glacial northeast Atlantic Ocean, Paleoceanography, 10(3), 563–578, 1995.

Bice, K. L., Layne, G. D. and Dahl K.: Application of secondary ion mass spectrometry to the determination of Mg/Ca in rare, delicate, or altered planktonic foraminifera: Examples from the Holocene, Paleogene, and Cretaceous, Geochem. Geophys. Geosyst., 6, 2005, Q12P07, doi:10.1029/2005GC000974.

Böning, P., Brumsack, H., Böttcher, M., Schnetger, B., Kriete, C., Kallmeyer, J. and Borchers, S.: Geochemistry of Peruvian near-surface sediments, Geochim. Cosmochim. Acta, 68, 4429–4451, 2004.

Bopp, L., LeQuere, C., Heimann, M., Manning, A. C. and Monfray, P.: Climate-induced oceanic oxygen fluxes: Implications for the contemporary carbon budget, Global Biogeochem. Cycles, 16, 2002, 10.1029/2001GB001445.

Boyer, T.P., J. I. Antonov, O. K. Baranova, H. E. Garcia, D. R. Johnson, R. A. Locarnini, A. V. Mishonov, D. Seidov, I. V. Smolyar, and M. M. Zweng: World Ocean Database 2009, Chapter 1: Introduction, NOAA Atlas NESDIS 66, Ed. S. Levitus, U.S. Gov. Printing Office, Wash., D.C. , 216 pp., 2009, DVD.

Boyle, E. A.: Cadmium, zinc, copper and barium in foraminifera tests, Geochim. Cosmochim. Acta, 47, 1815–1819, 1981.

Boyle, E.A.: Manganese carbonate overgrowths on foraminifera tests, Geochim. Cosmochim. Acta, 47, 1815, 1983.

Boyle, E. A., and Keigwin, L. D.: Comparison of Atlantic and Pacific paleochemical records for the last 215,000 years: Changes in deep ocean circulation and chemical inventories, Earth Planet. Sci. Lett., 76, 135–150, 1985.

Boyle, E. A.: Cadmium: Chemical tracer of deep-water paleoceanography, Paleoceanography, 3, 471–489, 1988.

Brady, H. B.: Supplementary note on the foraminifera of the Chalk of the New Britain Group, Geological Magazine, London, new series, 4(12), 534-536, 1877.

Brady, H. B.: Report on the foraminifera dredged by H.M.S. Challenger during the years 1873-1876, Reports of the scientific results of the voyage H.M.S. Challenger, 1873-1876, Zoology, 9, 1884.

Brink, K.H., Halpern, D., Huyer, A. and Smith, R.L.: The physical environment of the Peru upwelling system, Progress in Oceanography 12, 285-305, 1983.

Brockmann, C., Fahrbach, E., Huyer, A. and Smith, R. L.: The poleward undercurrent along the Peru coast—5 degrees S to 15 degrees S, Deep-Sea Res., A27(10), 847–856, 1980.

Burdige, D. J.: The biogeochemistry of manganese and iron reduction in marine sediments, Earth-Sci. Rev., 35, 249-284, 1993.

Came, R. E., Oppo, D. W. and Curry, W. B.: Atlantic Ocean circulation during the Younger Dryas: Insights from a new Cd/Ca record from the western subtropical South Atlantic, Paleoceanography, 18(4), 1086, 2003.

Codispoti L. A., Brandes, J. A,. Christensen, J. P., Devol, A. H., Naqvi, S. W. A., Paerl, H. W. and Yoshinari, T.: The oceanic fixed nitrogen and nitrous oxide budgets: Moving targets as we enter the Anthropocene?, Scientia Marina, 65 (suppl. 2), 85–105, 2001.

Cushman, J. A.: Shallow-water foraminifera of the Tortugas Region. Publications of the Carnegie Institution of Washington, no. 311, Department of Marine Biology, Papers, 17, 1-75, 1922.

Cushman, J. A.: Some Pliocene Bolivinas from California, Contributions from the Cushman Laboratory for Foraminiferal Research, 2, 40-46, 1926.

Cushman, J. A. and Wickenden, R.T.D.: Recent foraminifera from off Juan Fernandez Islands, Proceedings of the United States National Museum, Washington, D. C., U.S.A, 75, 2780, 1929.

Cushman, J. A. and McCulloch, I.: Some Virgulininae in the collections of the Allan Hancock Foundation, Southern California, University, Publications, Allan Hancock Pacific Expedition, Los Angeles, California, 6(4), 179-230, 1942.

Delaney, M.L.: Miocene benthic foraminiferal Cd/Ca records: South Atlantic and western Equatorial Pacific, Paleoceanography, 5, 743–760, 1990.

Dessier, A. and Donguy, J. R.: Response to El Nino signals of the epiplanktonic copepod populations in the eastern tropical Pacific, J. Geophys. Res., 92, 14,393-14,403, 1987.

Díaz-Ochoa, J.A., Lange, C.B., Pantoja, S., De Lange, G.J., Gutiérrez, D. Munoz, P. and Salamanca, M.: Fish scales in sediments from off Callao, central Peru, Deep-Sea Res. II, 56, 1124-1135, 2009.

D'Orbigny, A.: Tableau méthodique de la classe des Céphalopodes, Annales des Sciences Naturelles. Paris, 7, 245-314, 1826.

D'Orbigny, A.: Foraminiferes, *in* A. Bertrand (ed.), Ramon de la Sagra, Histoire physique et naturelle de l' Ile de Cuba, Paris, 1-224, 1839.

Doyle, W. L.: Distribution of mitochondria in the foraminiferan, *Iridia diaphana*, Science, 81, 387, 1935.

Duijnstee, I. A. P., Ernst, S. R., and van der Zwaan, G. J.: Effects of anoxia on the vertical distribution of benthic foraminifera: Marine Ecology Progress Series, 246, 85–94, 2003.

Eggins, S., De Deckker, P. and Marshall, J.: Mg/Ca variation in planktonic foraminifera tests: Implications for reconstructing paleoseawater temperature and habitat migration, Earth Planet. Sci. Lett., 6694, 1–16, 2003.

Eggins, S., Sadekov, A., and De Deckker, P.: Modulation and daily banding of Mg/Ca in Orbulina universa tests by symbiont photosynthesis and respiration: A complication for seawater thermometry?, Earth Planet. Sci. Lett., 225, 411–419, 2004.

Elderfield, H., and Ganssen, G.: Past temperature and $\delta^{18}O$ of surface ocean waters inferred from foraminiferal Mg/Ca ratios, Nature, 405, 442–445, 2000.

Ekman, V. W.: On the influence of the earth´s rotation on ocean currents, Arkiv för Matematik, Astronomi och Fysik, 2, 1-53, 1905.

Emeis, K.C., Whelan, J.K. and Tarafa, M.: Sedimentary and geochemical expression of oxic and anoxic conditions on the Peru shelf, *in* Tyson, R.V. and Pearson, T.H. (eds.), Modern and Ancient Continental Shelf Anoxia, Geological Society of London, pp. 155-170, 1991.

Erez, J.: The source of ions for biomineralization in foraminifera and their implications for paleoceanographic proxies, *in* Dove, P. M., De Yoreo, J. J., and Weiner, S. (eds.), Biomineralization: Mineralogical Society of America, Washington, D. C., 115–149, 2003.

Fairbanks, R. G.: A 17,000-year glacio-eustatic sea level record: Influence of glacial melting rates on the Younger Dryas event and deep-ocean circulation, Nature, 342, 637-642, 1989.

Falkowski, P. G.: Evolution of nitrogen cycle and its influence on the biological pump in the ocean, Nature, 342, 637-642, 1997.

Finlay, B. J., Span. A. S. W., and Harman, J. M. P.: Nitrate respiration in primitive eukaryotes, Nature, 303, 333–335, 1983.

Fhlaithearta, S. N., Reichart, G.-J., Jorissen, F. J., Fontanier, C., Rehling, E. J., Thomson, J. and De Lange, G. J.: Reconstructing the seafloor environment during sapropel formation using benthic foraminiferal trace metals, stable isotopes, and sediment composition, Paleoceanography, 25, 2010, PA4225, doi:10.1029/2009PA001869.

Foster, G.L.: Seawater pH, pCO_2 and $[CO_3^{2-}]$ variations in the Caribbean Sea over the last 130 kyr: a boron isotope and B/Ca study of planktic foraminifera, Earth and Planetary Science Letters, 271, 254–266, 2008.

Fréon, P., Barange, M. and Arístegui, J.: Eastern Boundary Upwelling Ecosystems: Integrative and comparative approaches, Progress in Oceanography, 83, 1-14, 2009.

Frerichs, W. E., Heiman, M. E., Borgman, L. E. and Bé, A. W. H.: Latitudinal variations in planktonic foraminiferal test porosity: Part 1. Optical studies, Journal of Foraminiferal Research, 2, 6-13, 1972.

Froelich P. N., Klinkhammer, G. P., Bender, M. L., Luedtke, N. A., Heath, G. R., Cullen, D., Dauphin, P., Hammond, D., Hartman, B. and Maynard, V.: Early oxidation of organic matter in pelagic sediments of the eastern equatorial Atlantic: suboxic diagenesis, Geochim. Cosmochim. Acta, 43, 1075-1090, 43.

Gaetani, G. A. and Cohen, A. L.: Element partitioning during precipitation of aragonite from seawater: A framework for understanding paleoproxies, Geochim. Cosmochim. Acta, 70, 4117-4137, 2006.

Ganeshram, R. S., Pedersen, T .F., Calvert, S. E. and Murray, J.W.: Large changes in oceanic nutrient inventories from glacial to interglacial periods, Nature, 376, 755–757, 1995.

Ganeshram, R. S., Pedersen, T. F., Calvert, S. E., McNeill, G. W. and Fontugne, M. R.: Glacial–interglacial variability in denitrification in the world's oceans: causes and consequences, Paleoceanography, 15 (4), 361–376, 2000.

Gehlen, M., Bassinot, F., Beck, L. and Khodja, H.: Trace element cartography of *Globigerinoides ruber* shells using particle-induced X-ray emission, Geochem. Geophys. Geosyst., 5(12), 2004, Q12D12, doi:10.1029/2004GC000822.

Geslin, E., Risgaard-Petersen, N., Lombard, F., Metzger, E., Langlet, D. and Jorissen, F.: Oxygen respiration rates of benthic foraminifera as measured with oxygen microsensors, Journ. Exp. Mar. Bio. and Eco., 396, 108-114, 2011.

Glock, N., Eisenhauer, A., Milker, Y., Liebetrau, V., Schönfeld, J., Mallon, J., Sommer, S. and Hensen, C.: Environmental influences on the pore-density in tests of *Bolivina spissa*, J. Foraminiferal Res., 41, 22-32, 2011a.

Glock, N., Schönfeld, J. and Mallon, J.: The functionality of pores in benthic foraminifera and bottom water oxygenation. *A Review, in* Altenbach, A.V., Bernhard, J.M. and Seckbach, J. (eds.), ANOXIA: Evidence for eukaryote survival and paleontological strategies, Springer, *in press*.

Glud, R. N., Thamdrup, B., Stahl, H., Wenzhoefer, F., Glud, A., Nomaki, H., Oguri, K., Revsbech, N. P., and Kitazato, H.: Nitrogen cycling in a deep ocean margin sediment (Sagami Bay, Japan), Limnology and Oceanography, 54, 723–734, 2009.

Goldstein, S. T. and Corliss, B. H.: Deposit feeding in selected deep-sea and shallow-water benthic foraminifera, Deep-Sea Res., 41, 229-241, 1994.

Gooday, A. J., Todo, Y., Uematsu, K. and Kitazato, H.: New organic- walled Foraminifera (Protista) from the ocean´s deepest point, the Challenger Deep (western Pacific Ocean), Zool. Journ. of the Linn. Soc., 153, 399-423, 2008.

Grasshoff, K.: Determination of oxygen, *in*: Grasshoff, K., Ehrhardt. M., and Kremling, K. (eds.) Methods of Seawater Analysis: Verlag Chemie Weinheim, New York, 61–72, 1983.

Greaves, M., Caillon, N., Rebaubier, H., Bartoli, G., Bohaty, S., Cacho, I., Clarke, L., Cooper, M., Daunt, C., Delaney, M., deMenocal, P., Datton, A. and Eggins, S.: Interlaboratory comparison of calibration standards for foraminiferal Mg/Ca thermometry, Geochem. Geophys. Geosyst., 9(8), 2008, Q08010, doi:10.1029/2008GC001974.

Gronovius, L. T.: Zoophylacii Gronoviani: Leyden, Theodorus Haak et Soc., 3, 241-380, 1781.

Gruber, N. and Sarmiento, J. L.: Global patterns of marine nitrogen fixation and denitrification, Global Biogeochemical Cycles, 11, 235–266, 1997.

Gruber N.: The dynamics of the marine nitrogen cycle and its influence on atmospheric CO_2 variations, *in* Follows, M. and Oguz, T. (eds.), The Ocean Carbon Cycle and Climate, NATO ASI Series, Kluwer Academic, Dordrecht, pp. 97–148, 2004.

Gutiérrez, D., Sifeddine, A., Field, D.B., Ortlieb, L., Vargas, G., Chávez, F.P., Velazco, F., Ferreira, V., Tapia, P., Salvatteci, R., Boucher, H., Morales, M.C., Valdés, J., Reyss, J.-L., Campusano, A, Boussafir, M., Mandeng-Yogo, M., García, M. and Baumgartner, T.: Rapid reorganization in ocean biogeochemistry off Peru towards the end of the Little Ice Age, Biogeosciences, 6, 835-848, 2009.

Gunther, E. R.: A report on oceanographical investigations in the Peru coastal current, Discovery Report, 13, 107-276, 1936.

Haley, B. A. and Klinkhammer, G. P.: Development of a flow-through system for cleaning and dissolving foraminiferal tests, Chem. Geol., 185, 51-69, 2002.

Haley, B. A., Klinkhammer, G. P. and Mix, A. C.: Revisiting the rare earth elements in foraminiferal tests, Earth and Planetary Science Letters, 239, 79-97, 2005.

Hall, J. M. and Chan, L.-H.: Ba/Ca in *Neogloboquadrina pachyderma* as an indicator of deglacial meltwater discharge into the western Arctic Ocean, Paleoceanography, 19, 9 pp., 2004a.

Hall, J. M. and Chan, L.-H.: Ba/Ca in benthic foraminifera: Thermocline and middepth circulation in the North Atlantic during the last glaciations, Paleoceanography, 19, 13 pp., 2004b.

Hallock, P., Röttger, R. and Wetmore, K.: Hypotheses on form and function in foraminifera, *in* Lee, J.J. and Anderson, O.R. (Ed.), Biology of Foraminifera, Academic Press, London, p. 41-72.

Haltia, T., Brown, K., Tegoni, M., Cambillau, C., Saraste, M., Mattila, K. and Djinovic-Carugo, K.: Crystal structure of nitrous oxide reductase from Paracoccus denitrificans at 1.6Å resolution, Biochemical Journal, 369, 77-88, 2003.

Hansen, H. J.: Pore pseudopodia and sieve plates of *Amphistigina*, Micropaleontology, 18, 223-230, 1972.

Hansen, H. J. and Buchardt, B.: Depth distribution of Amphistigina in the Gulf of Elat, Utrecht Micropaleontological Bulletin, 1, 225-239, 1977.

Harding, D. J., Arden, J. W. and Rickaby, R. E. M.: A method for precise analysis of trace element/calcium ratios in carbonate samples using quadrupole inductively coupled plasma mass spectrometry, Geochem. Geophys. Geosyst., 7, 2006, Q06003, doi:10.1029/2005GC001093.

Harmann, R. A.: Distribution of foraminifera in the Santa Barbara Basin, California, Micropaleontology, 10, 81–96, 1964.

Hart, T. Y., Currie, R. J.: The Benguela Current, Discovery Report, 31, 123-298, 1960.

Hemleben, C., Spindler, M. and Anderson, O. R.: Modern planktonic Foraminifera, Springer-Verlag, New York, pp 363, 1989.

Hastings, D. W., Emerson, S., Erez, J. and Nelson, B.K.: Vanadium incorporation in foraminiferal calcite as a paleotracer for seawater vanadium concentrations, Geochim. Cosmochim. Acta, 19, 3701-3715, 1996a.

Hastings, D. W., Emerson, S. E. and Nelson, B.: Determination of picogram quantities of vanadium in foraminiferal calcite and seawater by isotope dilution inductively coupled plasma mass spectrometrwy ith electrothermavla porization, Anal. Chem., 68, 371-378, 1996b.

Hastings, D. W., Emerson, S. R. and Mix, A. C.: Vanadium in foraminiferal calcite as a tracer for changes in the areal extent of reducing sediments, Paleoceanography, 11 (6), 665-678, 1996c.

Hastings, D. W., Russell, A. D. and Emerson, S. R.: Foraminiferal magnesium in Globeriginoides sacculifer as a paleotemperature proxy, Paleoceanography, 13(2), 161–169, 1998.

Hathorne, E. C., Alard, O., James, R. H. and Rogers, N. W.: Determination of intratest variability of trace elements in foraminifera by laser ablation inductively coupled plasma-mass spectrometry, Geochem. Geophys. Geosyst., 4(12), 8408, 2003, doi:10.1029/2003GC000539.

Hayward, B. W., Grenfell, H. R., Sabaa, A. T., Kay, J. and Clark, K.: Ecological distribution of the foraminifera in a tidal lagoon brackish lake, New Zealand, and its Holocene origins, Journal of Foraminiferal Research, 41, 124-137, 2011.

Helly, J. and Levin, L.: Global distribution of naturally occurring marine hypoxia on continental margins, Deep-Sea Res., 51, 1159–1168, 2004.

Hendrix, W.E.: Foraminiferal shell form, a key to sedimentary environment, Journal of Paleontology, 32, 649–659, 1958.

Heron-Allen, E. and Earland, A.: The foraminifera of the Kerimba Archipelago (Portuguese East Africa); Part 1, The Transactions of the Zoological Society, London, England, 20, 1914.

Hill E.A., Hickey, B.M., Shillington, F.A., Strub, P.T., Brink, K.H., Barton, E.D. and Thomas, A.C.: Eastern ocean boundaries, *in* Robinson, A.R. and Brink, K.H. (eds.), The Global Coastal Ocean—Regional Studies and Syntheses, Vol. 11 of The Sea—Ideas and Observations in the Study of the Seas, Wiley, pp. 29-67., 1998.

Høgslund, S., Revsbech, N. P. Cedhagen, T. Nielsen, L. P., and Gallardo, V. A.: Denitrification, nitrate turn over, and aerobic respiration by benthic foraminiferans in the oxygen minimum zone off Chile, Journal of Experimental Marine Biology and Ecology, 359, 85–91, 2008.

Hottinger, L., and Dreher, D.: Differentiation of protoplasm in Nummulitidae (Foraminifera) from Elat, Red Sea, Marine Biology, 25, 41–61, 1974.

Jahn, B.: Elektronenmikroskopische Untersuchungen an Foraminiferenschalen, Zeitschrift für Wissenschaftliche Mikroskopie und Mikrotechnik, 61, 294-297, 1953.

Joos, F., Plattner, G.-K., Stocker, T. F., Körtzinger, A. and Wallace, D. W. R.: Trends in marine dissolved oxygen: Implications for ocean circulation changes and the carbon budget, EOS Trans. AGU, 84, 197-204, 2003.

Jorissen, F. J., De Stigter, H. C., and Widmark, J. G. V.: A conceptual model explaining benthic foraminiferal microhabitats, Marine Micropaleontology, 26, 3–15, 1995.

Jorissen, F. J., Fontanier, C. and Thomas, E.: Paleoceanographical proxies based on deep-sea benthic foraminiferal assemblage characteristics, *in* Hillaire-Marcel, C. and de Vernal, A. (eds.), Proxies in Late Cenozoic Paleoceanography (Pt. 2): Biological tracers and biomarkers, pp. 500, 2007.

Kaiho, K.: Benthic foraminiferal dissolved-oxygen index and dissolved-oxygen levels in the modern ocean, Geology, 22, 719–722, 1994.

Kaldorf, M., Linne von Berg, K.-H., Maier, U. and Bothe, H.: The reduction of nitrous oxide by *Escherichia coli*, Archives of Microbiology, 160, 432-439, 1993.

Kasemann, S. A., Schmitt, D. N., Bijma, J. and Foster, G. L.: *In situ* boron isotope analysis in marine carbonates and its application for foraminifera and palaeo-pH, Chemical Geology, 260, 138-147, 2009.

Kellner, R., Mermet, J.-M., Otto, M. and Widmer, H. M.: Analytical Chemistry, Wiley VCH, Weinheim, 1998.

Knauss, J. A.: Introduction to physical oceanography, Prentice Hall, Upper Saddle River, New Jersey, 1997.

Kunioka D., Shirai K., Takahata N., Sano Y., Toyofuku T. and Ujiie Y.: Microdistribution of Mg/Ca, Sr/Ca and Ba/Ca ratios in Pulleniatina obliquiloculata test by using NanoSIMS: implication for the vital effect mechanism. Geochem. Geophys. Geosyst. 7, 2006, Q12P20. doi:10.1029/2006GC001280.

Kutzbach, J. E., P. J. Guetter, P. J. Behling, and R. Selin: Simulated climatic changes: Results of the COHMAP climate-model experiments, *in* Wright H. E. et al. (eds), Global Climates Since the Last Glacial Maximum, Univ. of Minn. press, Minnesota, pp. 24-93, 1993.

Lalucat, J., Bennasar, A., Bosch, R., García- Valdéz, E. and Palleroni, N. J.: Biology of *Pseudomonas stutzeri*, Microbiology and Molecular Biology Reviews, 70, 510-547, 2006.

Larsen, A. R.: Studies of recent Amphistegina, taxonomy and some ecological aspects, Israel Journal of Earth-Sciences, 25, 1-26, 1976.

Lam, P., Lavik, G., Jensen, M. M., van de Vossenberg, J., Schmid, M., Woebken, D., Gutiérrez, D., Amann, R., Jetten, M. S. M. and Kuypers, M. M. M.: Revising the nitrogen cycle in the Peruvian oxygen minimum zone, PNAS, 106 (12), 4752-4757, 2009.

Lambeck, K., Yokoyama, Y. and Purcell, A.: Into and out of Last Glacial Maximum: sea-level change during the oxygen isotope Stage 3 and 2, Quaternary Science Reviews 21, 343–360, 2002.

Langer, M. R.: Assessing the contribution of foraminiferan protists to global ocean carbonate production, J. Eukaryot. Microbiol., 55, 163-169, 2008.

Lea, D. W. and Boyle, E.A.: Barium content of benthic foraminifera controlled by bottom-water composition, Nature, 338, 751–753, 1989.

Lea, D. W. and Boyle, E. A.: Foraminiferal reconstruction of barium distributions in water masses of the glacial oceans, Paleoceanography, 5, 719– 742, 1990a.

Lea, D. W. and Boyle, E. A.: A 210,000-year record of barium variability in the deep northwest Atlantic Ocean, Nature, 347, 269–272, 1990b.

Lea, D. W., and Boyle, E. A.: Barium in planktonic foraminifera, Geochim. Cosmochim. Acta, 55, 3321– 3331, 1991.

Lea, D. W., and Spero, H. J.: Experimental determination of barium uptake in shells of the planktonic foraminifera Orbulina universa at 22°C, Geochim. Cosmochim. Acta, 56, 2673–2680, 1992.

Lea, D. W. and Spero, H. J.: Assessing the reliability of paleochemical tracers: Barium uptake in the shells of planktonic foraminifera, Paleoceanography, 9, 445– 452, 1994.

Lea, D. W., Mashiotta, T. A. and Spero, H. J.: Controls on magnesium and strontium uptake in planktonic foraminifera determined by live culturing, Geochim. Cosmochim. Acta, 63, 2369–2379, 1999.

Lea, D. W.: Trace elements in foraminiferal calcite Modern Foraminifera, in B. K. Sen Gupta (ed.) Kluwer Academic Publishers, New York, Boston, Dordrecht, London, Moscow, pp. 201-216, 2003.

Lear, C. H., Rosenthal, Y. and Slowey, N.: Benthic foraminiferal Mg/Ca-paleothermometry: A revised coretop calibration, Geochim. Cosmochim. Acta, 66(19), 3375–3387, 2002.

Lear, C. H., Rosenthal, Y. and Slowey, N.: Benthic foraminiferal Mg/Ca-paleothermometry: A revised coretop calibration, Geochim. Cosmochim. Acta, 66(19), 3375–3387, 2002.

Le Calvez, J.: Les perforations du test de *Discorbis erecta* (Foraminifère), Bulletin de Laboratoire Maritime de Dinard, 29, 1-4, 1947.

Lee, J.J., Anderson, O.R.: Symbiosis in Foraminifera, *in* Lee, J.J. & Anderson, O.R. (Ed.), Biology of Foraminifera, Academic Press, London, 157-222, 1991.

Lehodey, P., Bertignac, M., Hampton, J., Lewis, A. and Picaut, J.: El Nino Southern Oscillation and tuna in the western Pacific, Nature, 389, 715-718, 1997.

Leutenegger, S.: Ultrastructure de foraminiféres perforés et imperforés ainsi que de leurs symbiotes, Cahiers de Micropaléontologie, 3, 1-52, 1977.

Leutenegger, S. and Hansen, H. J.: Ultrastructural and radiotracer studies of pore function in foraminifera: Marine Biology, 54, 11–16, 1979.

Leutenegger, S.: Symbiosis in benthic foraminifera; specifity and host adaptations, Journal of Foraminiferal Research, 14, 16-35, 1984.

Levin, L. A., Huggett, C. L. and Wishner, K. F.: Control of deep-sea benthic community structure by oxygen and organic matter gradients in the eastern Pacific Ocean, Journal of Marine Research, 49, 763–800, 1991.

Levin, L. A., Gage, J. D., Martin, C. and Lamont, P. A.: Macrobenthic community structure within and beneath the oxygen minimum zone, NW Arabian Sea, Deep-Sea Research II, 47, 189–226, 2000.

Levin, L. A., Gutiérrez, D., Rathburn, A., Neira, C., Sellanes, J., Munoz, P., Gallardo, V. and Salamanca, M.: Benthic processes on the Peru margin: a transect across the oxygen minimum zone during the 1997-1998 El-Nino, Progress in Oceanography, 53, 1-27, 2002.

Linne: Systema Naturae. 10th edition, Stockholm, vol. 10, 824 pp., 1758.

Lisiecki, L.E and Raymo, M.E: A Pliocene-Pleistocene stack of 57 globally distributed benthic delta O-18 records, Paleoceanography 20(1), 2005, PA1003.

Loubere, P.: Remote vs. local control of changes in eastern equatorial Pacific bioproductivity from the Last Glacial Maximum to the Present, Global and Planetary Change, 35, 113-126, 2002.

Lückge, A. and Reinhardt, L.: CTD measurements in the water column off Peru, in Kudrass, H.R. (ed.), Cruise Report SO147 Peru Upwelling: Valparaiso—Callao, 29.05.-03.07.2000, BGR Hannover, pp. 35-37, 2000.

Lutze, G. F.: Variiationsstatistik und Ökologie bei rezenten Foraminiferen, Paläontologische Zeitschrift, 36, 252–264, 1962.

Lutze, G. F.: *Uvigerina* species of the eastern North Atlantic, *in* van der Zwaan G., J., Jorissen F. J., Verhallen P. J. J. M., and von Daniels C. H. (eds.), Atlantic-European Oligocene to Recent *Uvigerina*: Utrecht Micropaleontological Bulletins, 35, 21–46, 1986.

Lyle, M.: Climatically forced organic carbon burial in equatorial Atlantic and Pacific Oceans. Nature, 335, 529-532, 1988.

Lyle. M. D., Murray, W., Finney, B. P., Dymond, J., Robbins, J. M. and Brooksforce, K.: The record of Late Pleistocene biogenic sedimentation in the Eastern Tropical Pacific Ocean. Paleoceanography, 3, 39-59, 1988.

Mallon, J., Glock, N. and Schönfeld, J.: The response of benthic foraminifera to low-oxygen conditions of the Peruvian oxygen minimum zone, *in* Altenbach, A.V., Bernhard, J.M. and Seckbach, J. (eds.), ANOXIA: Evidence for eukaryote survival and paleontological strategies, Springer, *in press*.

Marchitto, T. M., Jr., Curry, W. B. and Oppo, D. W.: Zinc concentrations in benthic foraminifera reflect seawater chemistry, Paleoceanography, 15(3), 299–306, 2000.

Marchitto, T. M.: Precise multielemental ratios in small foraminiferal samples determined by sector field ICP-MS, Geochem. Geophys. Geosyst., 7, 2006, Q05P13, doi:10.1029/2005GC001018.

Marszalek, D. S. and Hay, W. W.: Function of the test in foraminifera, Trans. Gulf-Cst. Ass. Geol. Soc., 19, 341-352, 1969.

Martin, P. A. and Lea, D. W.: Comparison of water mass changes in the deep tropical Atlantic derived from Cd/Ca and carbon isotope records: Implications for changing Ba composition of deep Atlantic water masses, Paleoceanography, 13, 572– 585, 1998.

Matear, R. J. and Hirst, A. C.: Long-term changes in dissolved oxygen concentation in the ocean caused by protracted global warming, Gobal Biogeochem. Cycles, 17(4), 1125, 2003, doi:10.1029/2002GB001997.

McPhaden, M. J., Busalacchi, A. J., Cheney, R., Donguy, J.-R., Gage, K. S., Halpern, D., Ji, M., Julian, P., Meyers, G., Mitchum, G. T., Niiler, P. P., Picaut, J., Reynolds, R. W., Smith, N., and Takeuchi, K. The Tropical Ocean-Global Atmosphere observing system: A decade of progress, J. Geophys. Res., 14, 169-240, 1998.

Mix, A. C., Ruddiman, W. F. and McIntyre, A.: Late Quaternary paleoceanography of the tropical Atlantic, I. Spatial variablity of annual mean sea-surface temperatures, 0-20,000 years B.P, Paleoceanography, 1, 43-66, 1986.

Morales, C.E., Hormazábal, S.E. and Blanco, J.L.: Interannual variability in the mesoscale distribution of the depth of the upper boundary of the oxygen minimum layer off northern Chile (18-24°S): Implications for the pelagic system and biogeochemical cycling, Journal of Marine Research, 57, 909-932, 1999.

Moodley, L. and Hess, C.: Tolerance of infaunal benthic foraminifera for low and high oxygen concentrations, Biological Bulletin, 183, 94–98, 1992.

Munsel, D., Kramar, U., Dissard, D., Nehrke, G., Berner, Z., Bijma, J., Reichart, G.-J. and Neumann, T.: Heavy metal incorporation in foraminiferal calcite: results from multi-element enrichment culture experiments with *Ammonia tepida*, Biogeosciences, 7, 2339-2350, 2010.

Murray, J.W.: Biodiversity of living benthic foraminifera: How many species are there?, Marine Micropaleontology, 64, 163-176, 2007.

Myers, E. H.: Morphogenesis of the test and biological significance of dimorphism in the foraminifer *Patellina corrugata* Williamson, Bulletin of the Scripps Institution of Oceanography , Technical Series, 3, 393-404, 1935.

Ni, Y., Foster, G.L., Bailey, T., Elliott, T., Schmidt, D.N., Pearson, P., Haley, B. and Coath, C.: A core top assessment of proxies for the ocean carbonate system in surface dwelling Foraminifers, Paleoceanography 22 (3), 14pp, 2007.

Nikulina, A, Polovodova, I and Schönfeld, J.: Foraminiferal response to environmental changes in Kiel Fjord, SW Baltic Sea, eEarth, 3, 37-49, 2008.

Nikulina, A and Dullo, W.-C.: Eutrophication and heavy metal pollution in Flensburg Fjord: A reassessment after 30 years, Marine Pollution Bulletin, 58, 905-915, 2009.

Noffke, A., Hensen, C., Sommer, S., Scholz, F., Bohlen, L., Mosch, T. and Wallmann, K.: The benthic diagenetic phosphorus and iron source across the Peruvian oxygen minimum zone, *submitted to Limnol. Oceanogr.*.

Nomaki, H., Heinz, P., Nakatsuka, T., Shimanaga, M., Ohkouchi, N., Ogawa, N. O., Kogure, K., Ikemoto, E., and Kitazato, H.: Different ingestion patterns of ^{13}C-labeled bacteria and algae by deep-sea benthic foraminifera, Marine Ecology Progress Series, 310, 95–108, 2006.

Nürnberg, D.: Magnesium in tests of *Neogloboquadrina pachyderma* sinistral from high northern and southern latitudes, J. Foraminiferal Res., 25, 350–368, 1995.

Nürnberg, D., Bijma, J. and Hemleben, C.: Assessing the reliability of magnesium in foraminiferal calcite as a proxy for water mass temperatures, Geochim. Cosmochim. Acta, 60(5), 803–814, 1996.

Ohkouchi, N., Kawahata, H., Murayama, M., Ohkada, M., Nakamura, T. and Taira, A.: Was deep water formed in the North Pacific during the Late Quaternary? Cadmium evidence from the northwest Pacific. Earth and Planetary Science Letters, 124, 185–194, 1994.

Ohkouchi, N., Kawamura, K. and Taira A.: Fluctuations of terrestrial and marine biomarkers in the western tropical Pacific during the last 23,300 years, Paleoceanography, 12, 623-630, 1997.

Pakhomova, S. V., Hall, P. O. J., Kononets, M. Y., Rozanov, A. G., Tengberg, A. and Vershinin, A. V.: Fluxes of iron and manganese across the sediment-water interface under various redox conditions, Mar. Chem., 107, 319-331, 2007.

Palmer, M.R., Pearson, P.N. and Cobb, S.J.: Reconstructing past ocean pH–depth profiles, Science 282, 1468–1471, 1998.

Palmer, M.R. and Pearson, P.N.: A 23,000-year record of surface water pH and pCO2 in the western equatorial Pacific Ocean, Science 300, 480–482, 2003.

Patrick, A. and Thunell, R.: Tropical Pacific sea surface temperatures and upper water column thermal structure during the last glacial maximum, Paleoceanography, 12, 649-657, 1997.

Pearcy, W. G. and Schoener, A.: Changes in the marine biota coincident with the 1982-1983 El Nino in the northeastern subarctic Pacific Ocean, J. Geophys. Res., 92, 14, 417-14,248, 1987.

Pearson, P.N. and Palmer, M.R.: Atmospheric carbon dioxide concentrations over the past 60 million years, Nature 406, 695–699, 2000.

Pedersen, T. F.: Increased productivity in the eastern equatorial Pacific during the last glacial maximum (19,000 to 14,000 yr B.P.), Geology, 11, 16-19, 1983.

Pedersen, T. F., Pickering, M., Vogel, J. S., Southon, J. N. and Nelson, D. E.: The response of benthic foraminifera to productivity cycles in the eastern equatorial Pacific: Faunal and geochemical constraints on glacial bottom water oxygen levels, Paleoceanography, 3 (2), 157-168, 1988.

Pena, L. D., Calvo, E., Cacho, I., Eggins, S. and Pelejero, C.: Identification and removal of Mn-Mg-rich contaminant phases on foraminiferal tests: Implications for Mg/Ca past temperature reconstructions, Geochem. Geophys. Geosyst., 6, 2005, Q09P02, doi:10.1029/2005GC000930.

Pena, L. D., Cacho, I., Calvo, E., Pelejero, C., Eggins, S. and Sadekov, A.: Characterization of contaminant phases in foraminifera carbonates by electron microprobe mapping, Geochem. Geophys. Geosyst., 9, 2007, Q07012, doi:10.1029/2008GC002018.

Pennington, J.T., Mahoney, K.L., Kuwahara, V.S., Kolber, D., Calienes, R., and Chavez, F.P.: Primary production in the eastern tropical Pacific: A review, Prog. Oceanogr., 69, 285–317, 2006.

Perez-Cruz, L. L. and Machain-Castillo, M. L.: Benthic foraminifera of the oxygen minimum zone, continental shelf of the Gulf of Tehuantepec, Mexico, Journal of Foraminiferal Research, 20, 312–325, 1990.

Perks, H. M. and Keeling, R. F.: A 400 kyr record of combustion oxygen demand in the western equatorial Pacific: Evidence for a precessionally forced climate response. Paleoceanography, 13 (1), 63, 1998.

Philander, S. G. H.: El Nino Southern Ocean Phenomena, Nature, 302, 295-301, 1983.

Philander, S. G. H.: E1 Nino, La Nina, and the Southern Oscillation, Academic Press, San Diego, Calif., 293 pp., 1990.

Piña-Ochoa, E., Høgslund, S., Geslin, E., Cedhagen, T., Revsbech, N. P., Nielsen, L. P., Schweizer, M., Jorissen, F., Rysgaard, S. and Risgaard-Petersen, N.: Widespread occurence of nitrate storage and denitrification among Foraminifera and *Gromiida*, Proceedings of the National Acadamy of Sciences of the United States of America, 107, 1148-1153, 2010.

Polovodova, I., Nikulina, A., Schönfeld, J. and Dullo, W. C.: Recent benthic foraminifera from the Flensburg Fjord, Journal of Micropaleontology, 28, 131-142, 2009.

Rae, J. W. B., Foster, G. L., Schmitt, D. N. and Elliot, T.: Boron isotopes and B/Ca in benthic foraminifera: Proxies for the deep ocean carbonate system, Earth and Planetary Science Letters, 302, 403-413, 2011.

Rea, D. K., Pisias, G., and Newberry, T.: Late Pleistocene paleoclimatology of the Central Equatorial Pacific: Flux patterns of biogenic sediments, Paleoceanography, 6 (2), 227-244, 1991.

Reichart, G.-J., Jorissen, Mason, F. P. R. D. and Anschutz, P.: Single foraminiferal test chemistry records the marine environment, Geology, 31, 355–358, 2003.

Resig, J. M.: Benthic foraminiferal stratigraphy and paleoenvironments off Peru, Leg 1121, Proceedings of the Ocean Drilling Program, Scientific Results, 112, 263–296, 1990.

Richards F. A.: Anoxic basins and fjords, *in* Riley, J. P. and Skirrow, G. (eds.) Chemical Oceanography, Academic, New York, pp. 611–645, 1965.

Riester, J., Zumft, W. G. and Kroneck, P. M. H.: Nitrous oxide from *Pseudomonas stutzeri*, European Journal of Biochemistry, 178, 751-762, 1989.

Risgaard-Petersen, N., Langezaal, A. M., Ingvardsen, S., Schmid, M. C., Jetten, M. S., Op den Camp, H. J. M., Derksen, J. W. M., Pina-Ochoa, E., Eriksson, S. P., Nielsen, L. P., Revsbech, N. P., Cedhagen, T. and van der Zwaan, G. J.: Evidence for complete denitrification in a benthic foraminifer, Nature, v. 443, p. 93–96, 2006.

Rollion-Bard C., Erez J. and Zilberman T.: Intra-shell oxygen isotope ratios in the benthic genus Amphistegina and the influence of seawater carbonate chemistry and temperature on this ratio. Geochim. Cosmochim. Acta, 72, 6006–6014, 2008.

Rollion-Bard, C. and Erez, J.: Intra-shell boron isotope ratios in the symbiont-bearing benthic foraminiferan Amphistegina lobifera: Implications for $\delta^{11}B$ vital effects and paleo-pH reconstructions, Geochim. Cosmochim. Acta, 74, 1530-1536, 2010.

Rosenthal, Y., Boyle, E. A. and Slowey, N.: Temperature control on the incorporation of magnesium, strontium, fluorine, and cadmium into benthic foraminiferal shells from Little Bahama Bank: Prospects for thermocline paleoceanography, Geochim. Cosmochim. Acta, 61, 3633–3643, 1997.

Russell, A. D., Emerson, S., Nelson, B., Erez, J. and Lea, D. W.: Uranium in foraminiferal calcite as a recorder of seawater uranium concentrations, Geochim. Cosmochim. Acta, 58(2), 671–681, 1994.

Russell, A. D., Hönisch, B., Spero, H. J. and Lea, D. W.: Effects of seawater carbonate ion concentration and temperature on shell U, Mg, and Sr in cultured planktonic foraminifera, Geochim. Cosmochim. Acta, 68(21), 4347–4361, 2004.

Sadekov, A. Y., Eggins, S. M. and De Deckker, P.: Characterization of Mg/Ca distributions in planktonic foraminifera species by electron microprobe mapping, Geochem. Geophys. Geosyst., 6, 2005, Q12P06, doi:10.1029/2005GC000973.

Sano, Y., Shirai, K., Takahata, N., Hirata, T. and Sturchio N. C.: Nano-SIMS analysis of Mg, Sr, Ba, U in natural calcium carbonate, Anal. Sci., 21, 1091–1097, 2005.

Sanyal, A., Hemming, N.G., Hanson and G.N., Broecker,W.: Evidence for a higher pH in the glacial ocean from boron isotopes in foraminifera, Nature 373, 234–236, 1995.

Sanyal, A., Bijma, J., Spero, H.J. and Lea, D.: Empirical relationship between pH and the boron isotopic composition of Globigerinoides sacculifer: implications for the boron isotope paleo-pH proxy, Paleoceanography 16 (5), 515–519, 2001.

Scholz, F., Hensen, C., Noffke, A., Rhode, A. and Wallmann, K.: Early diagenesis of redox-sensitive trace metals in the Peru upwelling area – response to ENSO-related oxygen fluctuations in the water column, *submitted to Geochim. Cosmochim. Acta*.

Schrader, H. and Sorknes, R.: Spatial and temporal variation of Peruvian coastal upwelling during the latest Quaternary. Proc. Ocean Drill. Prog., Sci. Results 112, 391– 406, 1990.

Sen Gupta, B. K. and Machain-Castillo, M. L.: Benthic foraminifera in oxygen-poor habitats, Marine Micropaleontology, 20, 183–201, 1993.

Sen Gupta, B. K.: Introduction to modern foraminifera, *in* B. K. Sen Gupta (ed.), Modern Foraminifera, Kluwer Academic Publishers, New York, Boston, Dordrecht, London, Moscow, pp. 201-216, 2003.

Shaffer, G., Salinas, S., Pizarro, O., Vega , A. and Hormázabal, S.: Currents in the deep ocean off Chile (30°S), Deep-Sea Res., 42, 425–426, 1995.

Shaffer, G., Pizarro, O., Djurfeldt, L., Salinas, S. and Rutllant, J.: Circulation and low-frequency variability near the Chilean coast: remotely forced fluctuations during the 1991–92 El Nino, J. Phys. Ocean., 27, 217–235, 1997.

Siddall, M., Rohling, E.J., Almogi-Labin, A., Hemleben, Ch., Meischner, D., Schmelzer, I. and Smeed, D.A.: Sea-level fluctuations during the last glacial cycle, Nature 423, 853–856, 2003.

Sifeddine, A., Gutierrez, D., Ortlieb, L., Boucher, H., Velazco, F., Field, D., Vargas, G., Boussafir, M., Salvatteci, R., Ferreira, V., García, M., Valdes, J., Caquineau, S., Mandeng Yogo, M., Cetin, F., Solis, J., Soler, P., and Baumgartner, T.: Laminated sediments from the central Peruvian continental slope: A 500 year record of upwelling system productivity, terrestrial runoff and redox conditions, Prog. Oceanogr., 79, 190–197, 2008.

Silva, K. A., Corliss, B. H., Rathburn, A. E., and Thunell, R. C.: Seasonality of living benthic foraminifera from the San Pedro Basin, California Borderland, Journal of Foraminiferal Research, 26, 71–93, 1996.

Sliter, W. V.: *Bolivina doniezi* Cushman and Wickenden in Clone Culture, Contributions from the Cushman Foundation for Foraminiferal Research, 21, 87-100, 1970.

Sliter, W. V.: Test ultrastructure of some living benthic foraminifers, Lethaia, 7, 5-16, 1974.

Smith, R. L.: Circulation patterns in upwelling regimes, *in* Suess, E. and Thiede, J. (eds.): Coastal upwelling – its sediment record, Part A: Responses of the Sedimentary Regime to Present Coastal Upwelling, Plenum Press, NY, 13-35, 1983.

Spivack, A. J., You, C.-F. and Smith, H. J.: Foraminiferal boron isotope ratios as a proxy for surface ocean pH over the past 21 Myr, Nature 363, 149–151,1993.

Stramma, L., Johnson, G. C., Sprintall, J. and Mohrholz, V.: Expanding Oxygen-Minimum Zones in the Tropical Oceans, Science, 320, 655-658, 2008.

Suess, E., Kulm, L.D. and Killingley, J.S.: Coastal upwelling and a history of organic-rich mudstone deposition off Peru, *in* Brooks, J. and Fleet, A.J. (eds.), Marine Petroleum Source Rocks, Geological Society, pp. 181-197, 1986.

Suits N. S. and Arthur M. A.: Sulfur diagenesis and partitioning in Holocene Peru shelf and upper slope sediments, Chem. Geol. 163, 219–234, 2000.

Sverdrup, H. U., Johnson, M. W. and Fleming, R. H.: The Oceans: Their Physics, Chemistry and General Biology, Prentice-Hall inc, Engelwood Cliffs, New Jersey, 1942.

Toyofuku, T. and Kitazato, H.: Micromapping of Mg/Ca values in cultured specimens of the high-magnesium benthic foraminifera, Geochem. Geophys. Geosyst., 6, 2005, Q11P05, doi:10.1029/2005GC000961.

Thurman, H. V.: Introductory Oceanography 5th Edition, Merrill Publishing Company, Columbus, Toronto, London, Melbourne, 312-316, 1988.

Travis, J. L. and Bowser, S. S.: The motility of foraminifera, *in* J. J. Lee and O. R. Anderson (ed.), Biology of the foraminifera, Academic Press, London, pp. 91-155, 1991.

Tyson R. V., and Pearson T. H.: Modern and ancient continental shelf anoxia: an overview, *in* Tyson R. V. and Pearson T. H. (eds.), Modern and ancient continental shelf anoxia, Geological Society Special Publication No 58, The Geological Society, London, p 1-24, 1991.

Van de Graaf, A. A., Mulder, A., de Bruijn, P., Jetten, M. S. M. and Kuenen, J. G: Anaerobic oxidation of ammonium is a biologically mediated process, Appl. Environ. Microbiol. 61, 1246–1251, 1995.

Walker, G. T.: correlations in seasonal variations of weather, VIII. A preliminary study of world weather I, Mem. Indian Meteorol. Dept., 23**,** 75-131, 1923.

Walker, G. T.: Correlation in seasonal variations of weather IX: A further study of world weather, Mem. Indian Meteorol. Dept., 24, 275-332, 1924.

Walker, G. T.: World Weather III, Mem. R. Met. Soc. II, 17, 97-106, 1928.

Wefer, G., Heinze, P. and Suess, E.: Stratigraphy and sedimentation rates from oxygen isotope composition, organic carbon content, and grain-size distribution at the Peru upwelling region: Holes 680B and 686B, Proc. Ocean Drill. Prog., Sci. Results 112, 355–367, 1990.

Williamson, W. C.: On the Recent Foraminifera of Great Britain. Ray Society, London, England, 1858.

Wolf, A.: Zeitliche Variationen im peruanischen Küstenauftrieb seit dem Letzten Glazialen Maximum – Steuerung durch globale Klimadynamik, Dissertation, 2002.

Wooster, W. S. and Reid, J. L.: Eastern boundary currents, *in* M. N. Hill (ed.), The Sea, Wiley, NY, 253-280, 1963.

Wooster, W.S., Chow, T.J. and Barrett, I.: Nitrite distribution in Peru current waters, Journal of Marine Research 23, 211-221, 1965.

Wu, G., and Hillaire-Marcel, C.: Application of LP-ICP-MS to benthic foraminifers, Geochim. Cosmochim. Acta, 59, 409–414, 1995, doi:10.1016/0016-7037(94)00370-2.

Wyrtki, K.: Surface currents of the Eastern Tropical Pacific Ocean, Inter-American Tropical Tuna Commission Bulletin 4, 271-304, 1965.

Wyrtki, K.: Circulation and water masses in the eastern equatvfial Pacific Ocean, Int. J. Oceanol. Limnol., 1, 117-147, 1967.

Yokoyama, Y., Esat, T. M. and Lambeck, K.: Coupled climate and sea-level changes deduced from Huon Peninsula coral terraces of the Last Ice Age, Earth and Planetary Science Letters 193, 579–587, 2001.

Yokoyama, Y., Kido, Y., Tada, R., Minami, I., Finkel, R. and Matsuzaki, H.: Japan Sea oxygen isotope stratigraphy and global sea-level changes for the last 50,000 years recorded in sediment cores from Oki Ridge, Paleogeography Paleoclimatology Paleoecology, 247, 5-17, 2007.

Yu, J., Elderfield, H., Jin, Z. and Booth, L.: A strong temperature effect on U/Ca in planktonic foraminiferal carbonates, Geochim. Cosmochim. Acta, 72, 4988-5000, 2008.

Zumft, W. G.: Cell biology and molecular basis of denitrification, Microbiology and Molecular Biology Reviews, 61, 533–616, 1997.

Yu, J., Day, J., Greaves, M. and Elderfield, H.: Determination of multiple element/calcium ratios in foraminiferal calcite by quadrupole ICP-MS, Geochem. Geophys. Geosyst. , 6, 2005, Q08P01, doi:10.1029/2005GC000964.

Yu, J., Elderfield, H., Greaves, M. and Day, J.: Preferential dissolution of benthic foraminiferal calcite during laboratory reductive cleaning, Geochem. Geophys. Geosyst. 8, 17, 2007.

Yu, J., Elderfield, H., Jin, Z. and Booth, L.: A strong temperature effect on U/Ca in planktonic foraminiferal carbonates, Geochim. Cosmochim. Acta, 72, 4988-5000, 2008.

Zumft, W. G.: Cell biology and molecular basis of denitrification, Microbiology and Molecular Biology Reviews, 61, 533-616, 1997.